ผลของสภาวะการเป่าและการดึงฟิล์มต่อสมบัติของฟิล์มพอลิแลคติกเอซิดผสมด้วยยางธรรมชาติ

นายธวัชชัย วงษ์ชัยชนะ

วิทยานิพนธ์นี้เป็นส่วนหนึ่งของการศึกษาตามหลักสูตรปริญญาวิศวกรรมศาสตรมหาบัณฑิต
สาขาวิชาวิศวกรรมเคมี ภาควิชาวิศวกรรมเคมี
คณะวิศวกรรมศาสตร์ จุฬาลงกรณ์มหาวิทยาลัย
ปีการศึกษา 2556
ลิขสิทธิ์ของจุฬาลงกรณ์มหาวิทยาลัย

EFFECTS OF FILM BLOWING AND DRAWING CONDITIONS ON PROPERTIES OF
POLY(LACTIC ACID)/NATURAL RUBBER FILMS

Mr. Thawatchai Wongchaichana

A Thesis Submitted in Partial Fulfillment of the Requirements
for the Degree of Master of Engineering Program in Chemical Engineering
Department of Chemical Engineering
Faculty of Engineering
Chulalongkorn University
Academic Year 2013

| | |
|---|---|
| Thesis Title | EFFECTS OF FILM BLOWING AND DRAWING CONDITIONS ON PROPERTIES OF POLY(LACTIC ACID)/NATURAL RUBBER FILMS |
| By | Mr. Thawatchai Wongchaichana |
| Field of Study | Chemical Engineering |
| Thesis Advisor | Associate Professor Anongnat Somwangthanaroj, Ph.D. |
| Thesis Co-Advisor | Assistant Professor Wanchai Lerdwijitjarud, Ph.D. |

Accepted by the Faculty of Engineering, Chulalongkorn University in Partial Fulfillment of the Requirements for the Master's Degree

----------------------------------------------------------Dean of the Faculty of Engineering

(Professor Bundhit Eua-arporn, Ph.D.)

THESIS COMMITTEE

----------------------------------------------------------Chairman

(Associate Professor Siriporn Damrongsakkul, Ph.D.)

----------------------------------------------------------Thesis Advisor

(Associate Professor Anongnat Somwangthanaroj, Ph.D.)

----------------------------------------------------------Thesis Co-Advisor

(Assistant Professor Wanchai Lerdwijitjarud, Ph.D.)

----------------------------------------------------------Examiner

(Associate Professor Prasert Pavasant, Ph.D.)

----------------------------------------------------------External Examiner

(Assistant Professor Amornrat Lertworasirikul, D.Eng.)

ธวัชชัย วงษ์ชัยชนะ : ผลของสภาวะการเป่าและการดึงฟิล์มต่อสมบัติของฟิล์มพอลิแลคติกเอซิดผสมด้วยยางธรรมชาติ. (EFFECTS OF FILM BLOWING AND DRAWING CONDITIONS ON PROPERTIES OF POLY(LACTIC ACID)/NATURAL RUBBER FILMS) อ.ที่ปรึกษาวิทยานิพนธ์หลัก: รศ. ดร. อนงค์นาฏ สมหวังธนโรจน์, อ.ที่ปรึกษาวิทยานิพนธ์ร่วม: ผศ. ดร วันชัย เลิศวิจิตรจรัส, 101 หน้า.

วัตถุประสงค์ของงานวิจัยนี้คือเพื่อหาความสัมพันธ์ระหว่าง สัณฐานวิทยา สมบัติเชิงความร้อน สมบัติเชิงกลและการซึมผ่านได้ของแก๊สของฟิล์มพอลิแลคติกเอซิดผสมยางธรรมชาติและสภาวะของการเป่า ได้แก่ อัตราส่วนการดึง (TUR) และ อัตราส่วนการขยายตัว (BUR) ผลกระทบของการดึงในทิศทางเดียวที่อุณหภูมิสูงต่อสมบัติของฟิล์มที่ถูกดึงได้ถูกศึกษาเช่นกัน ฟิล์ม PLA ที่มียางธรรมชาติปริมาณร้อยละ 10 โดยน้ำหนักถูกผสมในสภาวะหลอมเหลวด้วยเครื่องอัดรีดเกลียวหนอนคู่และจึงเป่าเป็นฟิล์มด้วยเครื่องอัดรีดเกลียวหนอนเดียวที่ต่อกับชุดอุปกรณ์สำหรับการเป่าฟิล์ม จากการศึกษาพบว่าการเพิ่มขึ้นของอัตราส่วนการดึง (TUR) และอัตราการส่วนการขยายตัว (BUR) ได้แสดงถึงการเสียรูปของยางธรรมชาติและเพิ่มการเรียงตัวของสายโซ่พอลิเมอร์ สมบัติเชิงกลลดลงอย่างมีนัยสำคัญ ยกเว้นความต้านแรงดึงและมอดุลัสของยังซึ่งสามารถถูกอธิบายโดยการเสียรูปของโดเมนยางจากทรงกลมกลายเป็นลักษณะของวงรีหลังจากการดึงยืด นอกจากนี้ ค่าการซึมผ่านของแก๊สออกซิเจนของฟิล์มเป่า PLA/NR เพิ่มขึ้นเมื่ออัตราส่วนการดึง (TUR) เพิ่มขึ้น เป็นผลมาจากการเกิดช่องว่างขนาดไมโครเมตร การดึงยืดในทิศทางเดียวของฟิล์มที่ถูกเป่าในแนวตามเครื่องจักร (MD) และแนวขวางเครื่องจักร (TD) ที่อุณหภูมิ 65 องศาเซลเซียสและอัตราการดึง 150 มิลลิเมตรต่อนาที ทำสำเร็จได้ด้วยเครื่องทดสอบการดึงร่วมกับตู้ควบคุมอุณหภูมิสิ่งแวดล้อม พบว่าการเพิ่มขึ้นของอัตราส่วนในการดึงในแนวตามเครื่องจักร (MD) ปรับปรุงปริมาณผลึกร้อยละ 3.42 เป็น 11.52 ที่อัตราส่วนการดึงร้อยละ 100 ในการเปรียบเทียบกับฟิล์ม PLA/NR ที่ไม่มีการดึงยืด สมบัติเชิงกลของฟิล์มที่อัตราส่วนการดึงร้อยละ 100 ถูกเพิ่มขึ้นเช่นกัน ดังต่อไปนี้ ความต้านแรงดึงเพิ่มขึ้นร้อยละ 68 มอดุลัสของยังเพิ่มขึ้นร้อยละ 24 การยืดตัว ณ จุดขาดเพิ่มขึ้นร้อยละ 81 และความเหนียวเพิ่มขึ้นร้อยละ 114 นอกจากนี้ค่าการซึมผ่านออกซิเจนเพิ่มขึ้นและขึ้นไปถึงค่าสูงสุดเป็นผลมาจากการเกิดช่องว่างขนาดไมโครเมตรและสมบัติการขวางกันแก๊สของโครงสร้างผลึกของ PLA

| | | | |
|---|---|---|---|
| ภาควิชา | วิศวกรรมเคมี | ลายมือชื่อนิสิต | .......................................... |
| สาขาวิชา | วิศวกรรมเคมี | ลายมือชื่อ อ.ที่ปรึกษาวิทยานิพนธ์หลัก | .......... |
| ปีการศึกษา | 2556 | ลายมือชื่อ อ.ที่ปรึกษาวิทยานิพนธ์ร่วม | .......... |

# # 5570230321 : MAJOR CHEMICAL ENGINEERING

KEYWORDS: NATURAL RUBBER (NR) / POLY (LACTIC ACID) (PLA) / PLA NATURAL RUBBER (NR) BLOWN FILM / UNIAXIAL DRAWING / BLOWN FILM CONDITION

THAWATCHAI WONGCHAICHANA: EFFECTS OF FILM BLOWING AND DRAWING CONDITIONS ON PROPERTIES OF POLY(LACTIC ACID)/NATURAL RUBBER FILMS. ADVISOR: ASSOC. PROF. ANONGNAT SOMWANGTHANAROJ, Ph.D., CO-ADVISOR: ASST. PROF. WANCHAI LERDWIJITJARUD, Ph.D., 101 pp.

The aim of this research is to find the relationship between morphology, thermal and mechanical properties, and gas permeation property of poly(lactic acid) (PLA)/natural rubber (NR) films and film blowing conditions, such as take-up ratio (TUR) and blow-up ratio (BUR). The effect of uniaxial drawing at elevated temperature on the properties of drawn films was also investigated. PLA films containing 10 wt% NR were prepared by melt mixing in a twin screw extruder and then blown by a single screw extruder attached to a blown film line. It is found that increasing TUR and BUR shows the deformation of NR and enhanced orientation of polymer chains. The mechanical properties drop significantly, except tensile strength and Young's modulus, which can be explained by a deformation of NR domains from spherical into elliptical after stretching. Moreover, oxygen permeation of PLA/NR blown films increases when TUR increases, resulting from the microvoid formation. Uniaxial drawing of the obtained blown films in machine direction (MD) and transverse direction (TD) at $65^{\circ}$C and drawing rate of 150 mm/min was achieved in a tensile testing machine equipped with a temperature controlled environmental chamber. It is found that increasing drawing ratio in MD improves crystallinity from 3.42% to 11.52% at drawing ratio of 100%. In comparison with the blown PLA/NR films without drawing, the mechanical properties of films at drawing ratio of 100% are also enhanced as follows: tensile strength of 68%, Young' modulus of 24%, elongation at break of 81% and tensile toughness of 114%. Furthermore, the oxygen permeation increases and reaches maximum value as a result of microvoid formation and gas barrier property of crystalline structure of PLA.

| | | | |
|---|---|---|---|
| Department: | Chemical Engineering | Student's Signature | |
| Field of Study: | Chemical Engineering | Advisor's Signature | |
| Academic Year: | 2013 | Co-Advisor's Signature | |

## ACKNOWLEDGEMENTS

## CONTENTS

# LIST OF FIGURES

# LIST OF TABLES

CHAPTER I

INTRODUCTION

## 1.1 General introduction

Poly(lactic acid) (PLA) is a biodegradable thermoplastic polyester produced from various renewable biomass resources such as sugar, corn and beet; therefore, it can reduce waste from the petroleum-based plastic production. PLA has been widely used in many environmentally concerned applications, especially as food packaging, due to its biodegradability, biocompatibility, high transparency and good mechanical properties [1]. However, PLA is brittle and has low crystallization rate. Many recent studies have focused on the improvement of these drawbacks by blending with natural rubber (NR) [2-4]. NR not only is a biodegradable material which is available in Thailand, but also can enhance toughness and crystallization behavior of PLA [3]. Consequently, NR is a good candidate for an improvement of PLA without altering the biodegradability of the final products.

There are several polymers processing to obtain the PLA film for food packaging. Among them, blown film extrusion is an important technique, which can easily control layflat and thickness of film. Furthermore, by adjusting the processing parameters the molecular orientation of PLA during film blowing can be controlled. The molten polymer was drawn in a machine direction (MD), in which it was stretched by the mechanical force from the take-off unit, and in a transverse direction (TD), in which it was stretched by forces generated from an air flow inside a film bubble. The correlation between blown film processing and film properties for

polymers has been extensively studied for low density polyethylene (LDPE) [5], linear low density polyethylene (LLDPE) [6], Polyamide-6/LDPE blends [7] and copolyamide nanocomposites [8]. It is worth noting that this molecular orientation, depending on stretching ratio in MD and TD, has a major effect on the film properties including the degree of crystallinity and, in turn, the mechanical properties and gas permeability of the PLA blown films [9-11]. Unfortunately, a continuous blown film processing and rapid drawing of the molten polymer leads to the incomplete PLA orientation since PLA has slow crystallization rate. Hence, further uniaxial stretching at elevated temperature is a post-processing method to enhance the properties of PLA/NR films.

In this study, the conditions of film blowing technique, *i.e.*, blow-up ratio (BUR) and take-up ratio (TUR) on morphology, mechanical and thermal properties as well as gas permeability of PLA/NR blown films were varied and investigated. Also, uniaxial stretching in MD and TD at elevated temperature was conducted to improve the properties of the PLA/NR films.

**1.2 Objectives**

1. To study the effects of take-up ratio (TUR) and blow-up ratio (BUR) on the morphology, thermal properties, mechanical properties and gas permeability properties of PLA/NR films

2. To examine the effect of uniaxial drawing in machine direction (MD) and transverse direction (TD) on morphology, thermal properties, mechanical properties and gas permeability properties of PLA/NR films

**1.3 Scopes of the research**

　　1. Vary the effects of take-up ratio (TUR = 15, 20 and 25) and blow-up ratio (BUR = 1.6, 1.8 and 2)

　　2. Vary uniaxial drawing condition in machine direction (MD) and transverse direction (TD) to the drawing ratio of 50% and 100%

CHAPTER II

THEORY AND LITERATURE REVIEWS

## 2.1 Poly(lactic acid)/natural rubber blends

In order to overcome the brittleness of PLA, natural rubber (NR) is incorporated as a second phase polymer to enhance the toughness of the blends because NR exhibits high elasticity and high impact strength, and it is also obtained from eco-friendly renewable resource. Various types of NR have been investigated to be blended with PLA such as unmodified NR and chemically modified NR, such as epoxidized natural rubber (ENR) and natural rubber grafted with poly(methacrylate) (NR-$g$-PMMA) [4]. SEM micrographs of PLA/NR blends, as illustrated in Figure 2.1, indicated the phase-separated morphology between PLA and unmodified NR. It was also found that the size of the dispersed phase increased as a function of the concentration of NR due to the coalescence phenomena, which generally occurs in immiscible binary blends. Moreover, the thermal properties measurement from DSC revealed the no shift of glass transition temperature ($T_g$), which confirmed the immiscible PLA/NR blends [2, 3, 12].

It was found that unmodified NR gave the highest toughness of the blends. In contrast, incorporation of chemically modified NR resulted in a smaller domain size of NR in PLA matrix owing to the enhanced interfacial interaction between phases; however, the modified NR is too rigid to absorb the stress leading to poor toughness [4]. The previous studies also suggested that the addition of 10 wt% NR was an

optimal concentration to improve toughness of PLA. At this content, domain size of NR provided optimal balance between its coalescence and its enhancement of the polymer chain mobility as well as the physical and mechanical behavior of material. It was reported that the elongation at break of PLA blends containing 5 wt%, 10 wt% and 20 wt% NR are 48%, 200% and 73%, respectively [3], which can be explained by an increase in domain size as a result of coalescence when NR content increased. As described by the toughening mechanism, toughness ability of rubber decreased significantly when domain size of rubber was larger than the optimum value [13, 14].

(a)

(b)

(c)

(d)
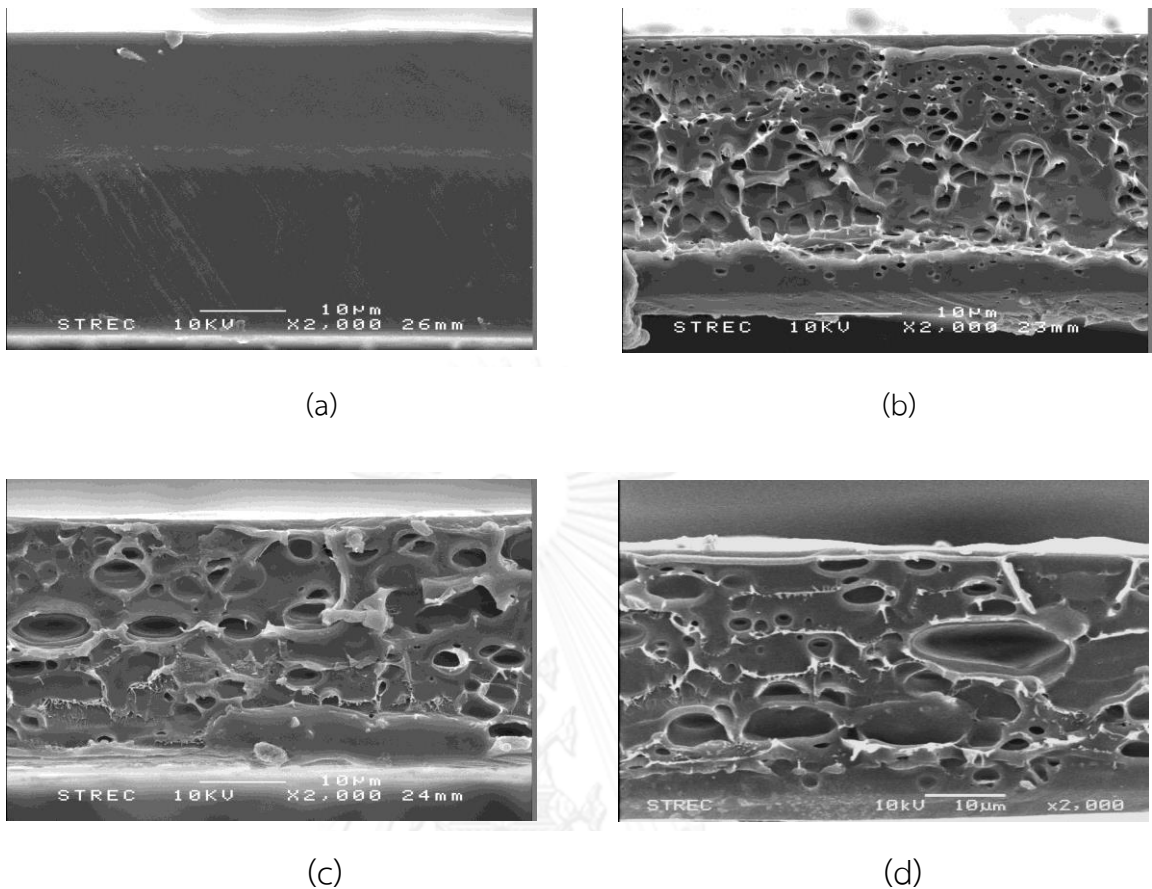
Figure 2.1 SEM micrographs of cross-sectional fractured surfaces of PLA blown films in MD: (a) neat PLA, (b) 5 wt% NR, (c) 10 wt% NR and (d) 15 wt% NR [12]

## 2.2 Blown film extrusion

Blown film extrusion is a process for producing a sheet or film that is better than flat film extrusion in terms of ability to adjust layflat width and film thickness without the need to change hardware. The equipment of blown film line is shown in Figure 2.2. Blown film extrusion is started by adding polymer pellet into a hopper feeder attached to extruder screw (1), which provides heat and shear force to melt polymer pellet into molten polymer and delivers to the blown film die (2). This unit is a thin annular channel to allow molten polymer flowing to the die exit. After that, air cooling ring unit (6) blows a cool air outside and inside to molten polymer. Internal

air keeps molten polymer expanding radially into bubble. Heat in the bubble is removed by external air, while the bubble is kept inflated and going through the lay-flat unit (3) to squeeze the bubble into a film. The take-off unit (4) pulls the film from die exit up to the top of tower. Eventually, the film goes via the deflection rolls at the other side down to the winder (5) where it is wound up to form a cylindrical roll. The important variables that affect the quality of the film are shown in Table 2.1.
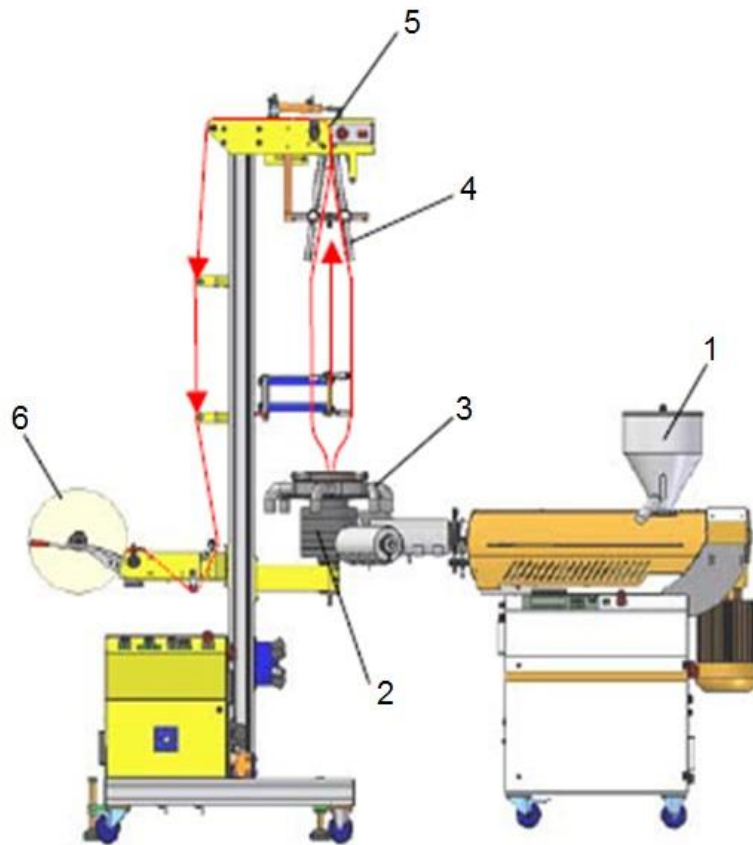


Figure 2.2 The major equipment in a blown film line (Collin, Blown film line BL 180/400E, Germany)

Table 2.1 The important variables on bubble geometry [15]

| Variable to increase | Film thickness | Bubble diameter | Frost-line height |
|---|---|---|---|
| Take-off speed | ↓★ | ↑ | ↑ |
| Screw speed | ↑★ | ↑ | ↑ |
| Cooling speed | ↑ | ↓ | ↓★ |
| Bubble volume | ↓ | ↑★ | ↓ |

★ Primary response

**Take-off speed:** When the take-off speed increases, the thickness of the films decreases because the molten polymer is stretched drastically in MD. As the film travels pass the cooling air more quickly, the height on the bubble where the temperature has dropped to the point of polymer solidification (the frost line) increases. As the frost-line height increases, the small diameter stalk below the frost line lengthens and the air volume in the bubble is displaced more to the top because the bubble contains a fixed volume of air. An increase in bubble volume above the frost line pushes the bubble outward to a higher diameter, contributing to the film thinning.

**Screw speed:** An increase in output of molten polymer from the extruder primarily leads to an increase in film thickness, while the external cooling speed remains constant. Consequently, it takes longer time to remove heat from the film, thus the frost-line height increases. Again, as the frost line moves upward, the bubble diameter increases. The slight thinning effect due to an increase in bubble diameter is far outweighed by an increase in thickness created by greater output rate.

**Cooling air speed:** Heat is suddenly removed from the bubble due to increasing the cooling rate. Since the film reaches solidification temperature sooner, the dominant effect is a decrease in frost line. From the constant internal air volume, the bubble diameter decreases. Moreover, the take-off speed is constant meaning that the film is stretched equally in MD and not significantly in TD. From this reason, film thickness increases as cooling rate is higher.

**Bubble volume:** The bubble volume increases when more air is blown into the bubble, and the diameter increases by stretching more in TD. Therefore, the film is thinner and cooled faster, resulting in a decrease in the frost-line height.

These processing parameters can be changed to a variable factor that can be measured as follows:

**Take-up ratio (TUR):** TUR represents the ratio of the film's velocity ($V_f$) to melt's velocity ($V_m$), TUR = $V_f/V_m$. This quantity indicates the amount of elongation of the film pulling in the MD. The film's velocity is equivalent to the take-off speed and the melt's velocity is the speed of molten polymer as it flows from die exit.

**Blow-up ratio (BUR):** BUR represents the ratio of the bubble diameter ($D_b$) to the outer die diameter ($D_d$), BUR = $D_b/D_d$. This quantity indicates the amount of elongation of film pulling in the TD. The bubble diameter can be either directly measured or calculated from layflat (LF) width ($D_b = 2LF/\pi$).

From the definitions of TUR and BUR, film can be more stretched in MD and TD with increasing TUR and BUR.

In semi-crystalline polymers such as LDPE or LLDPE, an increase in TUR led to an increase in tensile strength and elastic modulus since chain orientation in MD was significantly promoted in the polyethylene chains [5]. However, low tear strength in

MD was observed [16]. On the other hand, as BUR increased chain orientation of polymer in TD increased, resulting in low tear strength in TD [6]. Tear resistance or tear strength, is defined as a resistance to growth of a crack. Consequently, energy of tearing film is lower when the polymer chains are highly oriented in a tear direction.

The structures of polyamide-6/LDPE blends were oriented predominantly in MD by the effect of TUR, which produces the anisotropic material as well as enhance tensile strength of films [7]. For copolyamide nanocomposites, increasing stretching ratio strongly affected the silicate re-aggregation and polyamide crystal phase changed into the mesomorphic $\beta$-form, which has lower stiffness and tensile strength than those of the stable $\alpha$-phase, during the single-bubble blown film processing. Besides, barrier properties of film increased due to longer diffusive path that gas must travel in the presence of filler [8].

Briefly, the stretching during blown film processing does not have the effect of orientation in the amorphous phase to account for the difference in film properties [16, 17].

## 2.3 Drawing of PLA film

PLA is a slow crystallizing polymer like poly(ethylene terephthalate) (PET) [9]. According to the previous literatures, drawing films above $T_g$ can increase the degree of crystallinity of PLA films. In the drawing processes, PLA film was stretched at temperature above $T_g$ and below 80°C to minimize crystallization from thermal effect during the drawing of films [11] and this temperature range is the optimum temperature window as PLA film exhibits ideal stress strain curves without a pronounced yielding region and exhibiting strain hardening [18]. In addition, it was

found that the ratio of drawing to annealing temperature strongly influenced the crystallization [9-11, 19] and chain relaxation of PLA [10]. Namely, drawing rate and heat setting time slightly affected crystallization [10, 11]. Structural model for uniaxial constant width drawing is demonstrated in Figure 2.3. The chains become oriented along stretching direction, which resulted in the improved modulus and tensile strength [10].

Drawing   direction
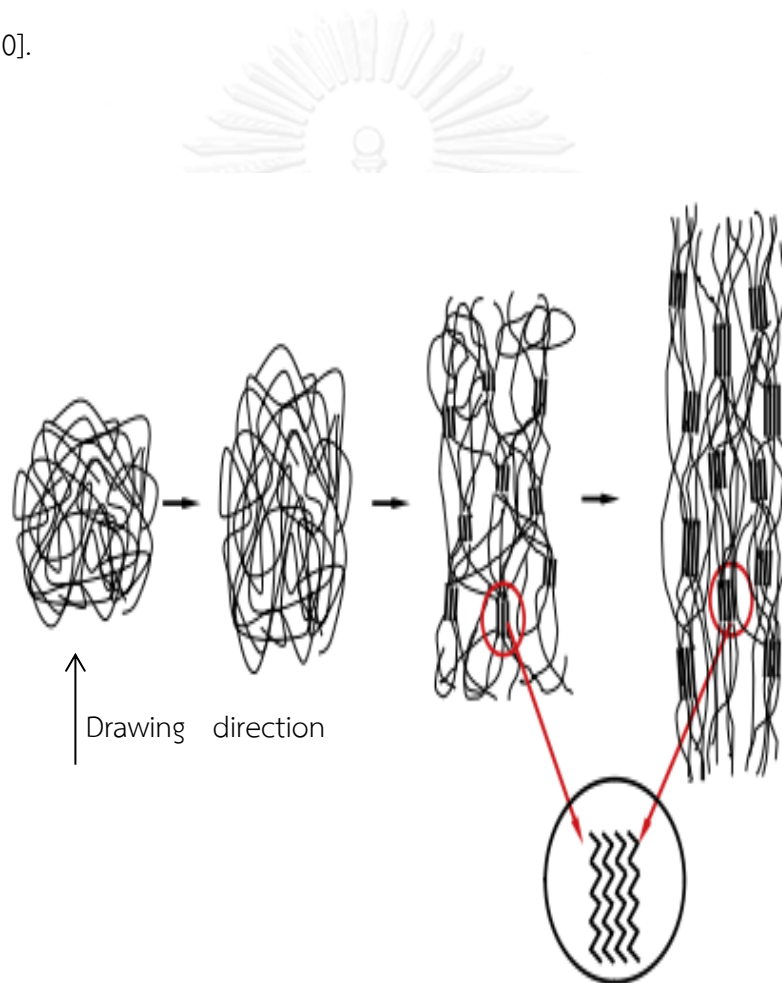
Figure 2.3 Structural model for uniaxial constant width drawing [9]

CHAPTER III

EXPERIMENTS

## 3.1 Materials

Poly(lactic acid) (PLA; grade: 2003D) was purchased from NatureWorks$^{®}$, USA. Commercial NR (grade: air dried sheet) was purchased from Hi Karn Yang Rayong, Thailand.

## 3.2 Preparation of PLA/NR blown films

The schematic diagram of the experiments in this study is demonstrated in Figure 3.1. PLA blends containing 10 wt% NR were prepared by melt blending in a co-rotating twin screw extruder (LabTech, Thailand; L/D = 40 and D = 20 mm). NR was cut into the same size as PLA pellet in on order to obtain the good dispersion of NR domain in PLA matrix during melt mixing The processing temperatures were 180-195°C from hopper feeder to die and the screw speed was 80 rpm. The extrudate was quenched in a water bath and then cut by a pelletizer. Eventually, the pellet of PLA/NR were dried at 60°C overnight in an oven and kept in PE zipped-lock plastic bag with silica gel inside to avoid the moisture absorption.

Blown films were obtained by using a single screw extruder (Collin; L/D = 25, D = 20 mm, die diameter 50 mm and die gap 0.8 mm) attached to blown film die (Collin, Blown film line BL 180/400E, Germany). The processing temperature profile was 180-210°C and a screw speed was 75 rpm. According to the previous work done by our group, PLA/NR were usually processed at TUR = 20 and BUR = 1.8 because it

is found that these film blowing conditions give the suitable thickness and layflat for fresh produces packaging. Furthermore, the varied TUR and BUR values should also provide the films with smooth surface in order to acquire reliable and satisfactory data, particularly mechanical properties. From our trial and error, PLA/NR films were collected at TUR = 15, 20, and 25 at fixed BUR, and BUR = 1.6, 1.8 and 2.0 at fixed TUR.

```
                          ┌─────────────────────┐
                          │  Prepare PLA/NR     │
                          │  films at 10wt% NR  │
                          └─────────────────────┘
```

Prepare PLA/NR films at 10wt% NR

Film blowing

Film drawing

Three TUR at fixed BUR

Three BUR at fixed TUR

PLA/NR films from the lowest TUR

PLA/NR films from the lowest BUR

Characterization

Uniaxial drawing to ratio 50% and 100% MD

Uniaxial drawing to ratio 50% and 100% TD

Morphology

Mechanical properties
- Tensile testing
- Impact testing
- Tear testing

Characterization

Gas permeability
- OP
- WVP

Mechanical properties
- Tensile testing

Gas permeability
- OP

Thermal properties

Thermal properties

Figure 3.1 Experimental procedure

**3.3 Condition of uniaxial drawing of PLA/NR films**

PLA/NR films fabricated from the lowest values of TUR were used for uniaxial drawing in MD and the films from the lowest values of BUR were used for uniaxial drawing in TD. Uniaxial drawing was performed by using a universal testing machine with a temperature controlled environmental chamber (Instron model 5567, USA). The specimen size of 20 mm wide and 50 mm long were kept in a chamber at 65℃ for 2.5 min before uniaxial drawing with a stretching rate 150 mm/min. The specimens were uniaxially stretched to 50% and 100% of original length.

**3.4 Characterization of PLA/NR films**

**3.4.1 Morphology**

The morphology of PLA/NR films in MD and TD were observed using a scanning electron microscope (SEM, JEOL JSM 5410 LV). All samples were quenched in liquid nitrogen and fractured to obtain the cross-sectional surfaces. Samples were stained with osmium tetroxide vapor and coated with gold before the observation to increase the contrast between PLA matrix and NR domains and to prevent the electrical discharge. The average size and size distribution of rubber domain size were determined by image analysis software (ImageJ software, Rasband, W.S., ImageJ, U.S. National Insitutes of Health, Bethesda, Maryland, USA). Typically, about 300 domains were analyzed per sample and the average Feret's diameter was calculated.

### 3.4.2 Thermal properties

Thermal properties of PLA/NR films were evaluated using a differential scanning calorimeter (Perkin Elmer, Diamond DSC, USA). About 10 mg of samples were sealed in an aluminum pan and then heated from $50^{\circ}$C to $200^{\circ}$C at a heating rate of 10°C/min. The samples were hold at this temperature for 5 min to eliminate the thermal history and residual PLA crystallites. Then, the samples were cooled to $50^{\circ}$C at a cooling rate of $10^{\circ}$C/min and reheated to $200^{\circ}$C at a heating rate of $10^{\circ}$C/min. The DSC measurements were operated under nitrogen atmosphere to avoid the thermal oxidative degradation. The thermal properties, *i.e.*, glass transition temperature ($T_g$), cold crystallization temperature ($T_{cc}$) and melting temperature ($T_m$), of PLA/NR films were determined from the heat flow. The degree of crystallinity (%$X_c$) was calculated as follows:

$$\%X_c = \frac{(\Delta H_m - \Delta H_{cc})}{(\Delta H_m^0 \times \Phi)} \times 100 \qquad (3.1)$$

where $\Delta H_m$ and $\Delta H_{cc}$ are the enthalpies of the melting and apparent cold crystallization of PLA/NR films, respectively. $\Delta H_m^0$ is the enthalpy of melting of 100% crystalline of PLA (93 J/g) [20]. $\Phi$ is a weight fraction of PLA in the samples [2].

### 3.4.3 Mechanical properties

Tensile testing of films was carried out according to ASTM D882 using a universal testing machine (Instron model 5567, USA) with a load cell of 1 kN and a crosshead speed of 12.5 mm/min. Rectangular samples from blown films (10 mm × 100 mm) and from drawn films (10 mm × 50 mm) were used for measurements.

Tensile strength, Young's modulus, elongation at break and tensile toughness of films were collected.

Impact testing of films was performed using an impact testing machine (Digital tester, Toyoseiki, Japan) according to ASTM D 3420. The pendulum energy was 1.5 J and sample was 100 mm × 100 mm.

Tear testing was conducted according to ISO 6383 using a tear testing machine (Digital Elmendorf type tearing tester model SA, SA-W, Toyoseiki, Japan). The pendulum of 16 N and rectangular samples of 63 mm × 75 mm were used.

In all measurements of mechanical properties, at least five specimens of samples were tested to obtain a mean value.

### 3.4.4 Gas Permeability

Oxygen permeation (OP) of PLA/NR films was determined using OX-TRAN[®] model 2/21 (Mocon, USA) at 23 ℃ and 90% relative humidity with an oxygen flow rate of 40 cm³/min according to ASTM F 1927. The area of specimens from blown films and from drawn films was 100 cm² and 5 cm², respectively.

Water vapor permeation (WVP) of PLA/NR films was recorded using PERMATRAN-W® model 398 (Mocon, USA) at 37.8 ℃ and 90% relative humidity with a nitrogen flow rate of 250 cm³/min according to ASTM F 1249. The area of specimens from blown films was 50 cm².

## CHAPTER IV

## RESULTS AND DISCUSSION

This study was designed to examine the relationship between the properties of PLA/NR blown films and film blowing conditions, i.e., blow-up ratio (BUR) and take-up ratio (TUR). The properties of films after uniaxial drawing at elevated temperature were also investigated.

### 4.1 Film blowing

PLA was blended with 10 wt% air dry sheet NR in a co-rotating twin screw extruder. Further, the blends were blown at different conditions. Eventually, the properties of PLA/NR blown films were characterized and discussed as follows:

#### 4.1.1 Effect of Take-up ratio (TUR)

##### *4.1.1.1 Morphology*

In order to investigate the effect of TUR on morphology of NR domains, including size and shape, in PLA/NR blown films, the blown film were cryofractured in liquid nitrogen and the cross-sectional fractured surfaces of blown films in TD were observed by SEM as illustrated in Figure 4.1. It is worth mentioning that the films stained with osmium tetroxide vapor shows the white matter of NR. The cross-sectional fractured surfaces in MD are insignificantly different as shown in

Appendix C. SEM micrographs demonstrate that NR domains are non-uniformly dispersed in PLA matrix due to the immiscibility between continuous PLA matrix and dispersed NR phase [2-4, 12, 21, 22]. Remarkably, interfacial adhesion between PLA and NR is relatively poor as can be seen by the debonding of NR domains. From the size distribution of NR domains, it is suggested that the average sizes of NR in the films prepared at TUR = 15, 20 and 25 are 7.97±1.38 µm 9.81±1.33 µm and 11.51±1.28 µm, respectively. Although the size of NR are insignificantly different, the shape of NR from the films prepared at TUR = 15 seems to be more spherical, whereas most NR domains in those prepared at TUR = 25 are ellipsoidal, which can be explained by that the mechanical force from the nip roll unit in MD greatly deforms the NR domains. This phenomenon is evidenced by SEM of the surfaces shown in Figure 4.2.
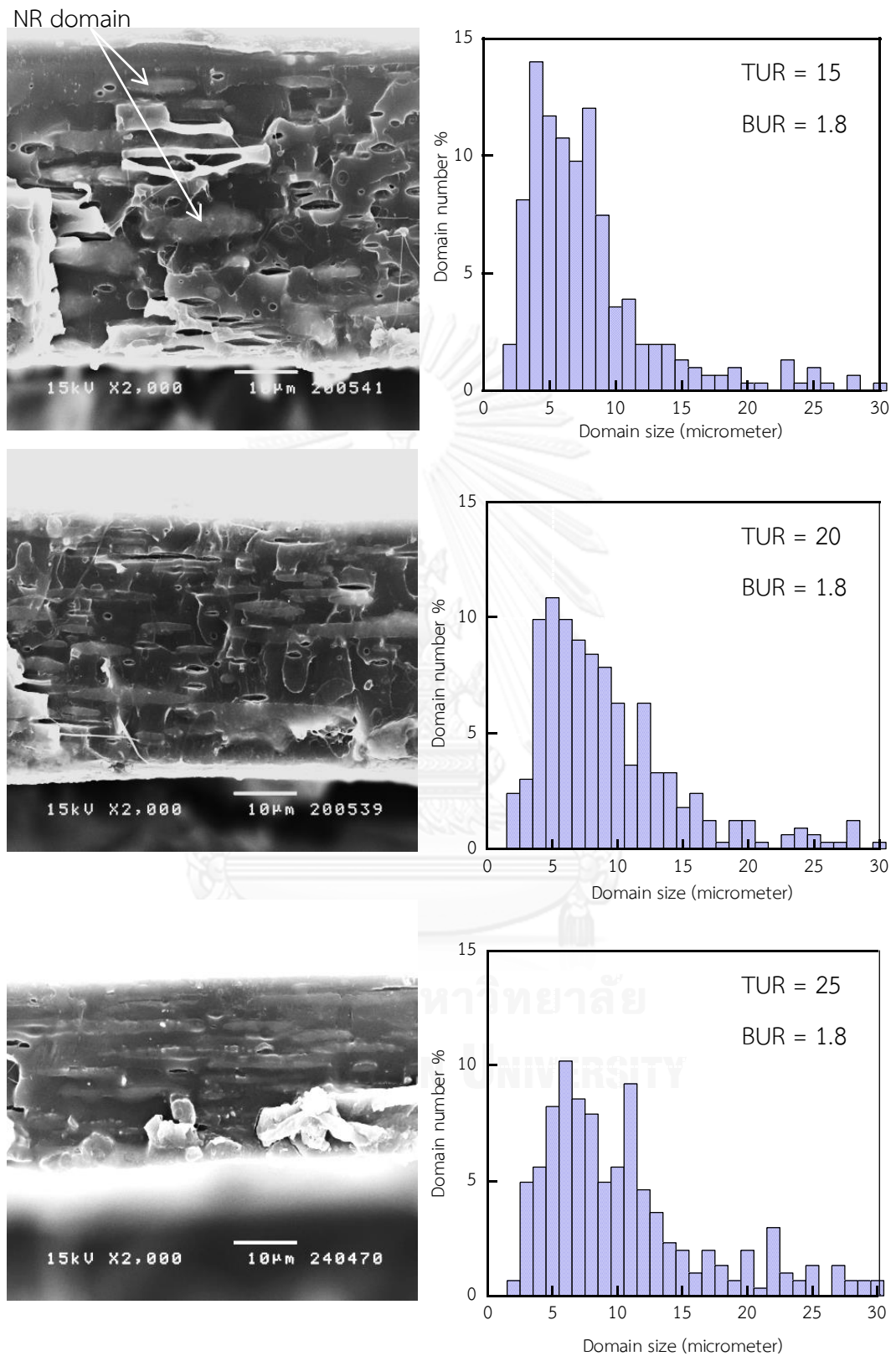
Figure 4.1 Morphology of cross-sectional fractured surfaces in TD and size distribution of NR domain in the PLA/NR films for different TUR at fixed BUR = 1.8

a

b

c

Machine direction (MD)
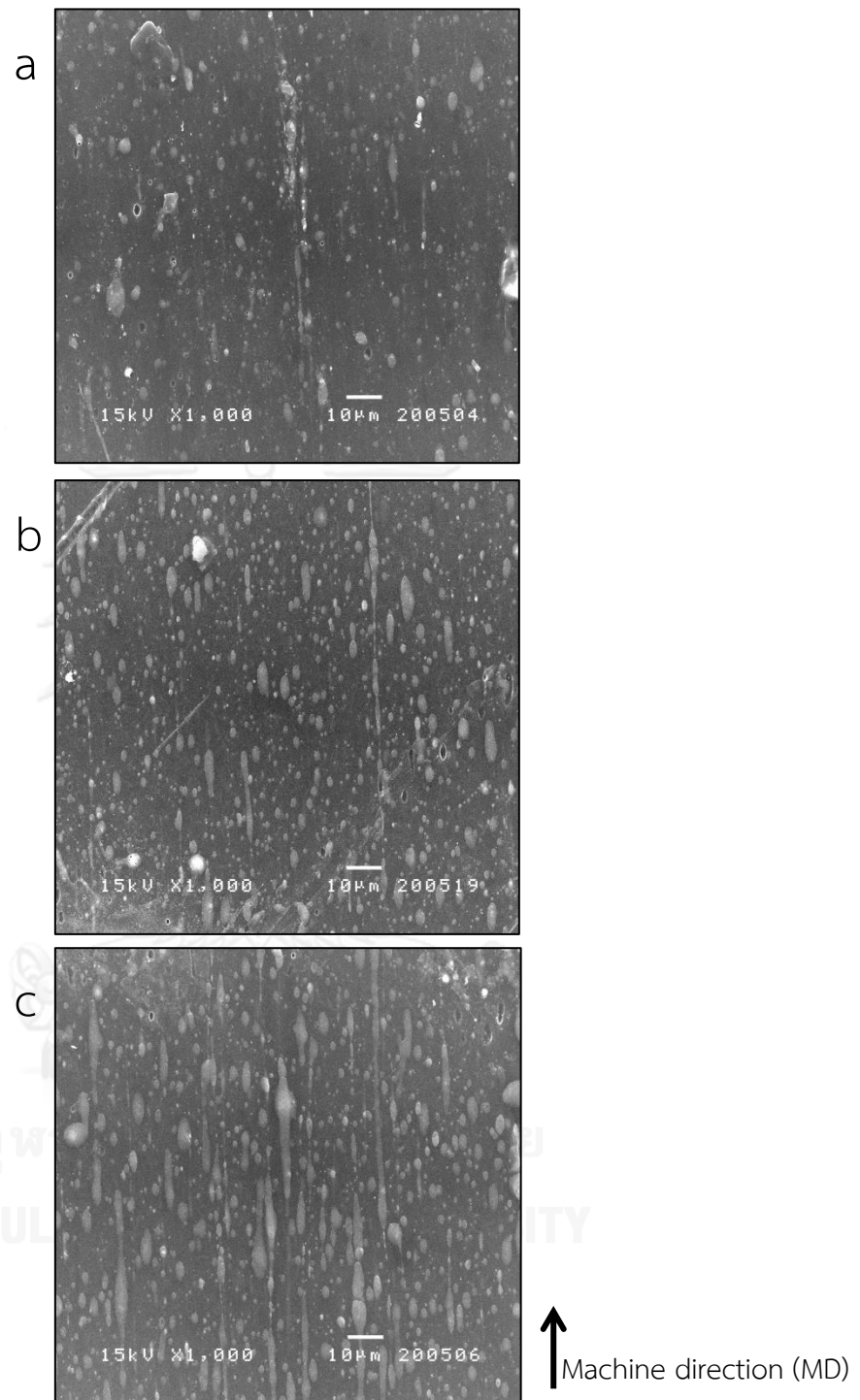
Figure 4.2 SEM micrographs of surfaces of PLA/NR films for different TUR at fixed
BUR = 1.8 (a) TUR = 15, (b) TUR = 20 and (c) TUR = 25

*4.1.1.2 Thermal properties*

In order to investigate the thermal properties and crystallization behavior of PLA/NR blown films, dynamic DSC measurements were performed. DSC thermograms of PLA/NR blown films at different TUR in the first and second heating scans are demonstrated in Figure 4.3. The values of cold crystallization temperature ($T_{cc}$), melting temperature at lower temperature ($T_{m1}$) and high temperature ($T_{m2}$), enthalpy of cold crystallization ($\Delta H_{cc}$), and degree of crystallinity %$X_c$ determined from DSC profiles are tabulated in Table 4.1. It is found that thermal properties of PLA/NR films insignificantly change with the increase of TUR. Interestingly, $\Delta H_{cc}$ of PLA/NR blown films slightly decreases when TUR increases. The considerable distinction between first and second heating is clearly observed. In the first DSC heating scan, $\Delta H_{cc}$ theoretically refers to the latent energy for converting the remaining amorphous structure from crystallization during processing to solid crystalline structure. The decrease in $\Delta H_{cc}$ might be due to a larger amount of polymer chains oriented [23] during film blowing with increasing TUR. On the other words, the polymer chains in an amorphous phase can easily be transformed into a crystalline structure. From the second DSC heating scan, it is noticed that blown film processing has the strong effect on the exothermic peak of cold crystallization of PLA/NR blown films, in which a peak of cold crystallization is broader and $T_{cc}$ shifts to higher temperature in comparison to that obtained from first heating scan. These behaviors imply that stretching the films by nip roll unit leads to the pronounced orientation of polymer chains in MD as a result of stress-induced crystallization [9]. Finally, the DSC profiles of PLA/NR blown films from first and second heating scans display distinct melting peaks. The melting peak at lower temperature ($T_{m1}$)

represents the imperfect crystalline structure of PLA, which was molten and then rearranged into a more perfect crystalline form that is detected at higher temperature ($T_{m2}$) [24-27].
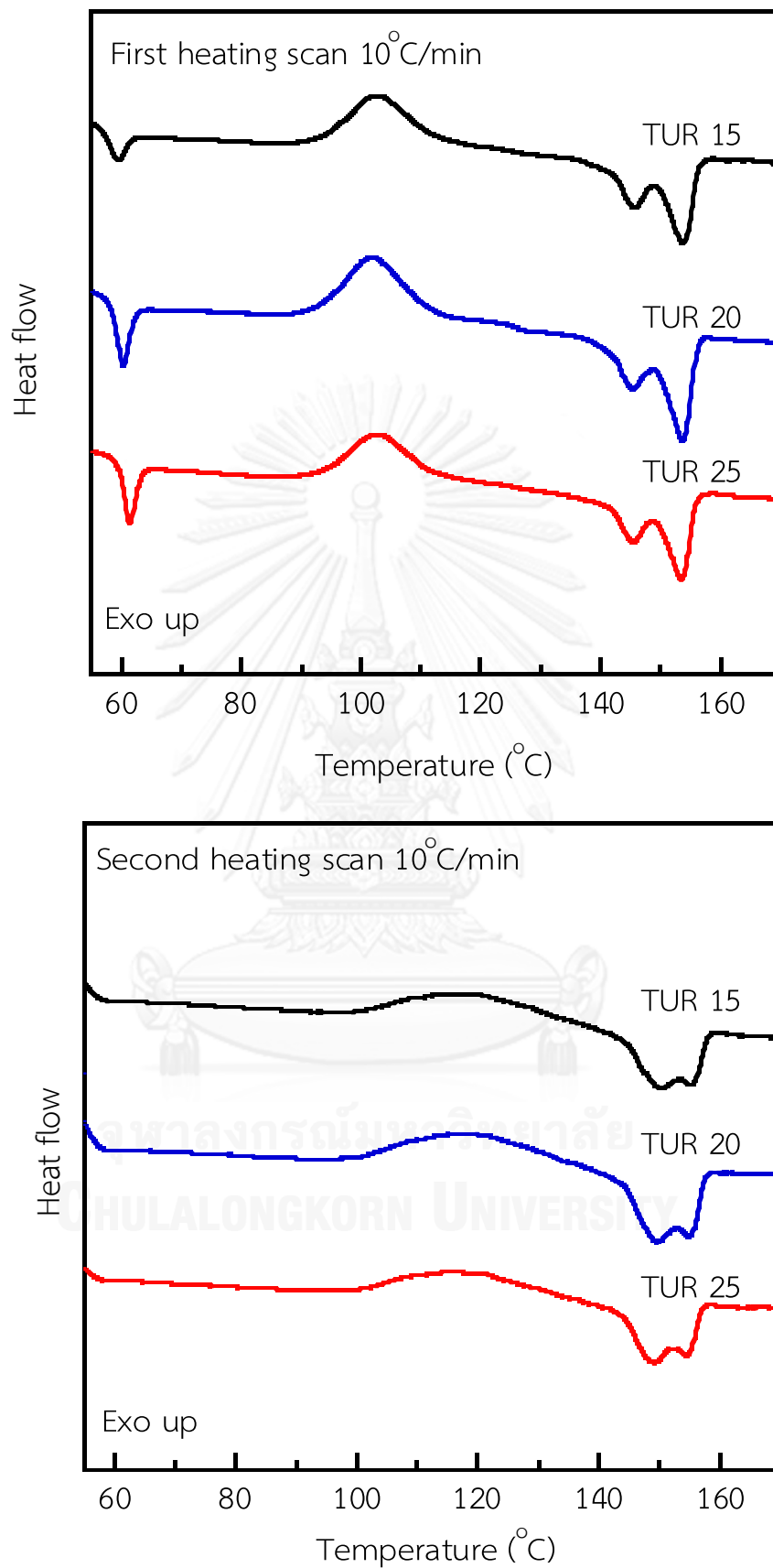
Figure 4.3 DSC thermograms of PLA/NR films for different TUR at
fixed BUR = 1.8

Table 4.1 Thermal properties of PLA/NR films for different TUR determined from the

   first DSC heating scan at fixed BUR = 1.8

| Samples | $T_g$ ($^o$C) | $T_{cc}$ ($^o$C) | $T_{m1}$ ($^o$C) | $T_{m2}$ ($^o$C) | $\Delta H_{cc}$ (J/g) | $\Delta H_m$ (J/g) | %$X_c$ |
|---------|------|------|------|------|------|------|------|
| TUR = 15 | 58.4 | 102.7 | 145.4 | 153.6 | 16.74 | 19.60 | 3.42 |
| TUR = 20 | 59.3 | 101.9 | 145.2 | 153.3 | 16.00 | 18.89 | 3.46 |
| TUR = 25 | 60.6 | 102.7 | 145.1 | 153.5 | 15.76 | 18.64 | 3.44 |

Table 4.2 Thermal properties of PLA/NR films for different TUR determined from the

   second DSC heating scan at fixed BUR = 1.8

| Samples | $T_g$ ($^o$C) | $T_{cc}$ ($^o$C) | $T_{m1}$ ($^o$C) | $T_{m2}$ ($^o$C) | $\Delta H_{cc}$ (J/g) | $\Delta H_m$ (J/g) | %$X_c$ |
|---------|------|------|------|------|------|------|------|
| TUR = 15 | 59.8 | 119.8 | 150.3 | 155.8 | 18.08 | 18.08 | 0.00 |
| TUR = 20 | 60.0 | 120.0 | 149.8 | 155.3 | 17.78 | 17.78 | 0.00 |
| TUR = 25 | 60.8 | 116.2 | 149.1 | 154.8 | 18.70 | 18.70 | 0.00 |

### *4.1.1.3 Mechanical properties*

At the later stage of tensile testing before breaking, the film specimens show the stress-whitening (Figure 4.4), resulting from crazing [28]. Principally, the dispersed NR acts as stress concentrator magnifying the stress in the matrix around NR. When the internal stress overcomes the interfacial adhesion between phases, the NR domains are debonded and microvoids formation at the interfacial boundary is noticed. Moreover, the stress-whitening occurs because the difference in refractive index of air in the microvoids and that of polymer chains, leading to the light scattering inside the specimens.

The effect of TUR on the mechanical properties of PLA/NR blown films is also investigated and shown in Figure 4.5 to Figure 4.11. The mechanical properties in both MD and TD decrease with increasing TUR. These results could be explained by the change in morphology of NR. As increasing TUR, the NR domains are lengthened, forming ellipsoid. According to the previous literatures [2, 4, 12], the mechanical properties is crucially related to the domain size of NR in the PLA/NR blown films. In the tensile testing, NR domain is less effective to absorb and dissipate energy as the domain size of NR phase increases [29] (as TUR increases), resulting in dropped elongation at break (Figure 4.8) and toughness (Figure 4.9). This mechanism is explainable during impact testing as shown in Figure 4.10. A steady Young's modulus for all films implies that the samples have similar rigidity in spite of the change in shape of dispersed phase.

It is found that the mechanical properties, excluding tear strength, in MD are better than those in TD, which can be described by the prominent polymer chain orientation and direction of the deformed NR particles in the film stretching direction (MD). Therefore, the orientation of most polymer chains and arrangement of domain dispersion hinders the required force to break the samples, leading to high tear strength in TD with respect to that in MD, as shown in Figure 4.11. The orientation of PLA chain and NR domains in PLA/NR films is schematically illustrated in Figure 4.12.

Figure 4.4 The photograph of deformed specimens after tensile testing
of PLA/NR film



Figure 4.5 Stress - strain curve of PLA/NR films at fixed BUR = 1.8
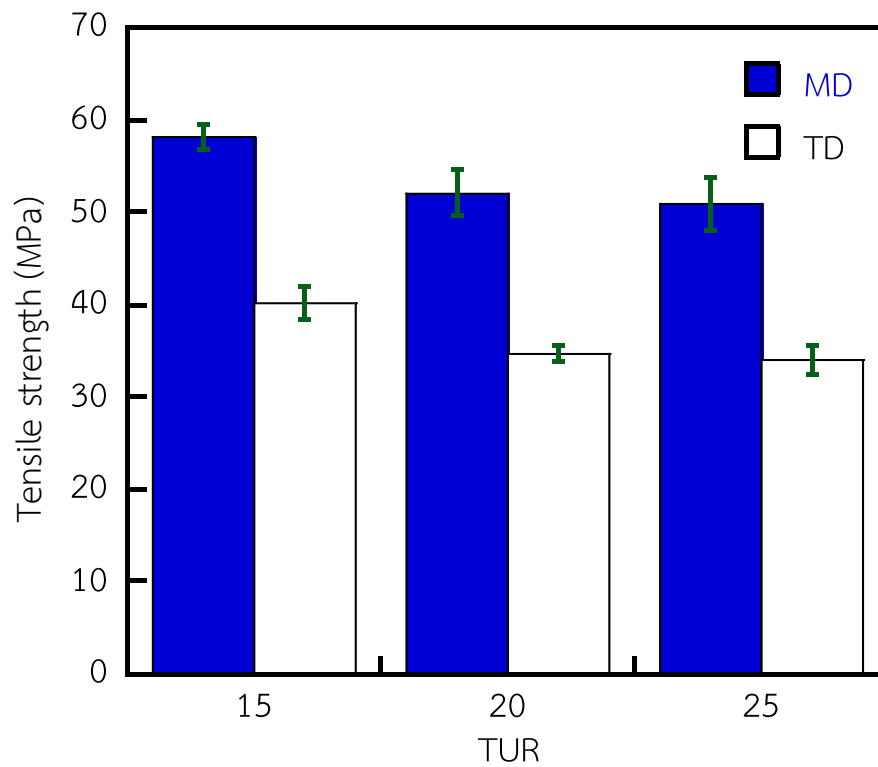
Figure 4.6 Tensile strength of PLA/NR films at fixed BUR = 1.8



Figure 4.7 Young's modulus of PLA/NR films at fixed BUR = 1.8

Figure 4.8 Elongation at break of PLA/NR films at fixed BUR = 1.8
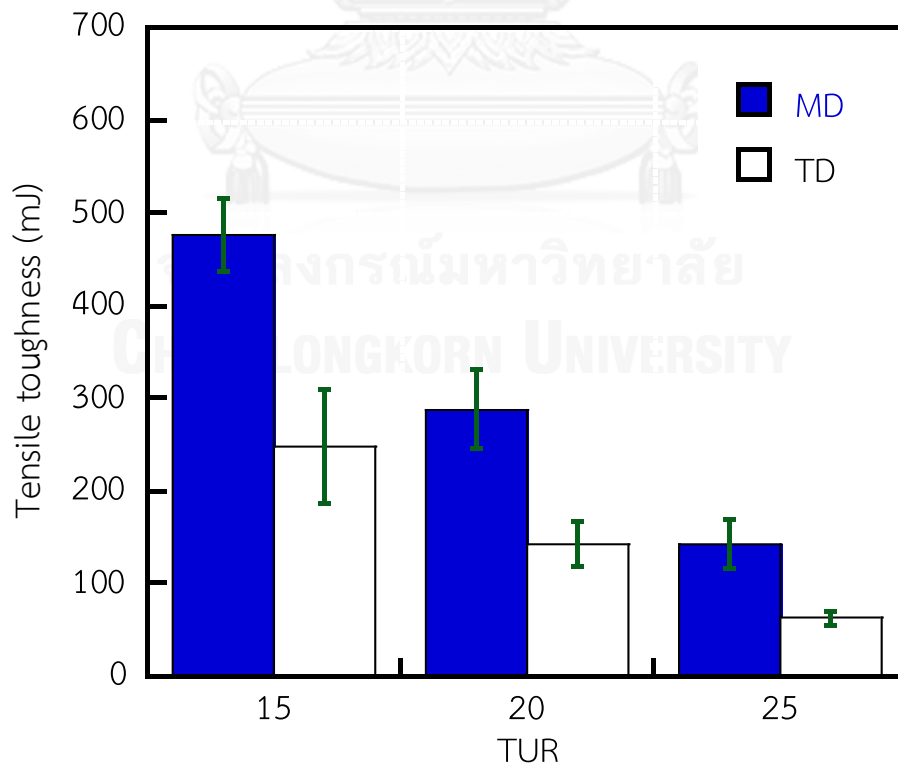


Figure 4.9 Tensile toughness of PLA/NR films at fixed BUR = 1.8
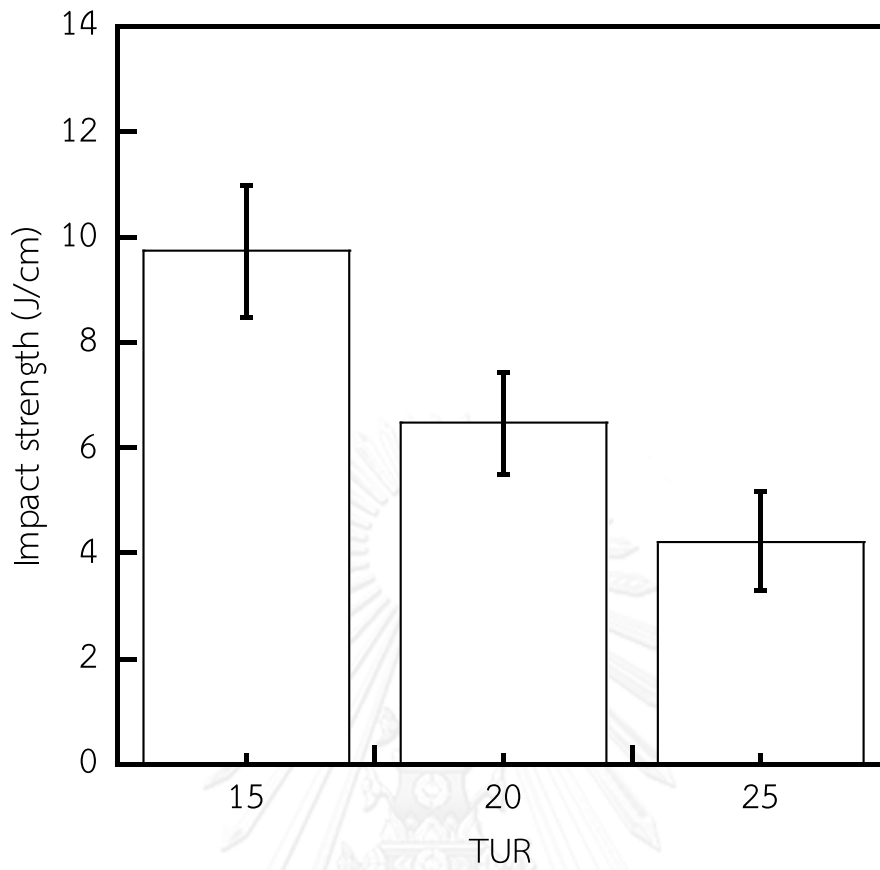
Figure 4.10 Impact strength of PLA/NR films at fixed BUR = 1.8



Figure 4.11 Tear strength of PLA/NR films at fixed BUR = 1.8
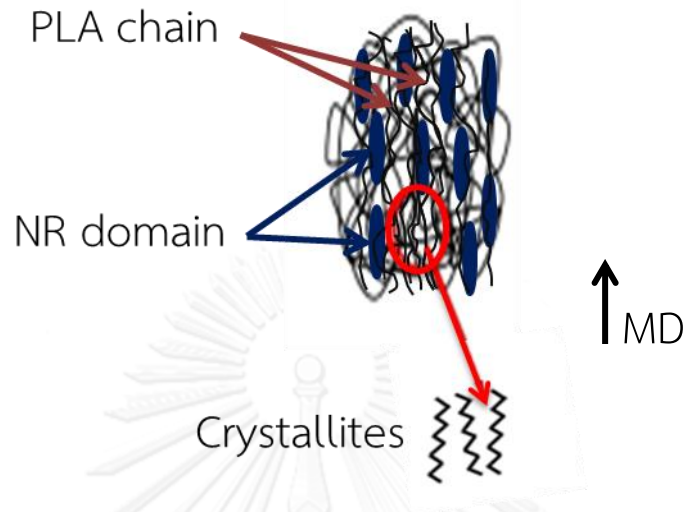
Figure 4.12 Schematic drawing of orientation of PLA chain and NR domain
in PLA/NR films

### 4.1.1.4 Gas Permeability

The values of oxygen permeation (OP) and water vapor permeation (WVP) of the PLA/NR blown films are shown in Figure 4.13. It can be seen that OP slightly increases when TUR increases because of the microvoid formation. As discussed earlier, the dispersed NR acts as stress concentrator. In principle, stress is much higher as the NR domain becomes larger. From this reason, the films prepared at TUR = 25, having the largest NR size in our study, have the highest content of microvoids created at the boundary of NR as a result of debonding when the internal stress overcomes the poor interfacial adhesion between dispersed NR and continuous PLA matrix. Hence, the gas easily passes through these microvoids in comparison to the PLA chains or amorphous NR, leading to enhanced OP. As TUR increases, WVP does not significantly change because the microvoids occurred in the

PLA phase and the fraction of polar PLA in the films is higher than non-polar NR [20]. Therefore, while polar water vapor passes through the microvoids in the PLA phase, it can be trapped between the free volume of PLA since PLA and water vapor have similar polarity. These two phenomena are the competitive mechanism taking place simultaneously. Conversely, oxygen passing through microvoids and oxygen passing through amorphous NR are irrelevantly.
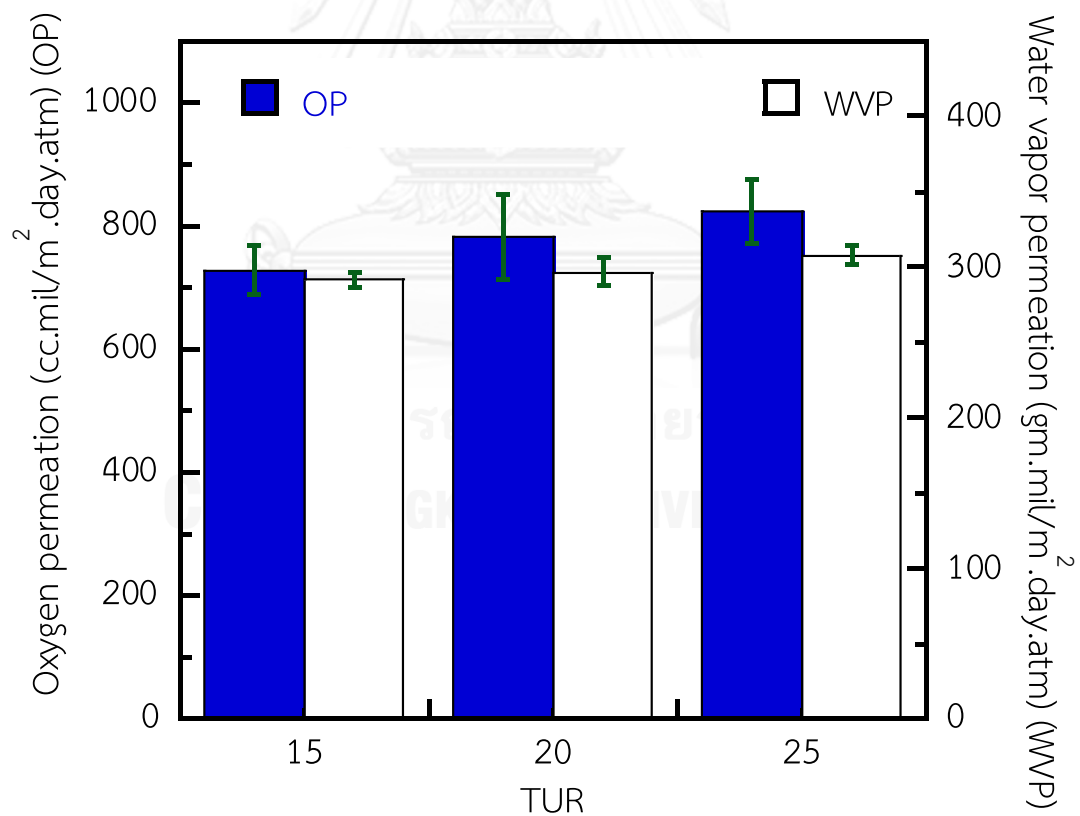


Figure 4.13 Oxygen and water vapor permeation of PLA/NR films at fixed BUR = 1.8

**4.1.2 Effect of Blow-up ratio (BUR)**

*4.1.2.1 Morphology*

Morphology of cross-sectional fractured surfaces of PLA/NR blown films in MD at different BUR is also observed by SEM analysis, as illustrated in Figure 4.14. It is found that the NR domains are lengthened in TD which is conceivably because NR domains were drawn by the pneumatic force from an air flow inside a film bubble when BUR increases. However, deformation of NR domains in TD is less than that in MD since the stretching force in MD by nip roll is usually higher than stretching force in TD generated by air flow.
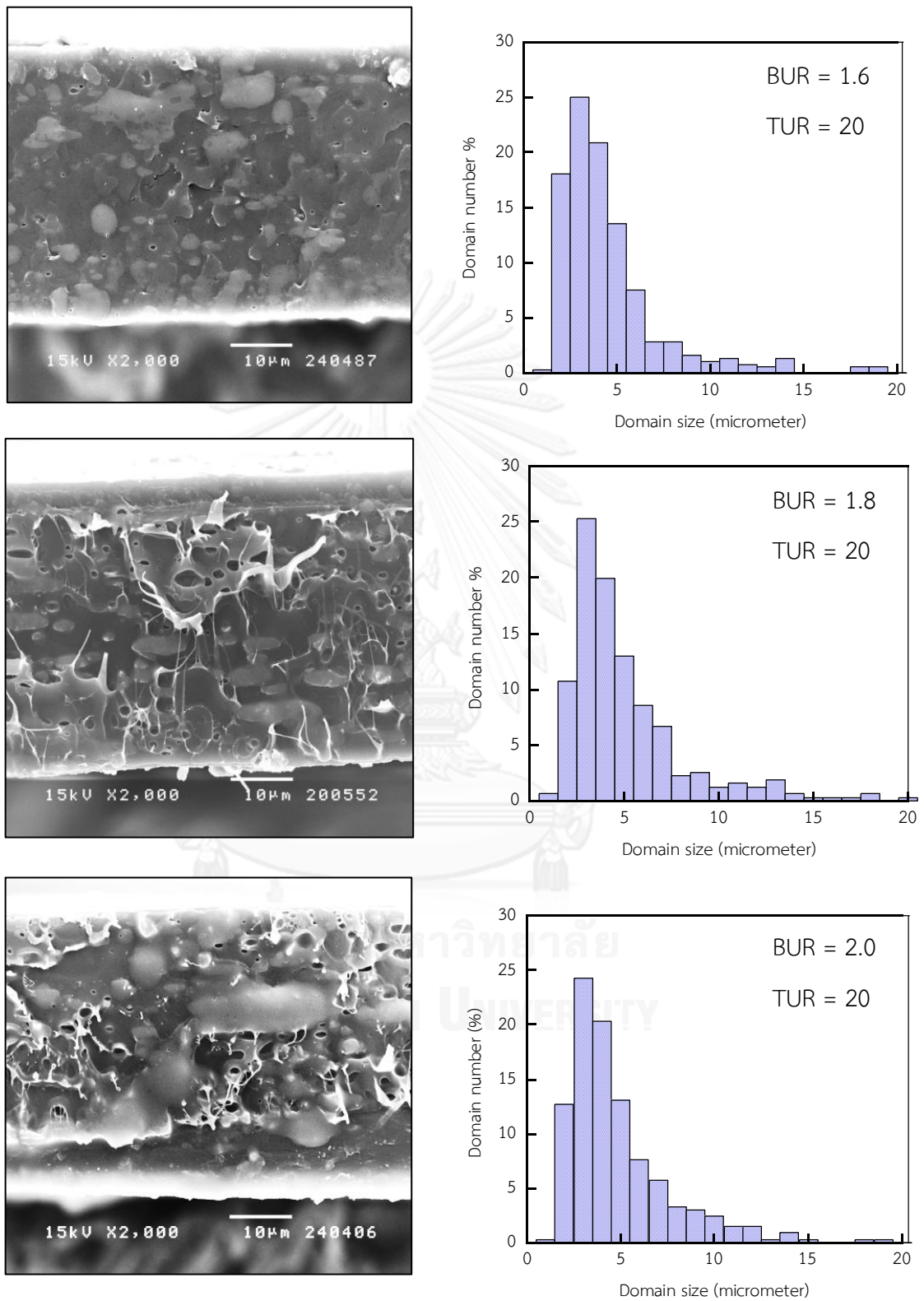
Figure 4.14 Morphology of cross-sectional fractured surfaces in MD and size distribution of NR domain in the PLA/NR films for different BUR at fixed TUR = 20

### 4.1.2.2 Thermal properties

As seen in Figure 4.15 and Table 4.3, thermal properties, *i.e.*, $T_{cc}$, $\Delta H_{cc}$ and $\%X_c$, of PLA/NR blown films are fairly constant. It is probably because low stretching forces generated from an air flow inside a film bubble was not high enough to orient PLA chains in TD.
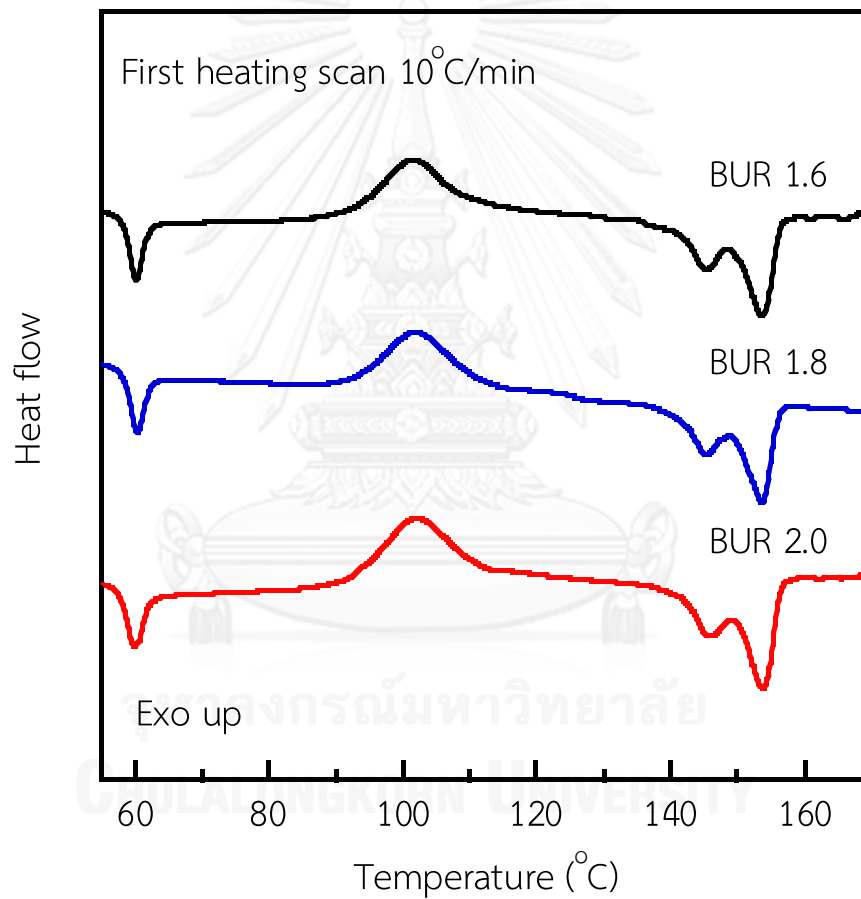


Figure 4.15 DSC thermograms of the PLA/NR films for different BUR at fixed TUR = 20

Table 4.3 Thermal properties of PLA/NR films for difference BUR determined from

the first DSC heating scan at fixed TUR = 20

| Samples | $T_g$ ($^o$C) | $T_{cc}$ ($^o$C) | $T_{m1}$ ($^o$C) | $T_{m2}$ ($^o$C) | $\Delta H_{cc}$ (J/g) | $\Delta H_m$ (J/g) | $\%X_c$ |
|---|---|---|---|---|---|---|---|
| BUR = 1.6 | 59.1 | 101.4 | 145.2 | 153.9 | 16.11 | 19.02 | 3.47 |
| BUR = 1.8 | 59.3 | 101.9 | 145.2 | 153.3 | 16.00 | 18.89 | 3.46 |
| BUR = 2.0 | 59.1 | 102.0 | 145.6 | 153.7 | 16.15 | 19.04 | 3.46 |

### *4.1.2.3 Mechanical properties*

Mechanical properties of PLA/NR blown films at different BUR are shown in Figure 4.17 to Figure 4.22 It is worth mentioning that the mechanical properties in TD exhibit the similar trends to those in MD. Moreover, the mechanical properties at varying BUR (fix TUR) also show the similar fashions to those varying TUR (fix BUR) discussed in the previous section. Namely, Tensile strength and Young's modulus are almost constant, while tensile toughness, elongation at break, impact strength and tear strength decrease as a function of BUR. These results can be explained by the reduction of interfacial area between dispersed NR domains and PLA matrix, resulting from a change in morphology of NR from sphere to ellipsoid.
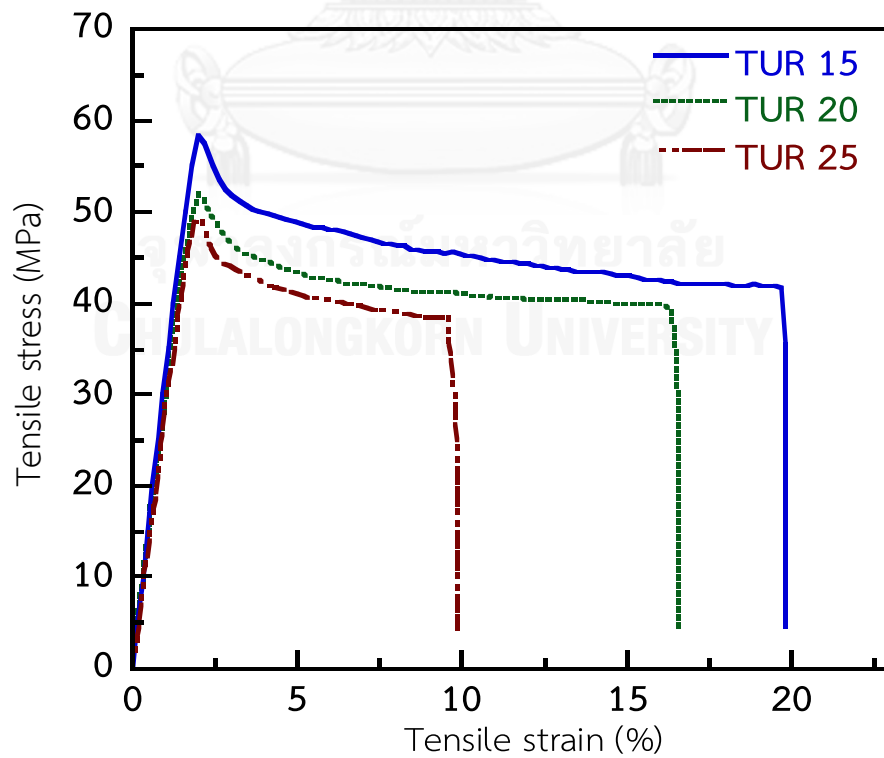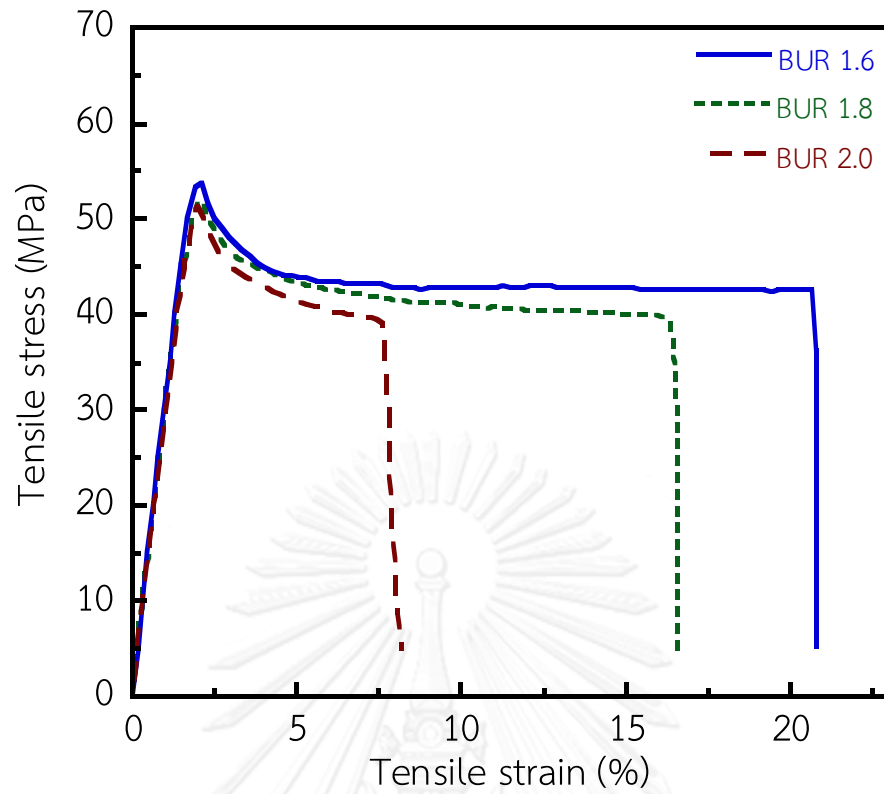
Figure 4.17 Stress - strain curve of PLA/NR films at fixed TUR = 20
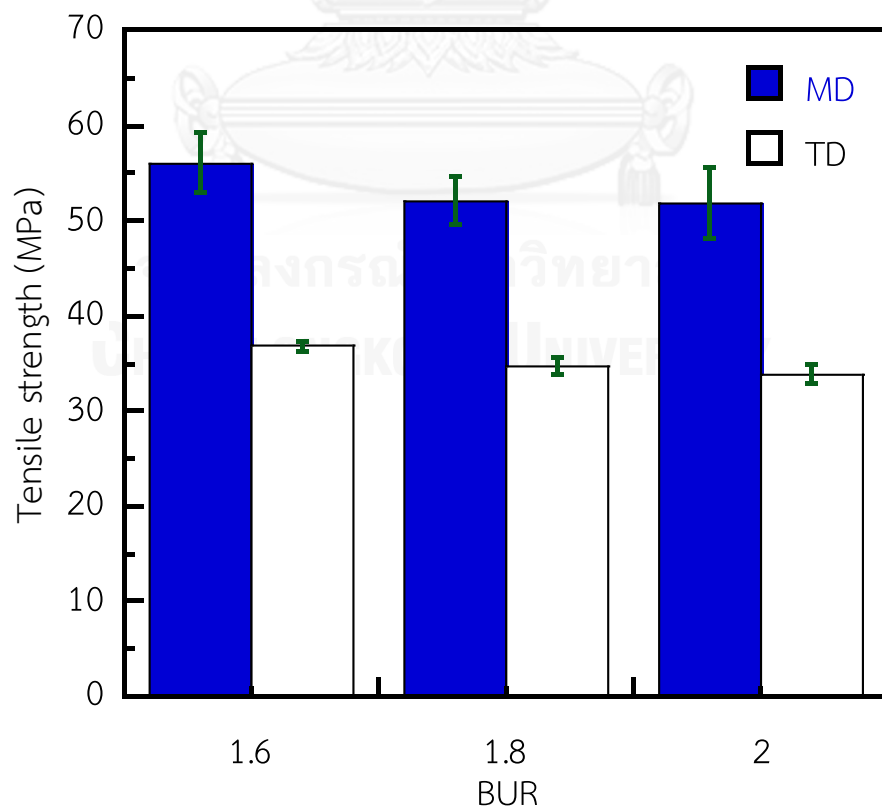


Figure 4.16 Tensile strength of PLA/NR films at fixed TUR = 20
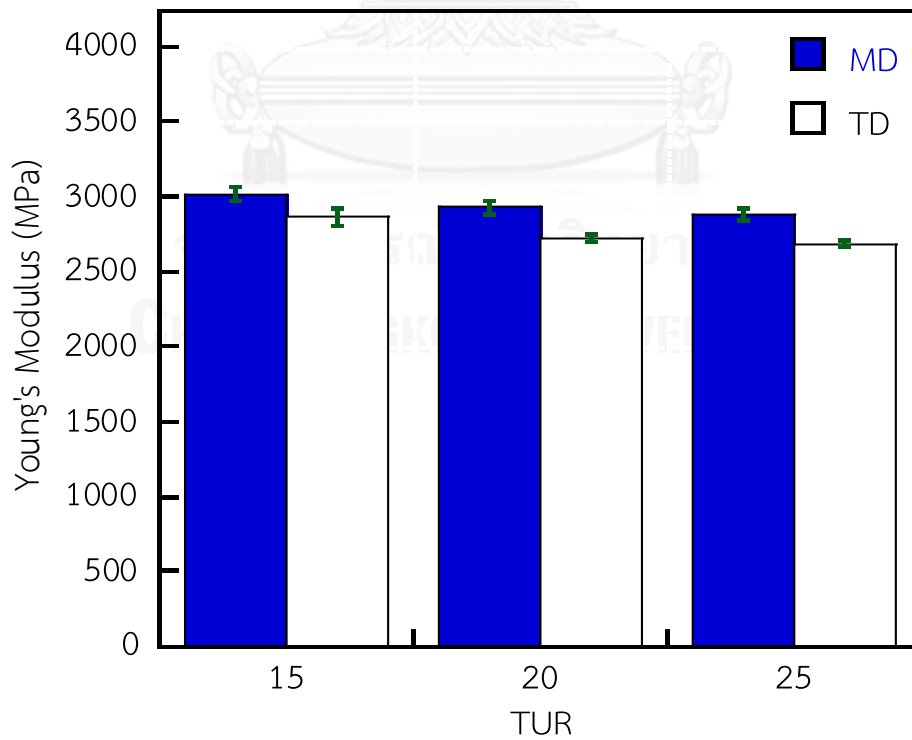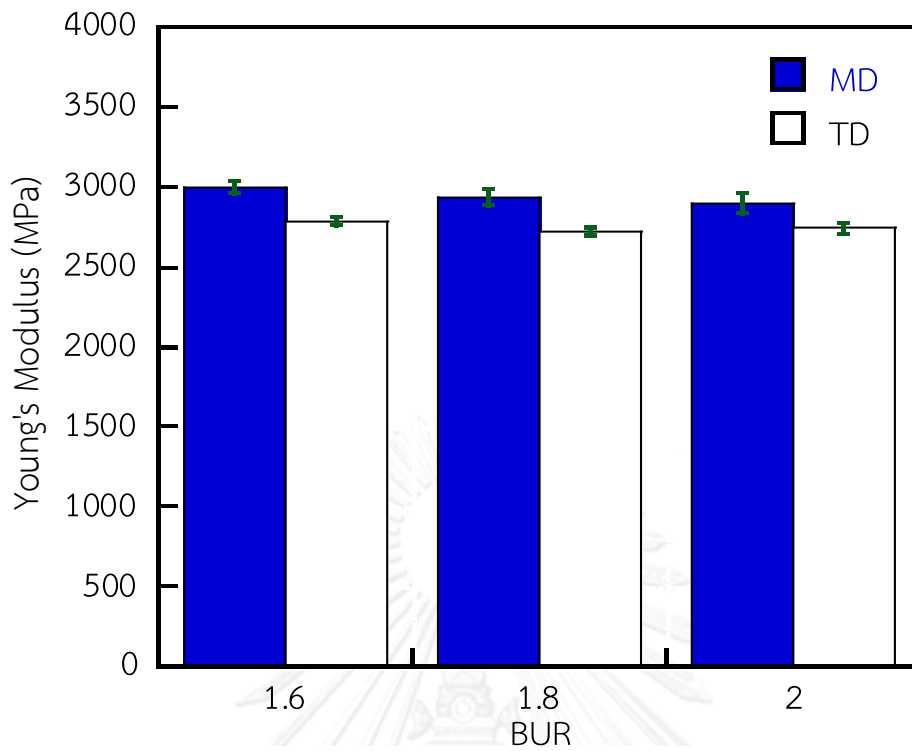
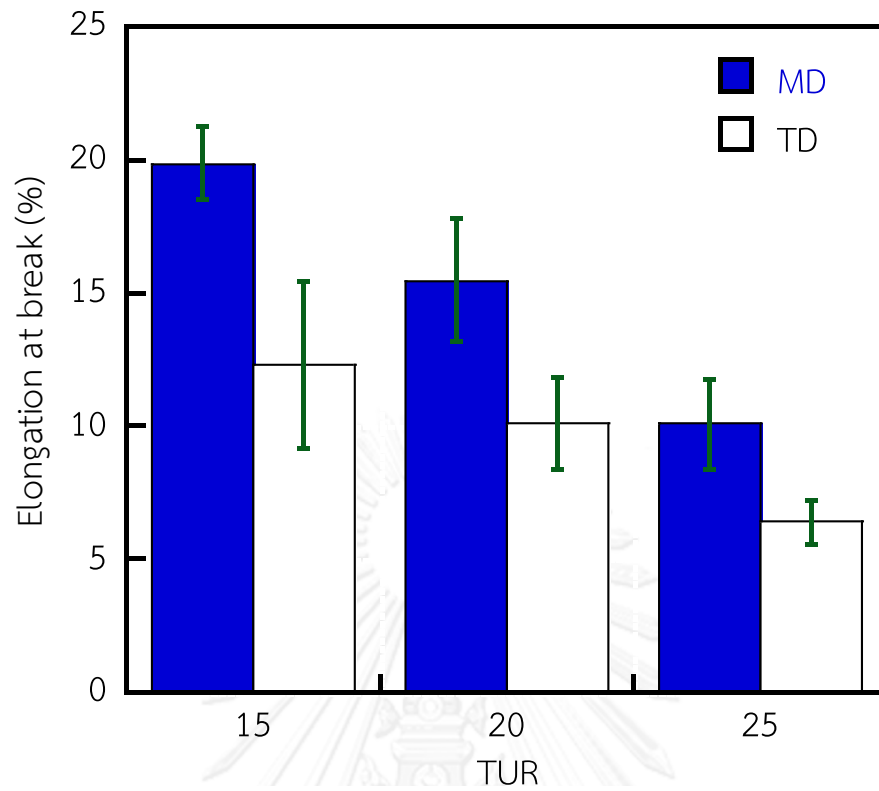Figure 4.18 Young's Modulus of PLA/NR films at fixed TUR = 20
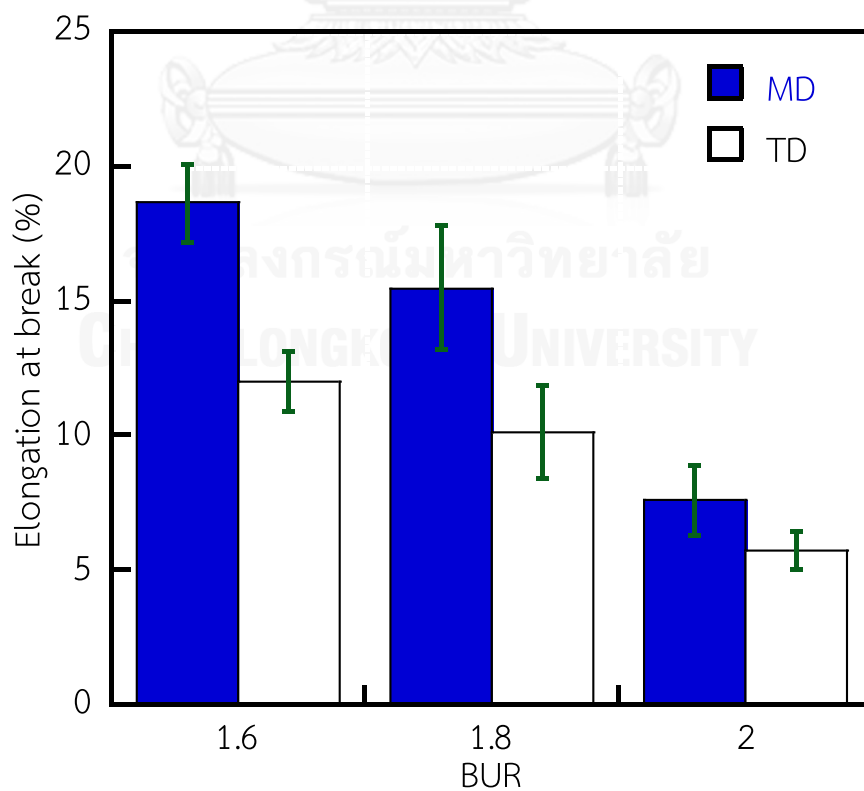


Figure 4.19 Elongation at break of PLA/NR films at fixed TUR = 20
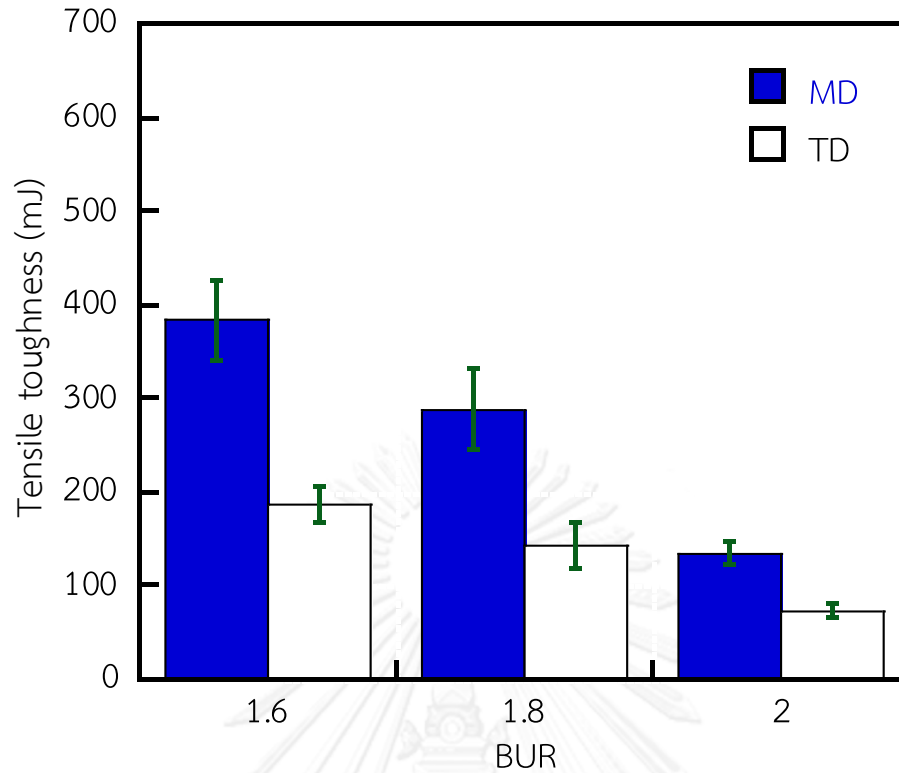
Figure 4.20 Tensile toughness of PLA/NR films at fixed TUR = 20
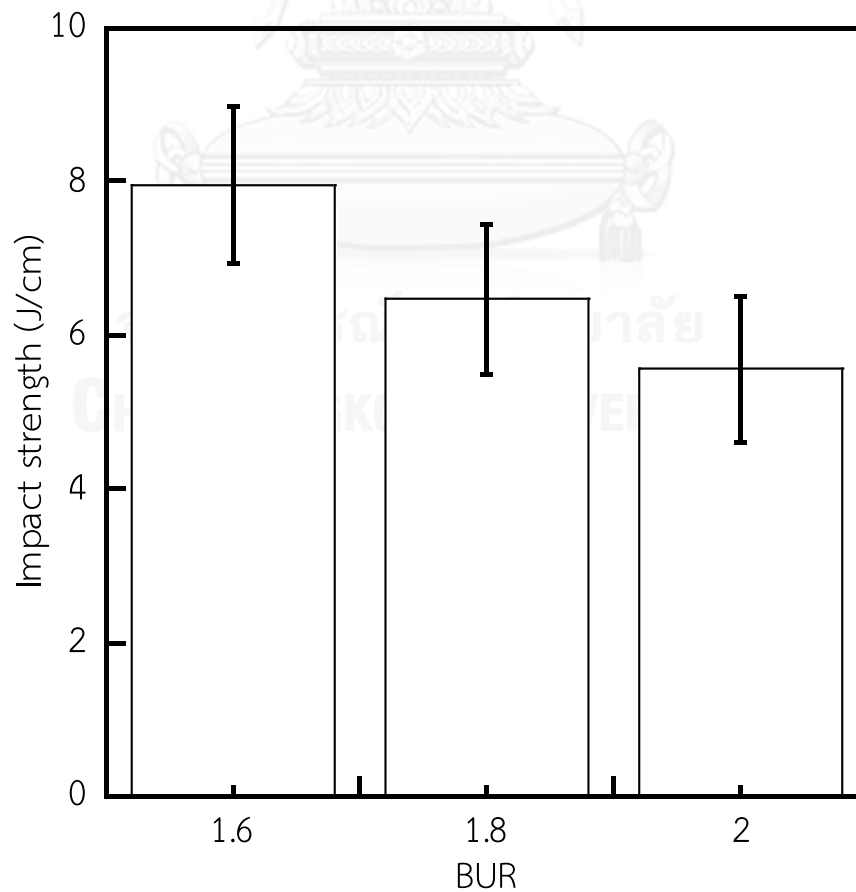


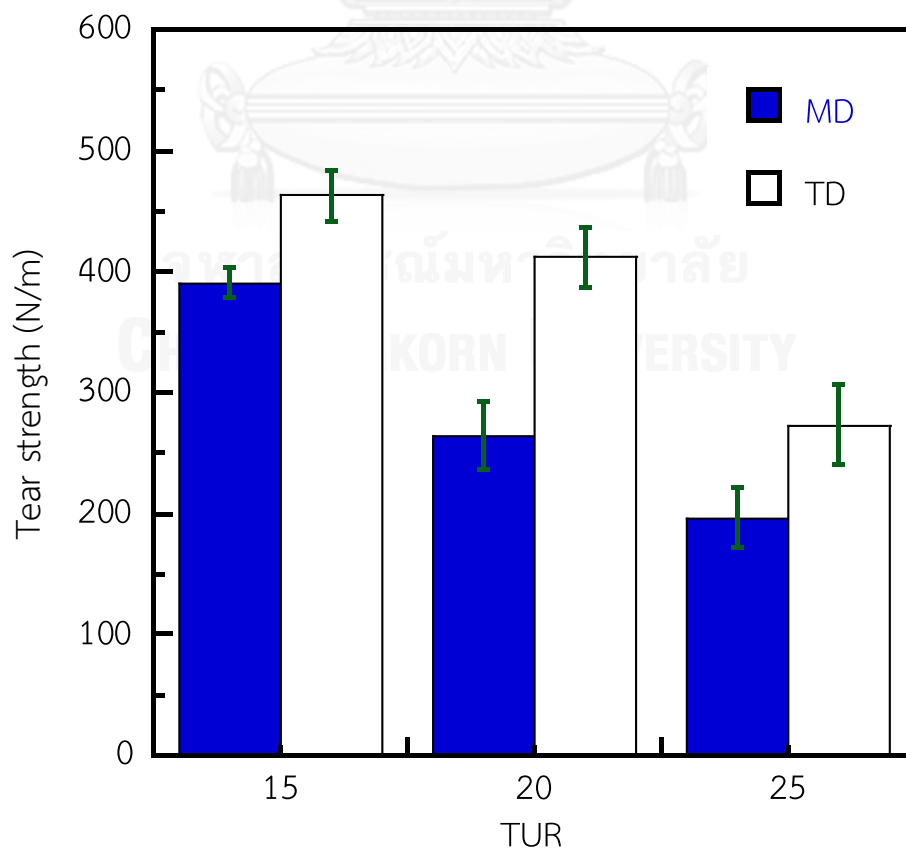Figure 4.21 Impact strength of PLA/NR films at fixed TUR = 20
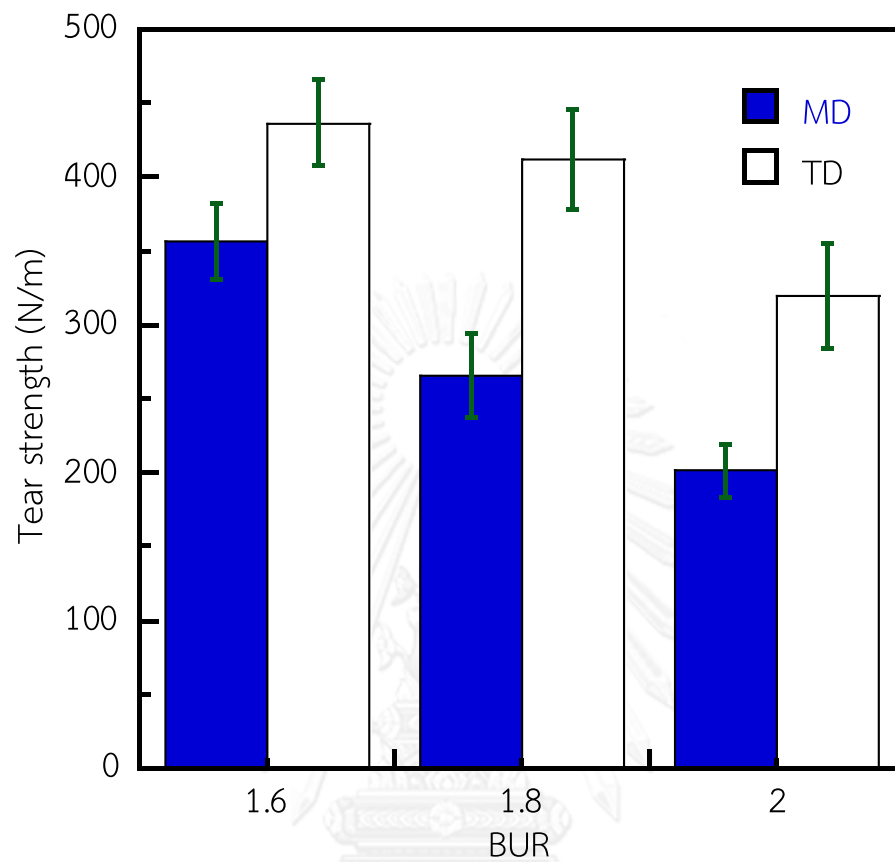
Figure 4.22 Tear strength of PLA/NR films at fixed TUR = 20

### 4.1.2.4 Gas Permeability

The values of OP and WVP of PLA/NR blown films with various BUR are illustrated in Figure 4.23. It is seen that OP and WVP of PLA/NR blown films are almost constant, which might be due to the fact that the pneumatic forces in TD are not significant difference and high enough to create a lot of voids, leading to the same content of microvoids at the interface.
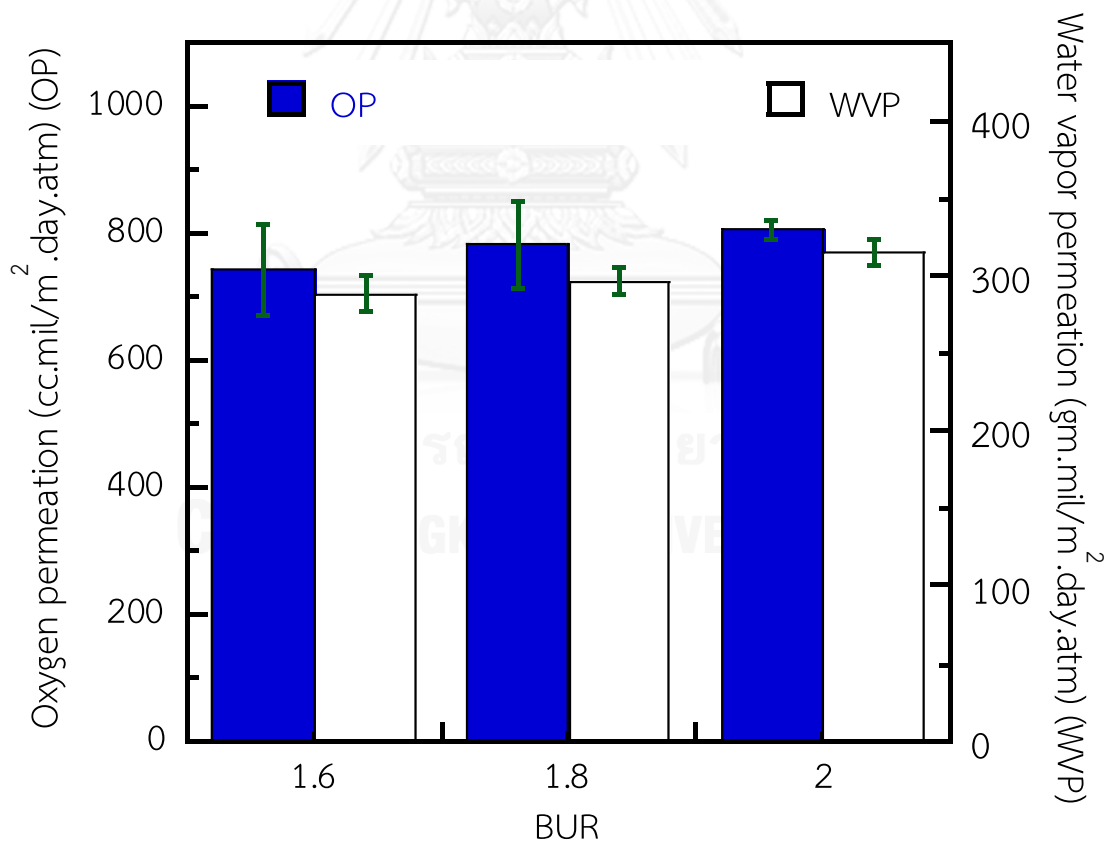


Figure 4.23 Oxygen and water vapor permeation of PLA/NR films at fixed TUR = 20

**4.2 Film drawing**

PLA/NR blown films were cut into rectangular specimens (5 × 2 cm$^2$) for further film drawing at elevated temperature, i.e., 65 $^\circ$C, in a temperature controlled environmental chamber of a tensile testing machine with a drawing rate of 150 mm/min. The photograph of the drawn films at the mentioned conditions is shown in Figure 4.24. It is worth mentioning that this temperature is selected because the PLA/NR drawn films still give the smooth surface, whereas drawing at other conditions exhibits the wrinkles on the film surfaces (Figure 4.25 and Figure 4.26) which are not suitable for measuring the mechanical properties and gas permeation property. In order to investigate the effect of drawing ratio on the film properties, the film specimens obtained from the blown film prepared at TUR = 15 were stretched in MD to the ratios of 50% and 100%, meanwhile the film specimens obtained from the blown film prepared at BUR = 1.6 were also stretched in TD to the same ratios.
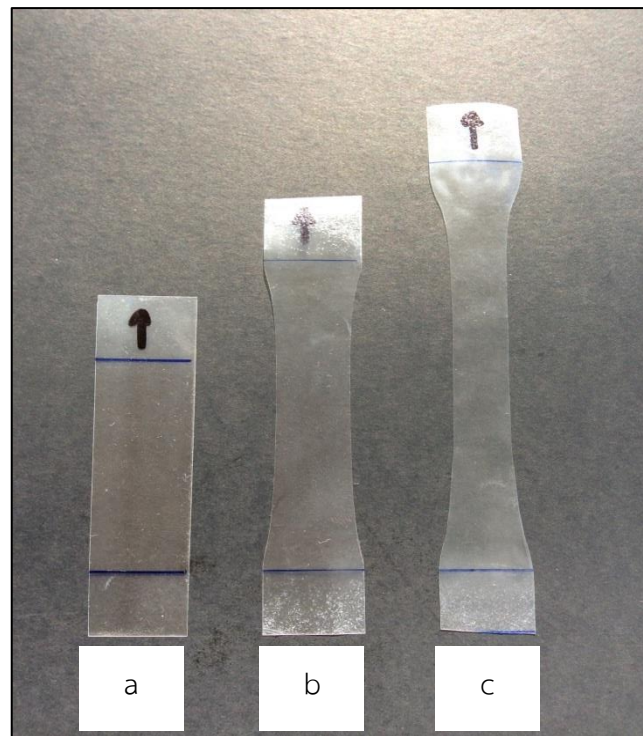
Figure 4.24 The photograph of specimens after drawing at different
drawing ratios (a) 0%, (b) 50% and (c) 100%
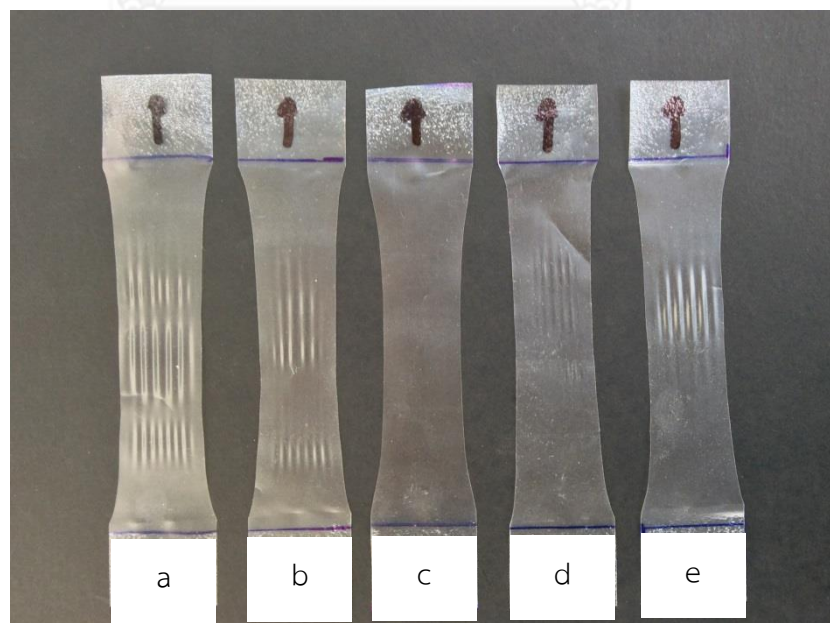


Figure 4.25 The photograph of specimens after drawing at different
drawing rates (mm/min) (a) 250, (b) 200, (c) 150, (d) 100 and
(e) 50
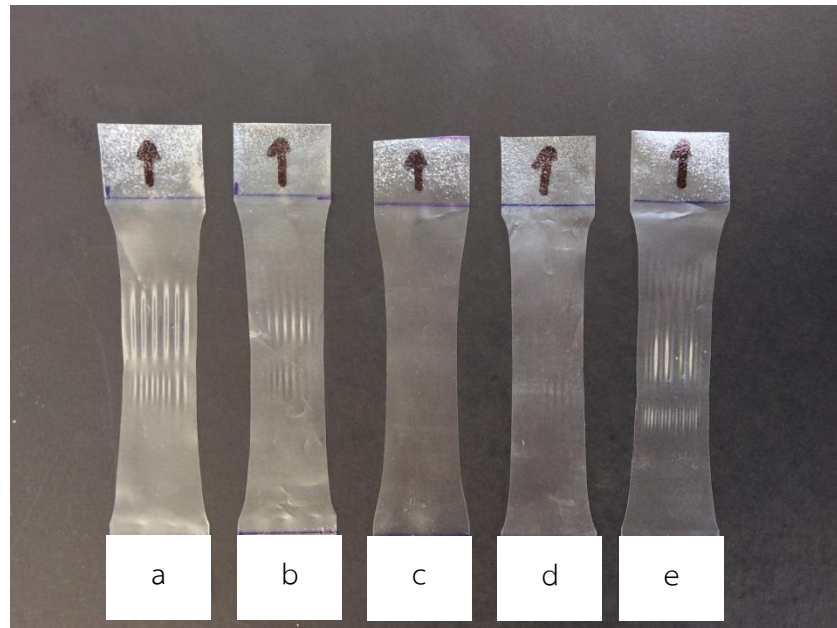
Figure 4.26 The photograph of specimens after drawing at different
temperatures (°C) (a) 75, (b) 70, (c) 65, (d) 60 and (e) 55

## 4.2.1 Effect of drawing in MD

### *4.2.1.1 Morphology*

The films after stretching were cryofractured in liquid nitrogen
to characterize the morphology of cross-section surfaces as shown in Figure 4.27. The
micrographs of PLA/NR drawn films show the similar trend to those of PLA/NR blown
films. Namely, NR domains in PLA matrix were considerably deformed in the drawing
direction, especially when the drawing ratio increases to 100%, because the polymer
chains of amorphous NR have higher mobility to deform at elevated temperature.
The average sizes of NR in the films prepared at drawing ratio of 0%, 50% and 100%
are 7.97±1.38 µm, 8.2±2.08 µm and 9.06±2.41 µm, respectively.

Figure 4.27 SEM micrographs of cross-sectional fractured surfaces in TD of the films drawn in MD for different drawing ratios (TUR = 15) (a) 0%, (b) 50% and (c) 100%

### *4.2.1.2 Thermal properties*

DSC thermograms of PLA/NR films after drawing are depicted in Figure 4.28 to Figure 4.30. The thermal properties obtained from first heating scan are summarized in Table 4.4. First heating scan is performed because the effect of processing parameter, which is drawing ratio in our study, on the thermal properties of stretched films can be directly acquired by this step. From DSC thermograms, it is noticed that the values of $T_{cc}$ and its exothermic enthalpy, which represent the rearrangement of PLA chains during a heating scan, are significantly different. The exothermic heat of cold crystallization decreases at a drawing of 50% (Figure 4.29), which might be due to the relaxation of the polymer chains during annealing before film drawing process [10]. However, the exothermic heat of cold crystallization further decreases and the endothermic heat of melting increases at a drawing ratio of 100% because the polymer chains were more oriented in the drawing direction, resulting from the stress-induced crystallization [9], leading to dramatically enhanced degree of crystallinity as shown in Figure 4.30.

Figure 4.28 DSC thermograms of drawn films in MD for different drawing ratios (TUR =15)
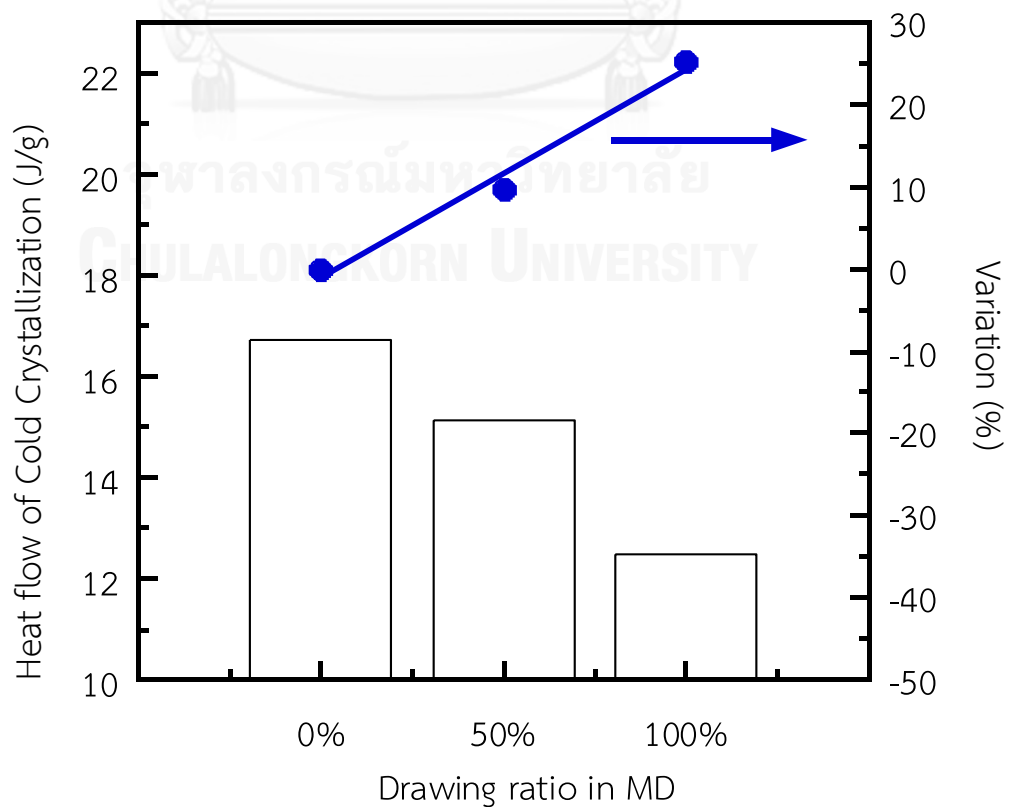


Figure 4.29 Heat flow of cold crystallization of drawn films in MD (TUR = 15)
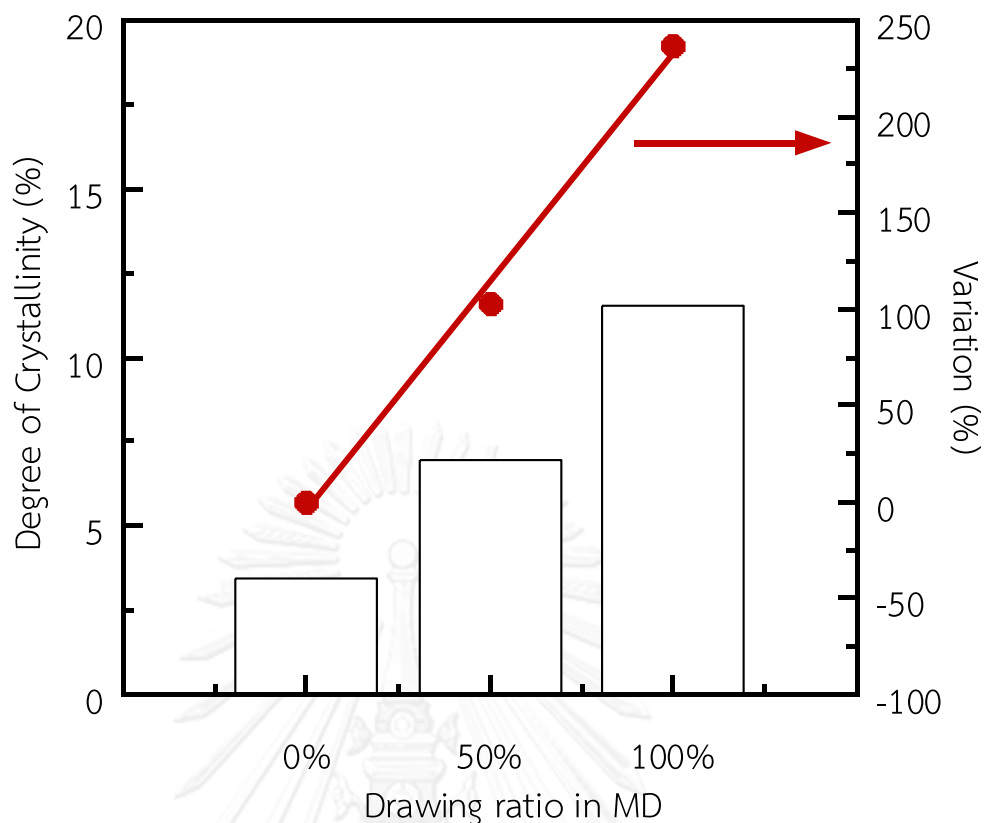
Figure 4.30 Degree of crystallization of drawn films in MD (TUR = 15)

Table 4.4 Thermal properties of drawn films in MD for different drawing ratios

determined from the first DSC heating scan (TUR = 15)

| Drawing ratio | $T_g$ ($^{\circ}$C) | $T_{cc}$ ($^{\circ}$C) | $T_{m1}$ ($^{\circ}$C) | $T_{m2}$ ($^{\circ}$C) | $\Delta H_{cc}$ (J/g) | $\Delta H_m$ (J/g) | %$X_c$ |
|---|---|---|---|---|---|---|---|
| 0% | 58.4 | 102.7 | 145.4 | 153.6 | 16.74 | 19.60 | 3.42 |
| 50% | 60.3 | 101.2 | 145.2 | 153.8 | 15.12 | 20.94 | 6.96 |
| 100% | 60.1 | 100.3 | 144.9 | 153.3 | 12.49 | 22.14 | 11.52 |

### *4.2.1.3 Mechanical properties*

From Figure 4.31 to Figure 4.35, it can be seen that a post-processing film drawing at elevated temperature can increase tensile strength, Young's modulus, and tensile toughness as a function of drawing ratio. This phenomenon could be explained by the improvement of degree of crystallinity when the drawing ratio is higher [10, 30] while domain size of NR was slightly increases. On the other hand, elongation at break reaches the maxima at 50% and drops at 100%. At the beginning of film drawing the polymer chains in the amorphous fraction, for example, tie chains that link the adjacent crystallites together, can be organized in the drawing direction owing to their high mobility, forming the packed of polymer chains or crystalline fraction. This phenomenon can be indicated by stress – strain curve at drawing ratio 50% as shown in Figure 4.31. It is noticed that after yield point stress becomes constant, which occurs because polymer chains slip over each other in direction parallel to the molecular axis. However, when the films were further stretched, the polymer chains in the crystalline fraction have already lost the ability of movement in comparison with those in amorphous fraction which can be observed by stress – strain curve at drawing ratio 100% (Figure 4.31). Stress in this curve dramatically increases because the polymer chains are packed tightly and cannot slip. Thus, the elongation at break declines. Moreover, the orientation of PLA chain and NR domain of films during drawing in MD is schematically in Figure 4.36.

Figure 4.31 Stress - strain curve of drawn films in MD (TUR = 15)



Figure 4.32 Tensile strength of drawn films in MD (TUR = 15)

Figure 4.33 Young's Modulus of drawn films in MD (TUR = 15)



Figure 4.34 Elongation at break of drawn films in MD (TUR = 15)

Figure 4.35 Tensile toughness of drawn films in MD (TUR = 15)
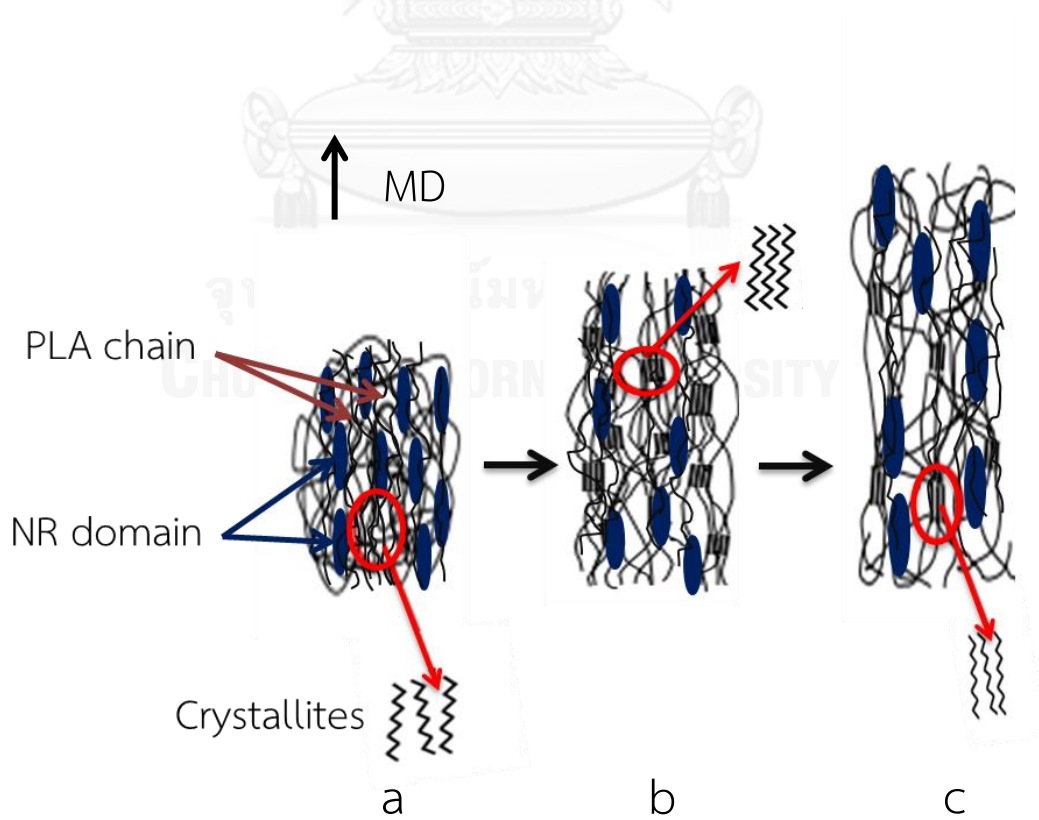


Figure 4.36 Schematic drawing of orientation of PLA chain and NR domains in
PLA/NR films during drawing in MD (TUR = 15) (a) 0%, (b) 50% and (c)
100%

### 4.2.1.4 Gas Permeability

OP of PLA/NR drawn films are demonstrated in Figure 4.37. The results show the similar pattern to the elongation at break. Namely, OP increases and then decreases after the drawing ratio of 50%. An increase in OP can probably be described by the microvoid formation at the interface or an enlargement of size of amorphous NR domain as a result of film drawing. Moreover, a decrease in OP at higher drawing ratio is due to the higher degree of crystallinity, obstructing the transportation of oxygen gas to pass through the films.
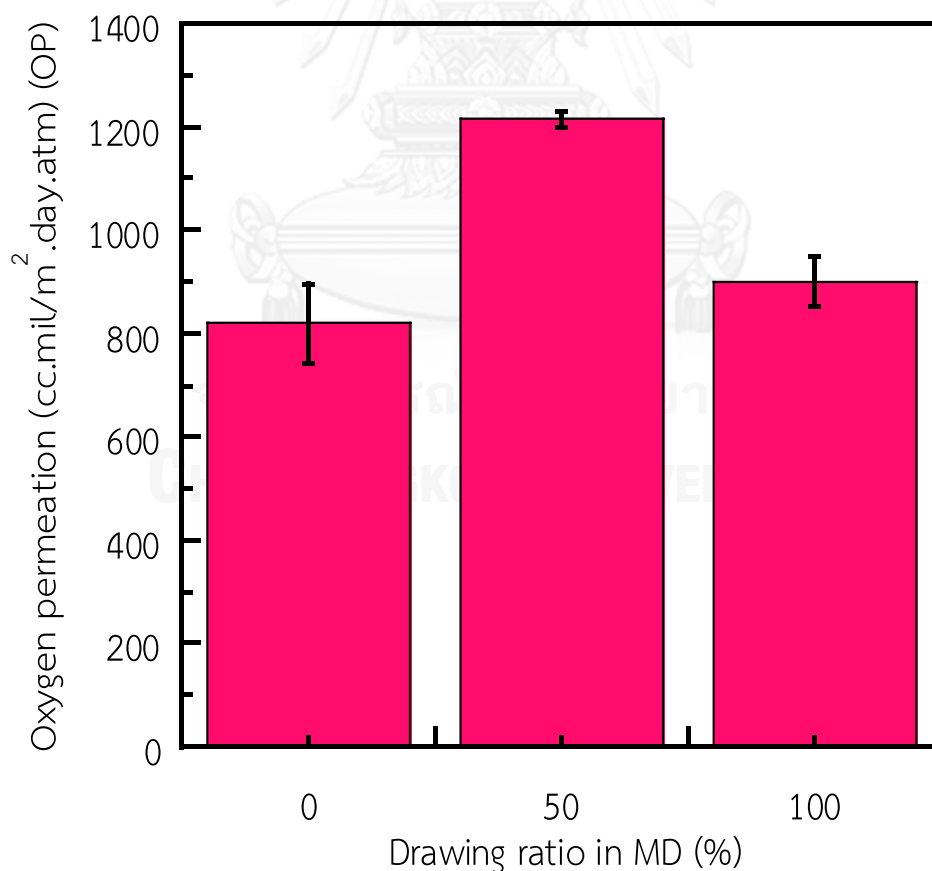


Figure 4.37 Oxygen permeation of drawn films in MD (TUR = 15)

**4.2.2 Effect of drawing in TD**

*4.2.2.1 Morphology*

As displayed in Figure 4.38, SEM micrographs of cross-sectional fractured surfaces of PLA/NR films after drawing in TD show the deformation of NR, that is, the characteristic of NR domains become ellipsoidal with the poles in TD (drawing direction) as increasing drawing ratio. The average sizes of NR in the films prepared at drawing ratio of 0%, 50% and 100% are 4.63±0.31 µm, 5.02±0.89 µm and 5.26±0.96 µm, respectively. Interestingly, it is also noticed that the magnitude of change in NR domain size in MD is higher than that in TD because the forces in machine direction generated by a nip roll have a greater extent than the forces in transverse direction produced from an air flow inside a bubble.
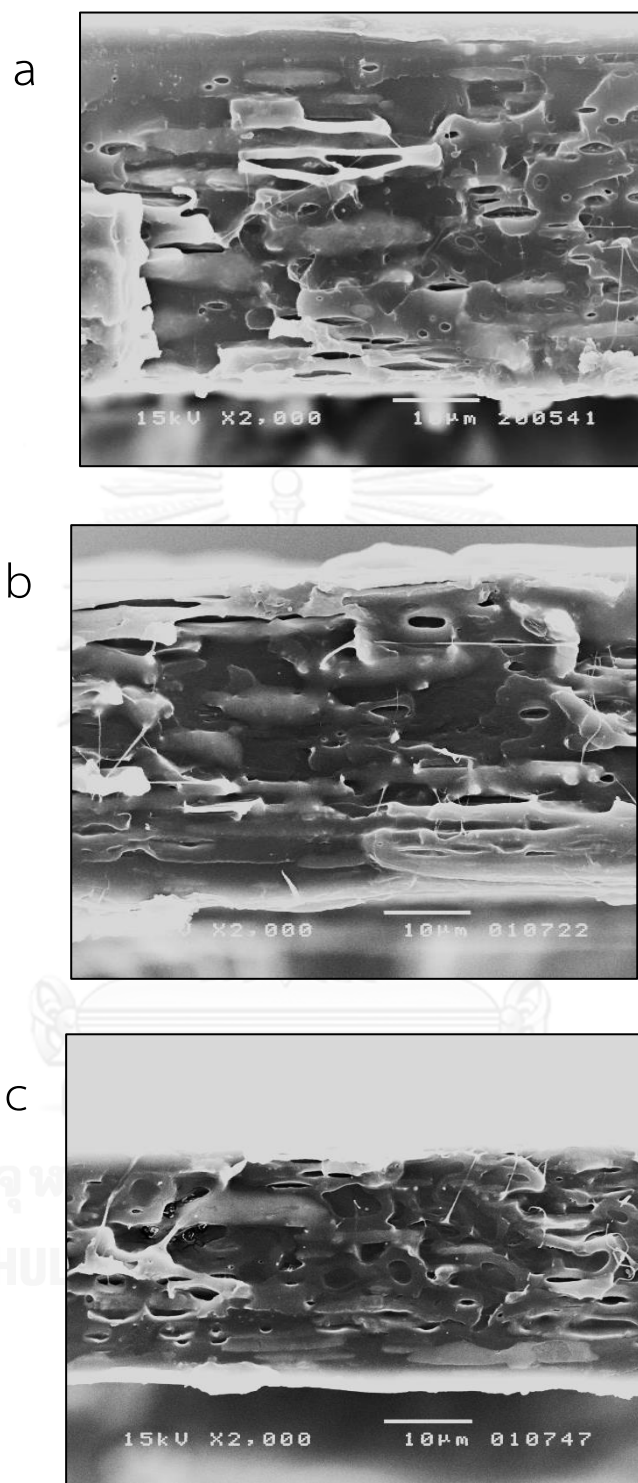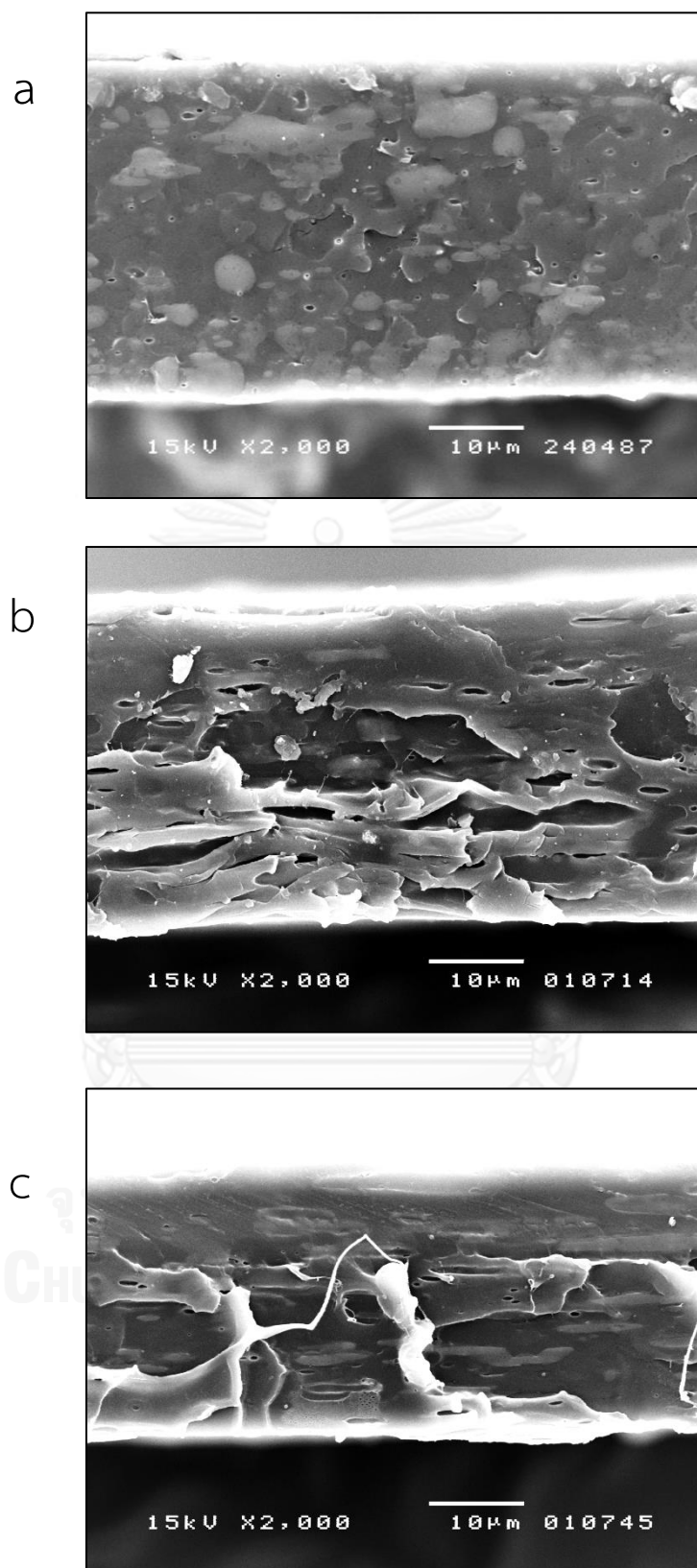
Figure 4.38 SEM micrographs of cross-sectional fractured surfaces in MD of the
drawn films in TD for different drawing ratios (BUR = 1.6) (a) 0%, (b)
50% and (c) 100%

### *4.2.2.2 Thermal properties*

As shown in Figure 4.39 to Figure 4.41, PLA/NR films drawn in TD exhibit the same thermal behavior comparing with those stretched in MD as discussed in the previous section. The thermal properties acquired from first heating scan of the PLA/NR films stretched in TD are listed in Table 4.5. Namely, heat of cold crystallization and crystallinity of films stretched in MD and TD are insignificantly distinct because the crystallinity of the starting PLA/NR blown films in MD and TD prior to drawing is also identical (see data in section 4.1.1.2 and 4.1.2.2). These results also imply that a post-processing drawing at elevated temperature in MD or TD has the similar effect on the thermal properties of the PLA/NR drawn films.
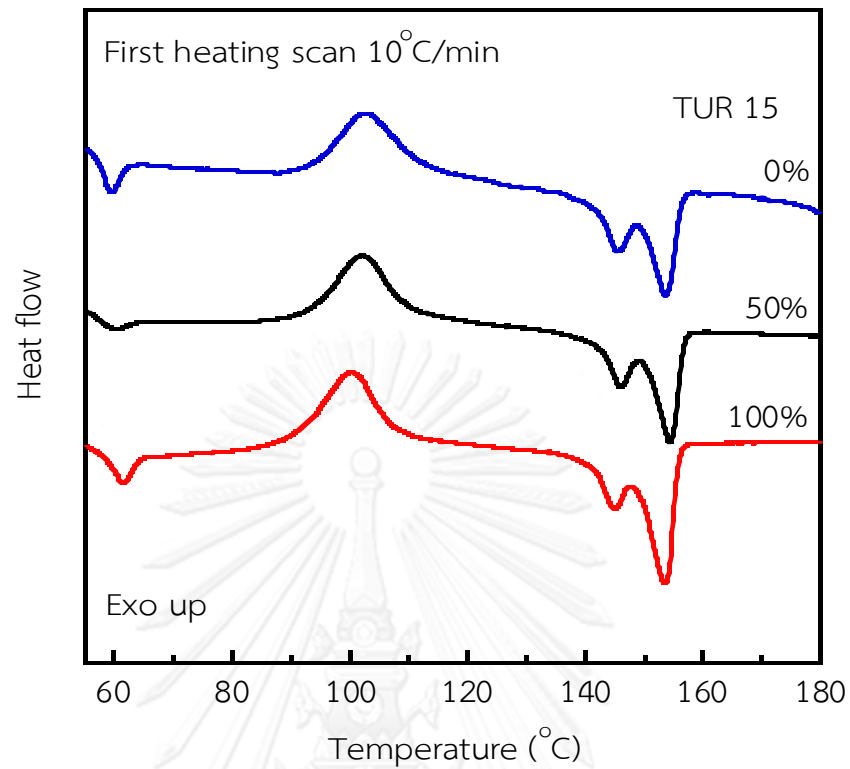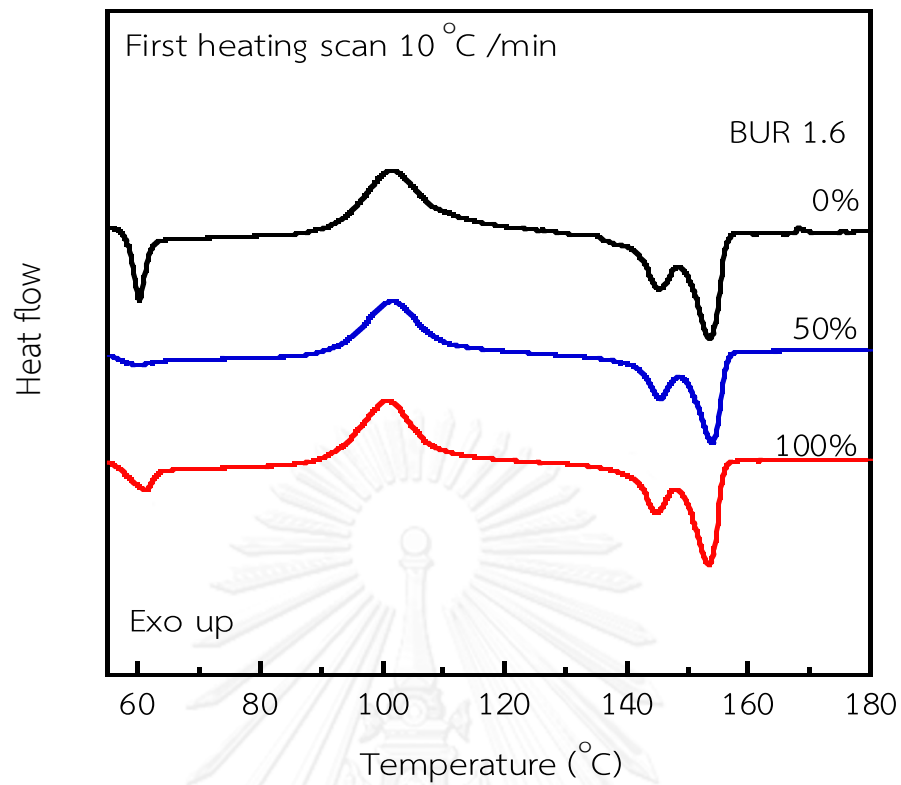
Figure 4.39 DSC thermograms of drawn films for different drawing ratios in TD (BUR = 1.6)
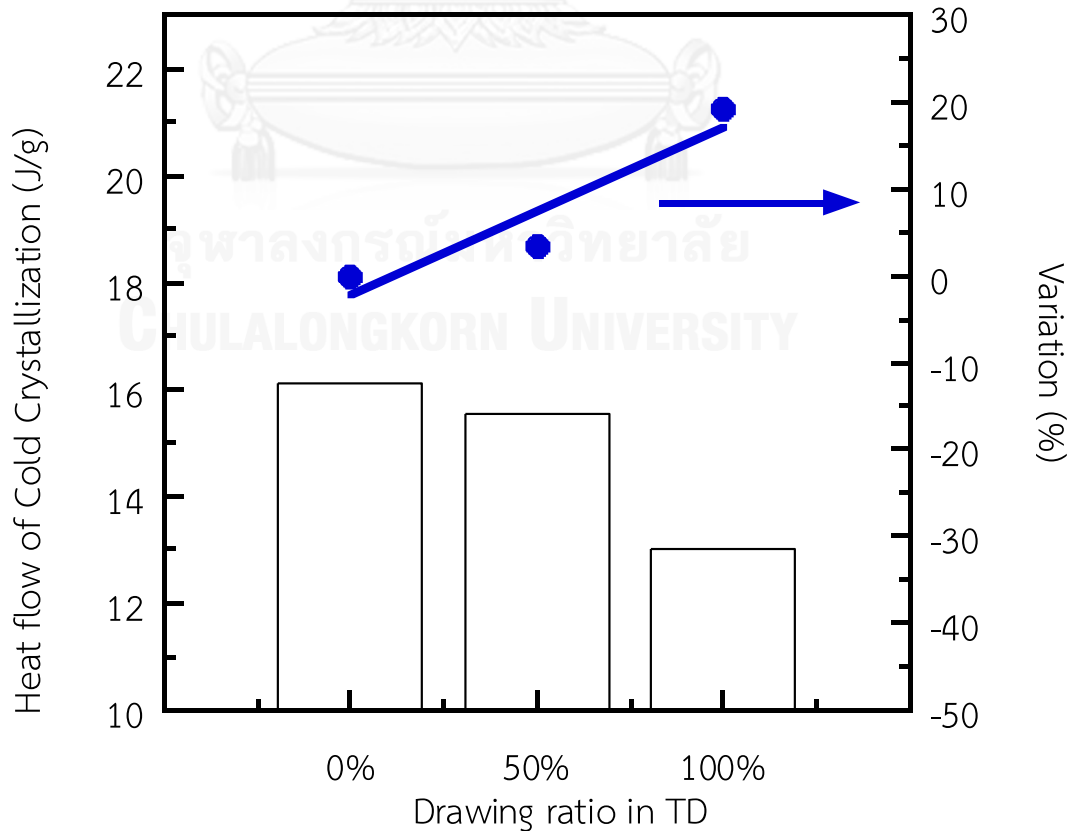


Figure 4.40 Heat flow of cold crystallization of drawn films in TD (BUR =1.6)
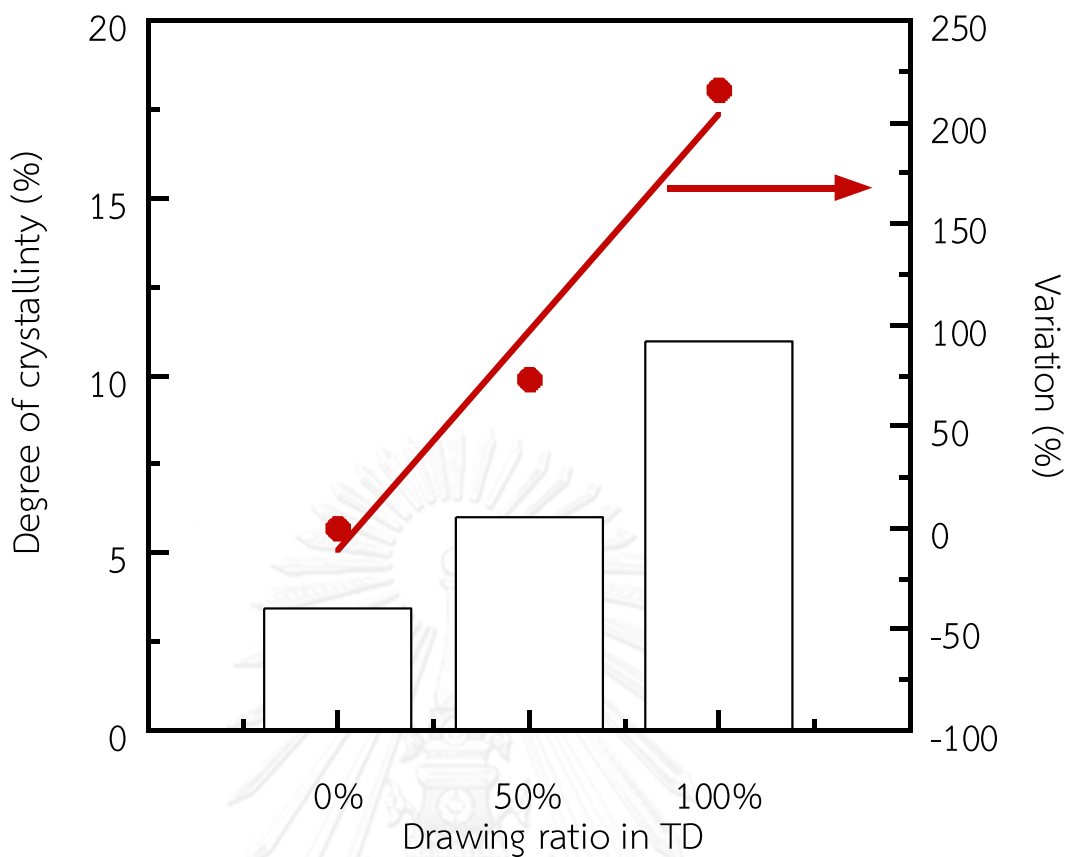
Figure 4.41 Degree of crystallinity of drawn films in TD (BUR =1.6)

Table 4.5 Thermal properties of drawn films in TD for different drawing ratios
determined from the first DSC heating scan (BUR = 1.6)

| Drawing ratio | $T_g$ (°C) | $T_{cc}$ (°C) | $T_{m1}$ (°C) | $T_{m2}$ (°C) | $\Delta H_{cc}$ (J/g) | $\Delta H_m$ (J/g) | $\%X_c$ |
|---|---|---|---|---|---|---|---|
| 0% | 59.1 | 101.4 | 145.2 | 153.9 | 16.11 | 19.02 | 3.47 |
| 50% | 60.9 | 101.6 | 145.5 | 154.0 | 15.55 | 20.59 | 6.03 |
| 100% | 60.9 | 100.6 | 144.9 | 153.5 | 13.01 | 22.18 | 10.96 |

### *4.2.2.3 Mechanical properties*

All tensile properties of drawn films in TD are shown in Figure 4.42 to Figure 4.46. It is worth mentioning that these properties increase with drawing ratio increases. Theoretically, at the early stage of transverse drawing a partial destruction of crystallized polymer chains oriented in MD, forming disordered crystalline phase, can be happened [9]. At higher extent of drawing, the polymer chains can reorient into a crystalline structure again, leading to higher degree of crystallinity. According to the DSC data, drawing in TD at drawing ratio of 50% is large enough for this reorientation of polymer chains. As seen in stress – strain curve in Figure 4.42, at drawing ratio of 50% the films show similar stress – strain behavior as those drawn in MD, as discussed in the previous section. Therefore, an enhancement of tensile strength and Young's modulus during tensile testing is achieved. Furthermore, the elongation at break and tensile toughness also improve which can be probably explained by the fact that the transverse drawing results in a formation of randomly oriented polymer chains [31] and a great extent of free volume, thus the polymer chains having high mobility in the amorphous phase can easily move in the intermolecular space during tensile loading . In addition, the orientation of PLA chain and NR domain of films during drawing in TD is schematically illustrated in Figure 4.47.
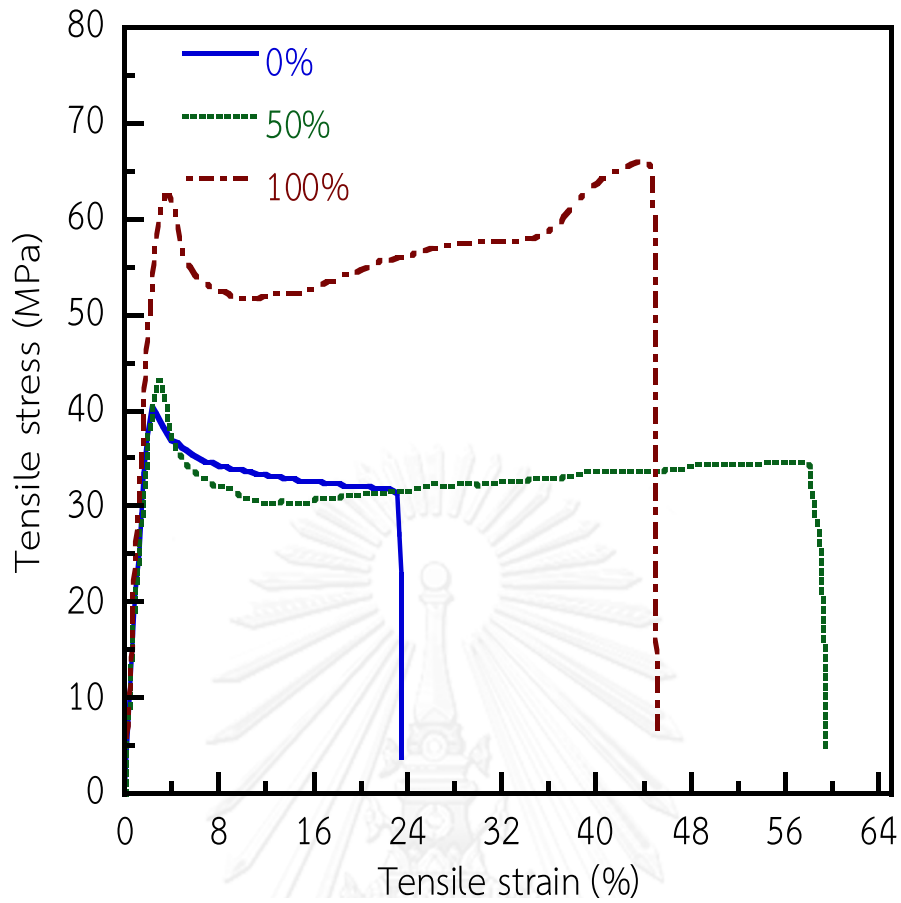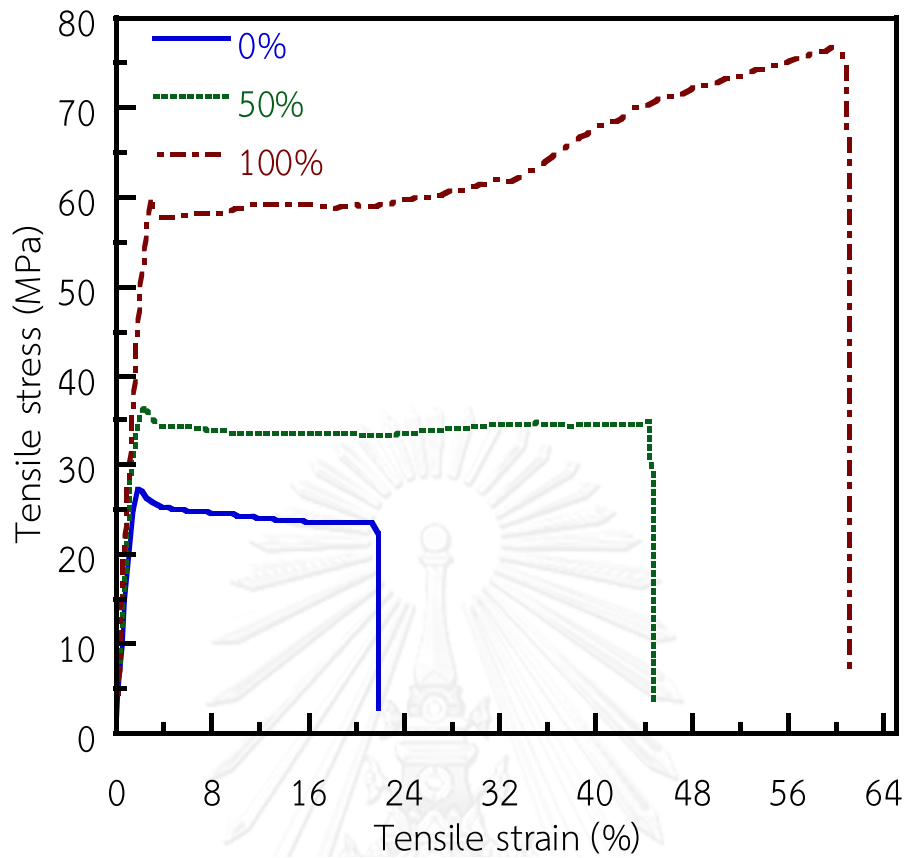
Figure 4.42 Stress - strain curve of drawn films in TD (BUR = 1.6)
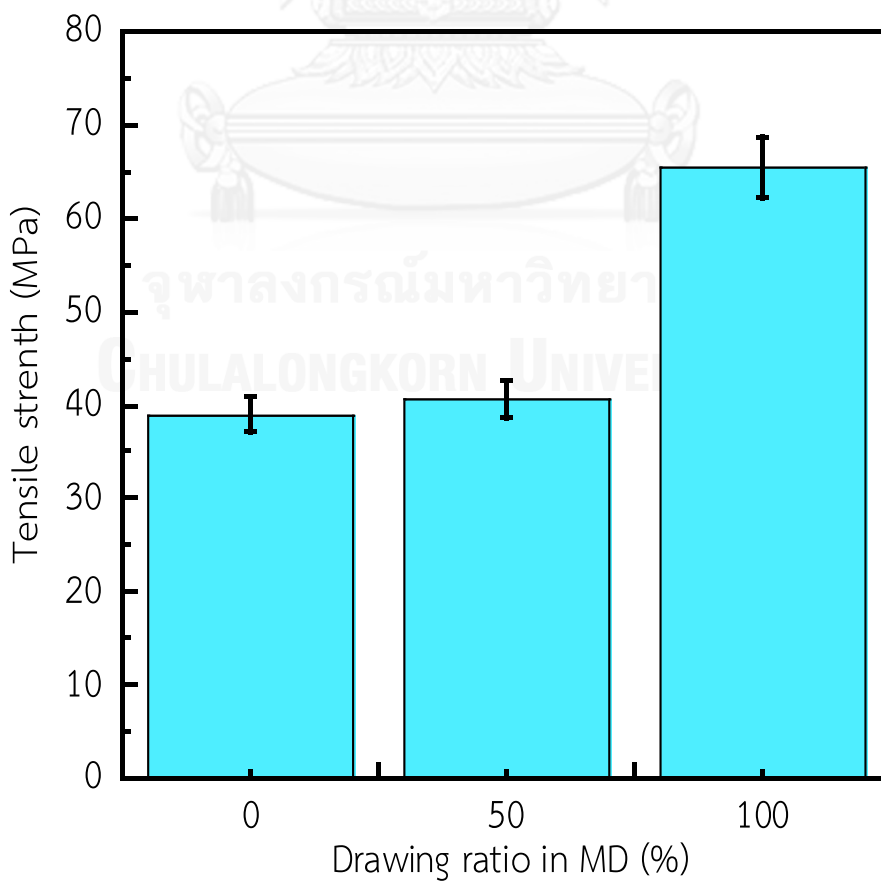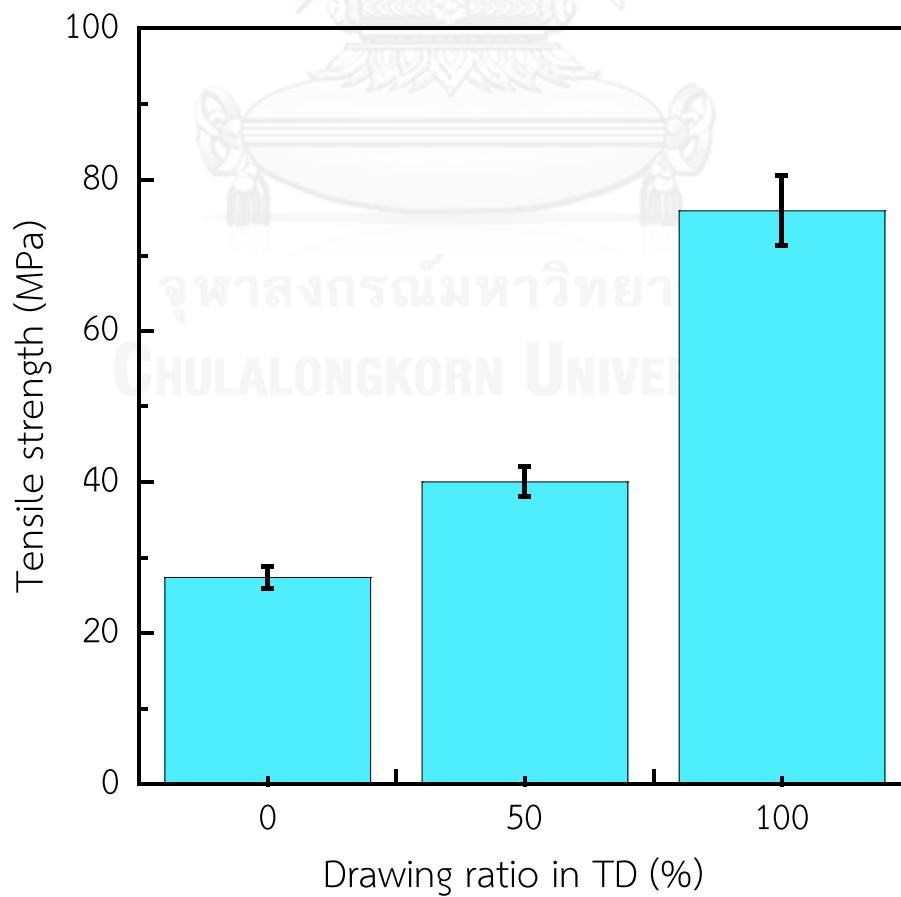


Figure 4.43 Tensile strength of drawn films in TD (BUR =1.6)
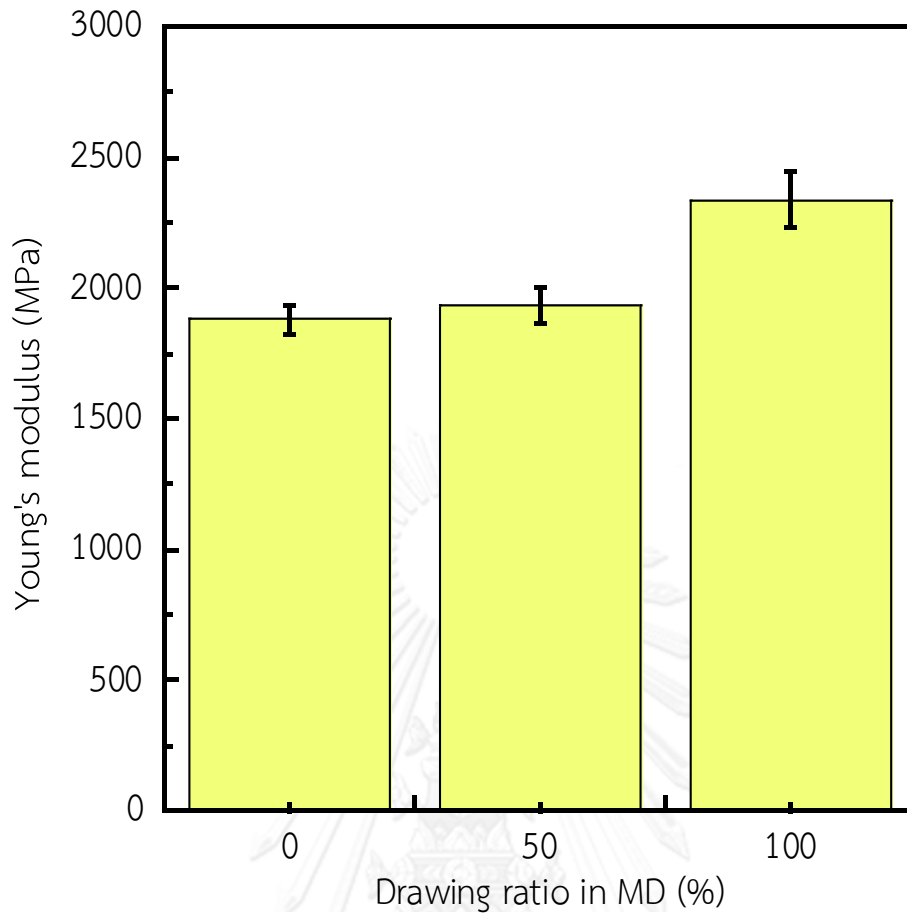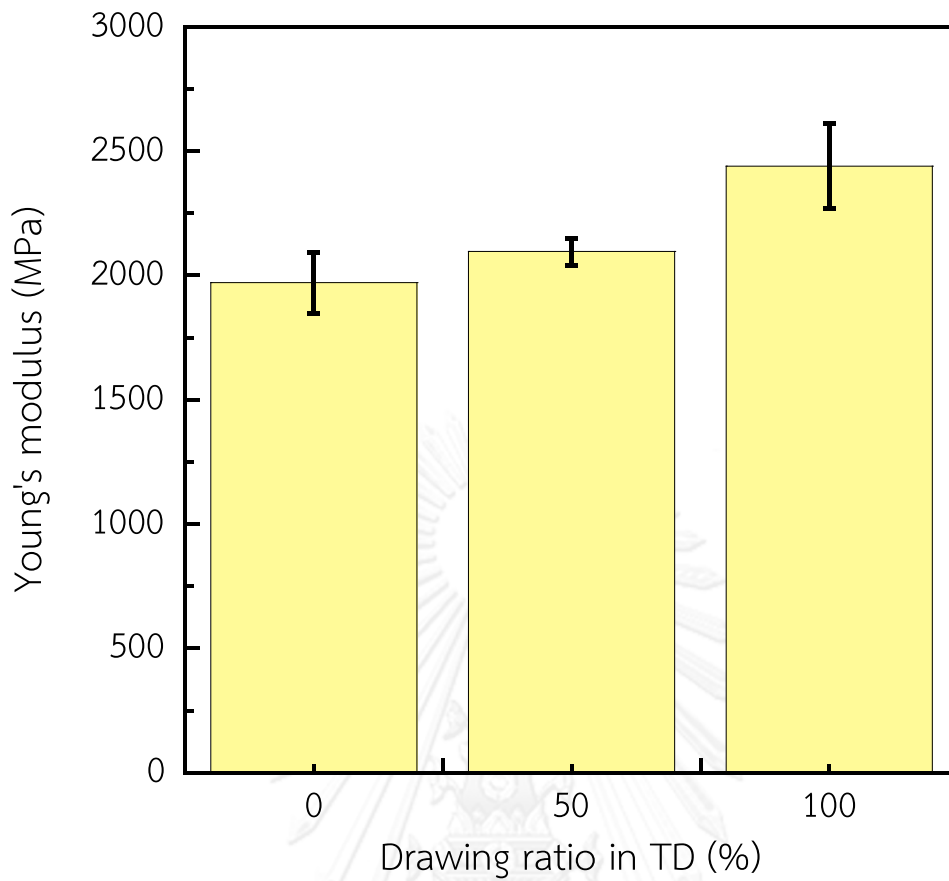
Figure 4.44 Young's Modulus of drawn films in TD (BUR =1.6)
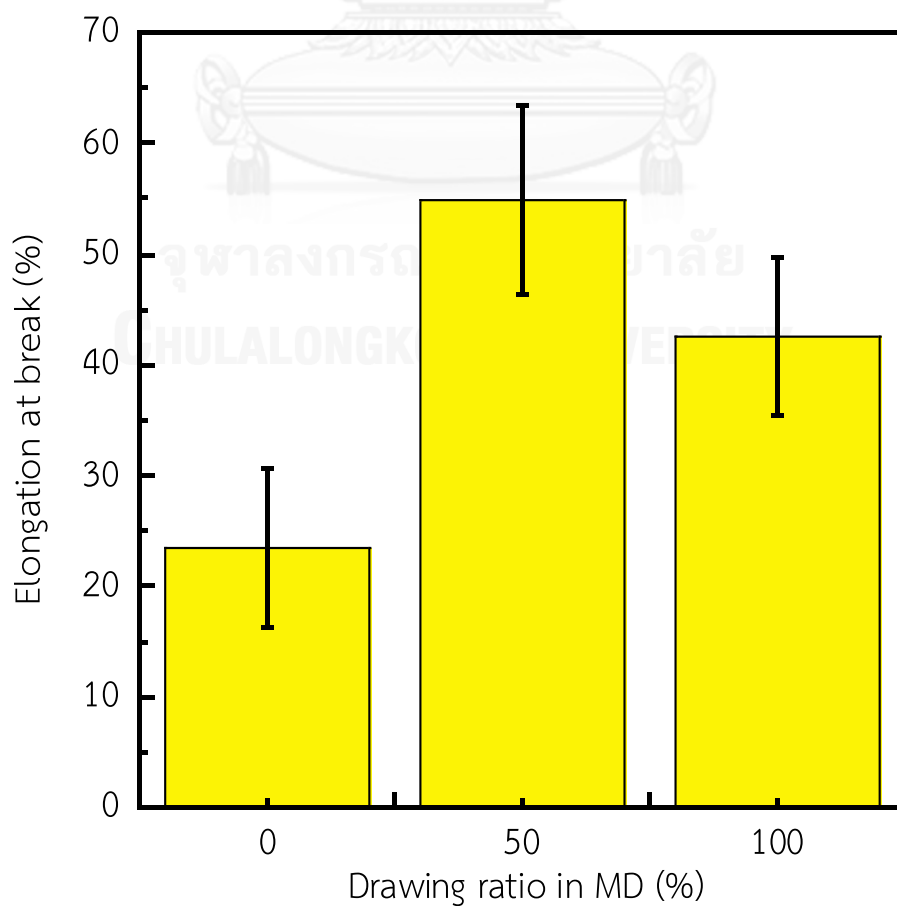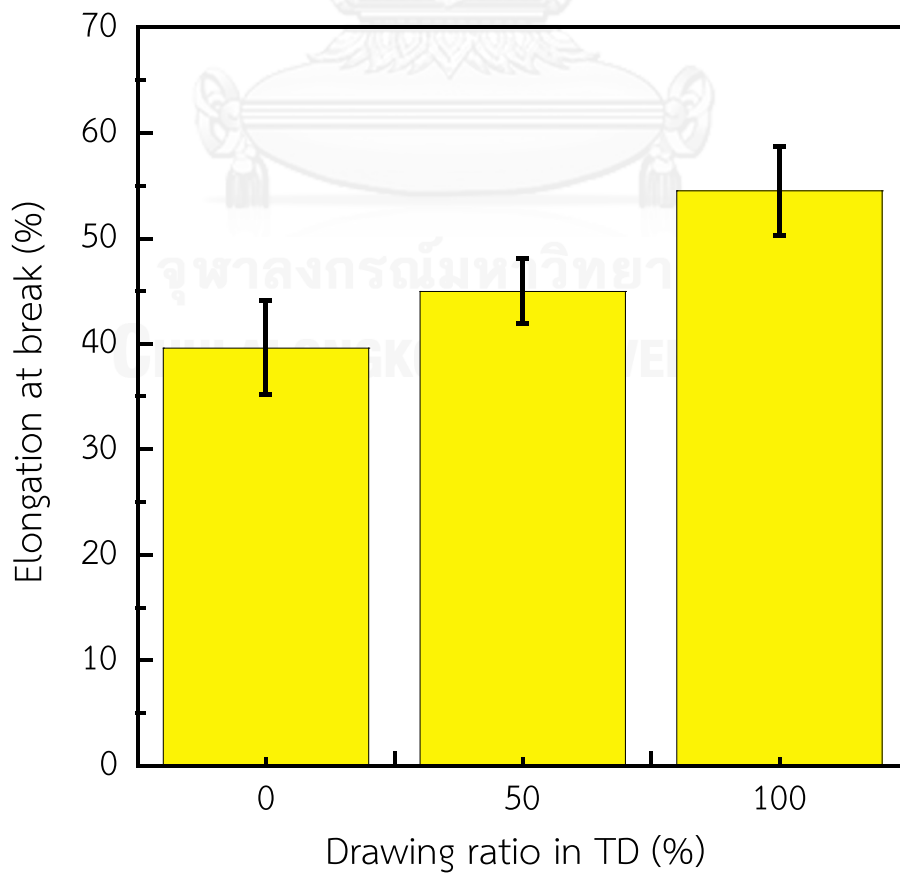


Figure 4.45 Elongation at break of drawn films in TD (BUR =1.6)
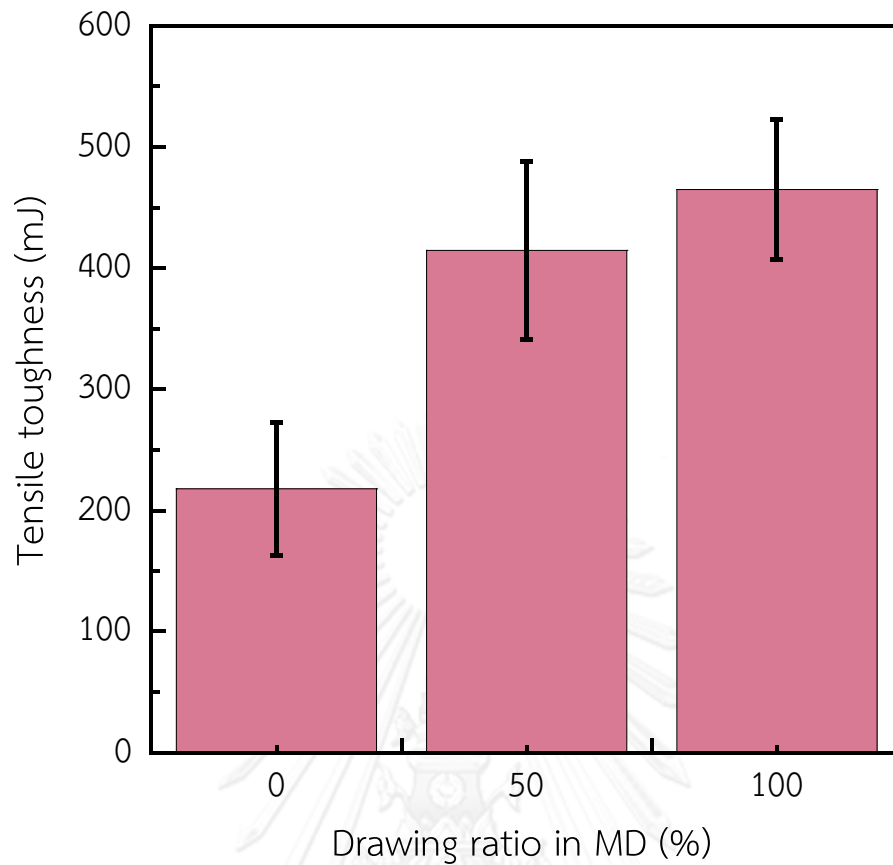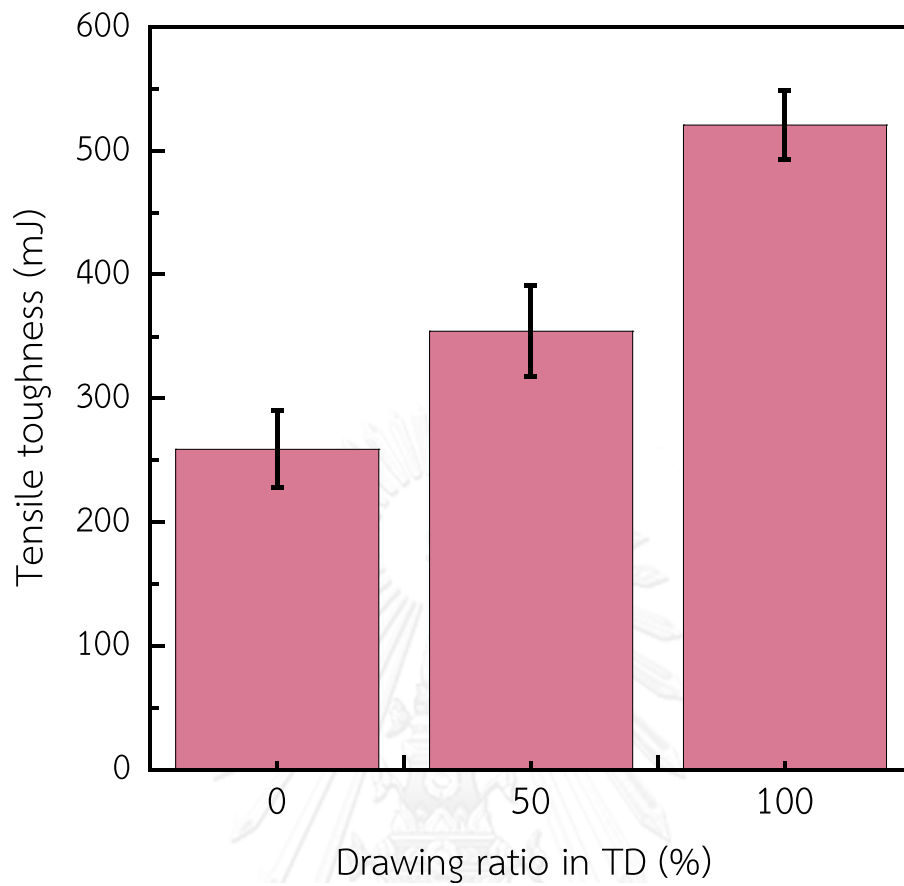
Figure 4.46 Tensile toughness of drawn films in TD (BUR =1.6)
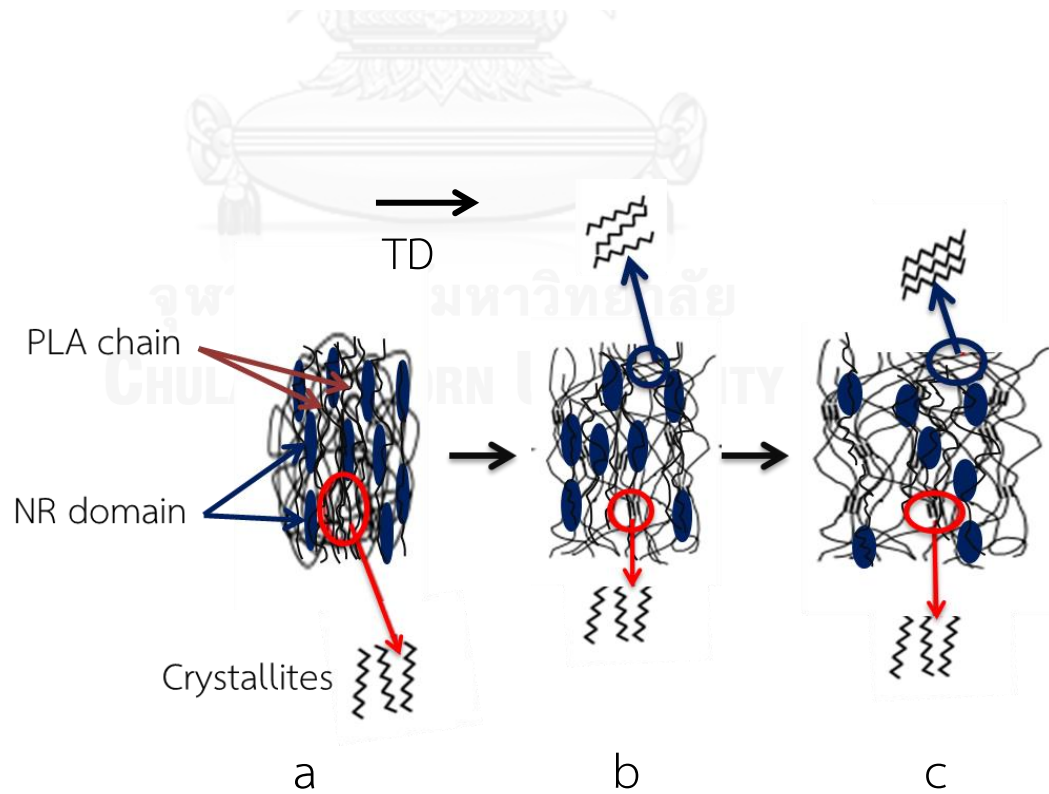


Figure 4.47 Schematic drawing of orientation of PLA chain and NR domains in PLA/NR films during drawing in TD (BUR = 1.6) (a) 0%, (b) 50% and (c) 100%

### 4.2.2.4 Gas Permeability

As illustrated in Figure 4.48, OP increases and reaches the maximum value at a drawing ratio of 50%. An increase in OP is possibly due to the microvoid formation at the interface between PLA matrix and dispersed NR domain. However, the development of crystalline structure at higher extent of drawing ratio is a competitive mechanism that inhibits the permeation of oxygen through the films.
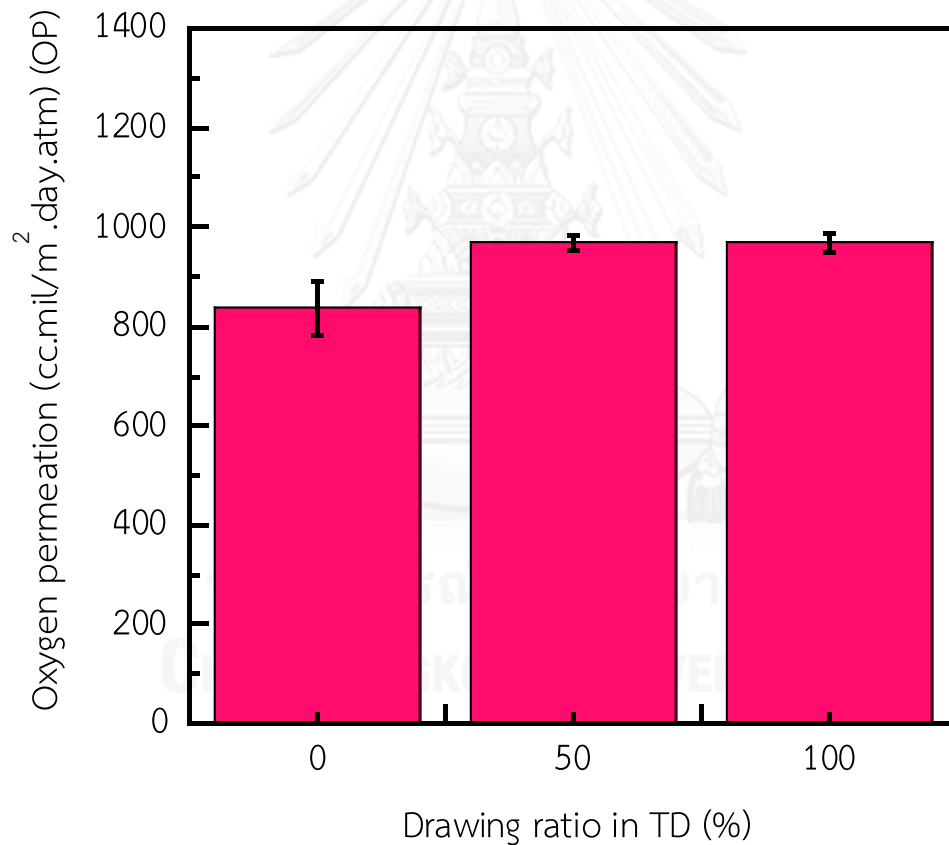


Figure 4.48 Oxygen permeation of drawn films in TD (BUR =1.6)

CHAPTER V

CONCLUSIONS AND RECOMMENDATION

## 5.1 Conclusions

In brief, the PLA blown films containing 10 wt% NR were prepared by melt-blending in a twin screw extruder following by film blowing at different Take-up ratios (TUR) and Blow-up ratios (BUR). Subsequently, films were cut from the PLA/NR blown films in machine direction (MD) and transverse direction (TD) and further stretched at elevated temperature at various drawing ratios, i.e., 50% and 100%. The important properties including morphology, thermal and mechanical properties, as well as gas permeation properties were evaluated. The conclusions of this research are described as follows:

PLA/NR blown films prepared at different TUR (fixed BUR at 1.8) and different BUR (fixed TUR at 20) show the deformation of NR domains from sphere to oval. Varying TUR has the stronger effect on the morphology of NR in comparison with varying BUR because forces mechanically generated from a nip roll is usually greater than the pneumatic forces produced from an air flow inside the bubble. The crystallinities of all blown film specimens are almost identical, 3 - 4 %, in spite of varying TUR and BUR, suggesting that a change in the processing conditions of blown film are not suitable enough to orient the polymer chains of PLA since PLA has a slow crystallization rate. The mechanical properties of the PLA/NR blown films significantly decrease as TUR or BUR increases , except tensile strength and Young's

modulus, which can be explained by a reduction of interfacial area of NR when NR shape changes. However, the improvement of oxygen permeation with increasing of TUR is also detected as a result of microvoid formation.

For the film drawing at elevated temperature, the film specimens were uniaxially stretched at different ratios. From SEM micrographs, NR domains greatly deform in the drawing direction as the drawing ratio increases. Further, the uniaxial drawing in MD and TD leads to a decrease in heat of cold crystallization and a considerable increase in crystallinity. Additionally, it is expected that the stress-induced crystallization happened upon drawing is responsible for significantly improved crystallinity. The uniaxial drawing in MD at drawing ratio of 100% gives enhanced mechanical properties shown as follows: tensile strength of 68.24 %, Young's modulus of 24.24 %, elongation at break of 81.54 % and tensile toughness of 113.52 %. Oxygen permeation increases and reaches maxima of about 23.64 % at drawing ratio in MD of 50% owing to the two competitive factors; microvoid formation and barrier property of crystalline structure of PLA. The mechanical properties and gas permeation of films stretched in TD exhibit the similar trends to films stretched in MD, omitting elongation at break and oxygen permeation which decrease at drawing ratio of 100% in MD.

## 5.2 Recommendation

•   Owing to the limitation of the equipment, the highest drawing ratio is only 100%. Thus, a drawing ratio over 100% should be investigated because we expect that it can highly improve the tensile properties of the films.

•       The grips of a chamber should be larger for holding a larger film specimen. So that, impact strength and tear strength can be measured. If possible, it is crucial to have other grips that can hold the films in both X- and Y-direction. As the result, the films can be stretched simultaneously or sequentially, not only uniaxially.

•       Functionalization of NR should be tried to consider the effect of interfacial adhesion.

# REFERENCES

[1]     Auras, R.A., Harte, B., Selke, S., and Hernandez, R., Mechanical, Physical, and Barrier Properties of Poly(Lactide) Films. Journal of Plastic Film and Sheeting, 2003. 19(2): p. 123-135.

[2]     Suksut, B. and Deeprasertkul, C., Effect of Nucleating Agents on Physical Properties of Poly(lactic acid) and Its Blend with Natural Rubber. Journal of Polymers and the Environment, 2010. 19(1): p. 288-296.

[3]     Bitinis, N., Verdejo, R., Cassagnau, P., and Lopez-Manchado, M.A., Structure and properties of polylactide/natural rubber blends. Materials Chemistry and Physics, 2011. 129(3): p. 823-831.

[4]     Jaratrotkamjorn, R., Khaokong, C., and Tanrattanakul, V., Toughness enhancement of poly(lactic acid) by melt blending with natural rubber. Journal of Applied Polymer Science, 2012. 124: p. 5027-5036.

[5]     La Mantia, F.P., Canfora, L., and Dintcheva, N.T., Filmability and properties of compatibilized PA6/LDPE blends. Polymer Engineering & Science, 2005. 45(9): p. 1297-1302.

[6]     Chen, H.Y., Bishop, M.T., Landes, B.G., and Chum, S.P., Orientation and property correlations for LLDPE blown films. Journal of Applied Polymer Science, 2006. 101(2): p. 898-907.

[7]     Lopez-Barron, C.R., Robledo-Ortiz, J.R., Rodrigue, D., and Gonzalez-Nunez, R., Film Processability, Morphology, and Properties of Polyamide-6/Low Density Polyethylene Blends. Journal of Plastic Film and Sheeting, 2007. 23(2): p. 149-169.

[8]     Garofalo, E., Fariello, M.L., Di Maio, L., and Incarnato, L., Effect of biaxial drawing on morphology and properties of copolyamide nanocomposites produced by film blowing. European Polymer Journal, 2013. 49(1): p. 80-89.

[9]     Ou, X. and Cakmak, M., Influence of biaxial stretching mode on the crystalline texture in polylactic acid films. Polymer, 2008. 49(24): p. 5344-5352.

[10]    Yu, L., Liu, H., Xie, F., Chen, L., and Li, X., Effect of annealing and orientation on microstructures and mechanical properties of polylactic acid. Polymer Engineering & Science, 2008. 48(4): p. 634-641.

[11]    Tsai, C.-C., Wu, R.-J., Cheng, H.-Y., Li, S.-C., Siao, Y.-Y., Kong, D.-C., and Jang, G.-W., Crystallinity and dimensional stability of biaxial oriented poly(lactic acid) films. Polymer Degradation and Stability, 2010. 95(8): p. 1292-1298.

[12]    Ketwattha, U. The development of toughness and gas permeability of poly(lactic acid)/ maleic anhydride-g-natural rubber blown film. Master Degree, Chemical engineering, Chulalongkorn university, 2011.

[13]   Collyer, A.A. and Walker, I., Rubber toughened engineering plastics. Vol. 1. 1994, London: Chapman & Hall. 666.

[14]   Bicerani, J., T.Seitz, J., and Arends, C.B., Polymer toughening. Vol. 30. 1996, New York: Marcel Dekker. 415.

[15]   Cantor, K., Blown Film Extrusion : an introduction. Vol. 1. 2006, Munich: Hanser publishers. 165.

[16]   Zhang, X.M., Elkoun, S., Ajji, A., and Huneault, M.A., Oriented structure and anisotropy properties of polymer blown films: HDPE, LLDPE and LDPE. Polymer, 2004. 45(1): p. 217-229.

[17]   Zhang, X., Ajji, A., and Jean-Marie, V., Processing–structure–properties relationship of multilayer films. 1. Structure characterization. Polymer, 2001. 42(19): p. 8179-8195.

[18]   Kokturk, G., Piskin, E., Serhatkulu, T.F., and Cakmak, M., Evolution of phase behavior and orientation in uniaxially deformed polylactic acid films. Polymer Engineering & Science, 2002. 42(8): p. 1619-1628.

[19]   Smith, P.B., Leugers, A., Kang, S., Hsu, S.L., and Yang, X., An analysis of the correlation between structural anisotropy and dimensional stability for drawn poly(lactic acid) films. Journal of Applied Polymer Science, 2001. 82(10): p. 2497-2505.

[20]   Zhang, C., Wang, W., Huang, Y., Pan, Y., Jiang, L., Dan, Y., Luo, Y., and Peng, Z., Thermal, mechanical and rheological properties of polylactide toughened by expoxidized natural rubber. Materials & Design, 2013. 45: p. 198-205.

[21]   Jantipa, M., The development of poly(lactic acid) packaging films with natural rubber, ed. S. Anongnat, T. Pramuan, and E. Chulalongkorn University. Faculty of. 2013: Chulalongkorn University.

[22]   Ishida, S., Nagasaki, R., Chino, K., Dong, T., and Inoue, Y., Toughening of poly(L-lactide) by melt blending with rubbers. Journal of Applied Polymer Science, 2009. 113(1): p. 558-566.

[23]   Wu, J.-H., Yen, M.-S., Wu, C.-P., Li, C.-H., and Kuo, M.C., Effect of Biaxial Stretching on Thermal Properties, Shrinkage and Mechanical Properties of Poly (Lactic Acid) Films. Journal of Polymers and the Environment, 2012. 21(1): p. 303-311.

[24]   Sarasua, J.-R., Prud'homme, R.E., Wisniewski, M., Le Borgne, A., and Spassky, N., Crystallization and Melting Behavior of Polylactides. Macromolecules, 1998. 31(12): p. 3895-3905.

[25]   Zhang, J., Tashiro, K., Tsuji, H., and Domb, A.J., Disorder-to-Order Phase Transition and Multiple Melting Behavior of Poly(l-lactide) Investigated by

Simultaneous Measurements of WAXD and DSC. <u>Macromolecules</u>, 2008. 41(4): p. 1352-1357.

[26]  Saeidlou, S., Huneault, M.A., Li, H., and Park, C.B., Poly(lactic acid) crystallization. <u>Progress in Polymer Science</u>, 2012. 37(12): p. 1657-1677.

[27]  Radjabian, M., Kish, M.H., and Mohammadi, N., Characterization of poly(lactic acid) multifilament yarns. I. The structure and thermal behavior. <u>Journal of Applied Polymer Science</u>, 2010. 117(3): p. 1516-1525.

[28]  Stoclet, G., Lefebvre, J.M., Séguéla, R., and Vanmansart, C., In-situ SAXS study of the plastic deformation behavior of polylactide upon cold-drawing. <u>Polymer</u>, 2014. 55(7): p. 1817-1828.

[29]  Bastani, D., Esmaeili, N., and Asadollahi, M., Polymeric mixed matrix membranes containing zeolites as a filler for gas separation applications: A review. <u>Journal of Industrial and Engineering Chemistry</u>, 2013. 19(2): p. 375-393.

[30]  Velazquez-Infante, J.C., Gamez-Perez, J., Franco-Urquiza, E.A., Santana, O.O., Carrasco, F., and Ll Maspoch, M., Effect of the unidirectional drawing on the thermal and mechanical properties of PLA films with different L-isomer content. <u>Journal of Applied Polymer Science</u>, 2013. 127(4): p. 2661-2669.

[31]  Tabatabaei, S.H. and Ajji, A., Crystal structure and orientation of uniaxially and biaxially oriented PLA and PP nanoclay composite films. <u>Journal of Applied Polymer Science</u>, 2011: p. n/a-n/a.

# APPENDIX

## Appendix A

## Mechanical properties

**Table A.1 Tensile properties of PLA/NR films at TUR 15 in MD**

| No. | Tensile strength (MPa) | Young's Modulus (MPa) | Elongation at break (%) | Tensile toughness (mJ) |
|---|---|---|---|---|
| 1 | 59.22 | 3050.34 | 18.43 | 496.26 |
| 2 | 56.24 | 2985.95 | 21.84 | 532.23 |
| 3 | 58.31 | 3047.44 | 19.80 | 437.81 |
| 4 | 59.30 | 2965.48 | 18.69 | 442.54 |
| 5 | 57.90 | 3053.88 | 20.48 | 475.90 |
| Avg. | 58.19 | 3020.62 | 19.85 | 476.95 |
| S.D. | 1.24 | 41.69 | 1.38 | 39.20 |

**Table A.2 Tensile properties of PLA/NR films at TUR 20 in MD**

| No. | Tensile strength (MPa) | Young's Modulus (MPa) | Elongation at break (%) | Tensile toughness (mJ) |
|---|---|---|---|---|
| 1 | 52.12 | 2895.62 | 16.56 | 334.63 |
| 2 | 48.76 | 2893.72 | 13.63 | 246.63 |
| 3 | 52.12 | 2954.90 | 14.57 | 260.35 |
| 4 | 56.00 | 3006.00 | 19.02 | 332.99 |
| 5 | 51.53 | 2895.07 | 13.61 | 266.67 |
| Avg. | 52.10 | 2929.06 | 15.48 | 288.26 |
| S.D. | 2.58 | 50.27 | 2.31 | 42.22 |

Table A.3 Tensile properties of PLA/NR films at TUR 25 in MD

| No. | Tensile strength (MPa) | Young's Modulus (MPa) | Elongation at break (%) | Tensile toughness (mJ) |
|-----|-----|-----|-----|-----|
| 1 | 53.76 | 150.51 | 9.15 | 150.51 |
| 2 | 47.26 | 119.71 | 8.57 | 119.71 |
| 3 | 51.31 | 172.22 | 9.97 | 172.22 |
| 4 | 53.49 | 159.26 | 12.91 | 159.26 |
| 5 | 48.89 | 112.58 | 9.86 | 112.58 |
| Avg. | 50.94 | 142.85 | 10.09 | 142.85 |
| S.D. | 2.84 | 25.70 | 1.67 | 25.70 |

Table A.4 Tensile properties of PLA/NR films at BUR 1.6 in MD

| No. | Tensile strength (MPa) | Young's Modulus (MPa) | Elongation at break (%) | Tensile toughness (mJ) |
|-----|-----|-----|-----|-----|
| 1.00 | 52.51 | 2953.18 | 17.20 | 338.70 |
| 2.00 | 56.38 | 2978.63 | 17.37 | 374.70 |
| 3.00 | 53.90 | 2962.47 | 17.67 | 352.02 |
| 4.00 | 53.76 | 3050.73 | 20.74 | 437.86 |
| 5.00 | 58.97 | 3004.80 | 19.86 | 435.95 |
| Avg. | 55.11 | 2989.96 | 18.57 | 387.85 |
| S.D. | 2.58 | 39.21 | 1.62 | 46.60 |

Table A.5 Tensile properties of PLA/NR films at BUR 1.8 in MD

| No. | Tensile strength (MPa) | Young's Modulus (MPa) | Elongation at break (%) | Tensile toughness (mJ) |
|---|---|---|---|---|
| 1.00 | 52.12 | 2895.62 | 16.56 | 334.63 |
| 2.00 | 48.76 | 2893.72 | 13.63 | 246.63 |
| 3.00 | 52.12 | 2954.90 | 14.57 | 260.35 |
| 4.00 | 56.00 | 3006.00 | 19.02 | 332.99 |
| 5.00 | 51.53 | 2895.07 | 13.61 | 266.67 |
| Avg. | 52.10 | 2929.06 | 15.48 | 288.26 |
| S.D. | 2.58 | 50.27 | 2.31 | 42.22 |

Table A.6 Tensile properties of PLA/NR films at BUR 2.0 in MD

| No. | Tensile strength (MPa) | Young's Modulus (MPa) | Elongation at break (%) | Tensile toughness (mJ) |
|---|---|---|---|---|
| 1.00 | 52.47 | 2914.25 | 6.08 | 121.95 |
| 2.00 | 48.52 | 2868.61 | 7.51 | 129.56 |
| 3.00 | 57.69 | 2993.97 | 6.79 | 134.74 |
| 4.00 | 51.34 | 2845.22 | 8.16 | 153.98 |
| 5.00 | 48.95 | 2873.58 | 9.40 | 131.53 |
| Avg. | 51.80 | 2899.13 | 7.59 | 134.35 |
| S.D. | 3.68 | 58.55 | 1.28 | 11.94 |

Table A.7 Tensile properties of PLA/NR films at TUR 15 in TD

| No. | Tensile strength (MPa) | Young's Modulus (MPa) | Elongation at break (%) | Tensile toughness (mJ) |
|---|---|---|---|---|
| 1 | 40.13 | 2851.81 | 9.16 | 250.90 |
| 2 | 41.43 | 2904.87 | 13.68 | 254.39 |
| 3 | 42.21 | 2936.45 | 11.99 | 207.51 |
| 4 | 37.84 | 2775.47 | 16.83 | 277.58 |
| 5 | 39.32 | 2864.66 | 9.69 | 259.97 |
| Avg. | 40.19 | 2866.65 | 12.27 | 250.07 |
| S.D. | 1.73 | 60.97 | 3.13 | 25.91 |

Table A.8 Tensile properties of PLA/NR films at TUR 20 in TD

| No. | Tensile strength (MPa) | Young's Modulus (MPa) | Elongation at break (%) | Tensile toughness (mJ) |
|---|---|---|---|---|
| 1 | 33.74 | 2704.67 | 9.40 | 130.47 |
| 2 | 34.10 | 2688.23 | 12.61 | 180.87 |
| 3 | 34.68 | 2724.40 | 8.50 | 121.80 |
| 4 | 35.86 | 2731.00 | 11.17 | 154.90 |
| 5 | 35.30 | 2760.30 | 8.91 | 130.67 |
| Avg. | 34.74 | 2721.72 | 10.12 | 143.74 |
| S.D. | 0.86 | 27.36 | 1.73 | 24.15 |

Table A.9 Tensile properties of PLA/NR films at TUR 25 in TD

| No. | Tensile strength (MPa) | Young's Modulus (MPa) | Elongation at break (%) | Tensile toughness (mJ) |
|---|---|---|---|---|
| 1 | 32.01 | 2667.30 | 5.66 | 57.51 |
| 2 | 35.92 | 2701.60 | 7.70 | 67.07 |
| 3 | 33.42 | 2703.60 | 5.69 | 61.62 |
| 4 | 34.95 | 2708.50 | 6.38 | 73.20 |
| 5 | 33.51 | 2664.80 | 6.59 | 54.22 |
| Avg. | 33.96 | 2689.16 | 6.40 | 62.73 |
| S.D. | 1.51 | 21.26 | 0.83 | 7.57 |

Table A.10 Tensile properties of PLA/NR films at BUR 1.6 in TD

| No. | Tensile strength (MPa) | Young's Modulus (MPa) | Elongation at break (%) | Tensile toughness (mJ) |
|---|---|---|---|---|
| 1.00 | 37.43 | 2800.55 | 12.49 | 195.58 |
| 2.00 | 35.90 | 2795.80 | 10.11 | 152.73 |
| 3.00 | 36.98 | 2755.00 | 12.29 | 195.42 |
| 4.00 | 37.04 | 2801.80 | 12.14 | 186.91 |
| 5.00 | 36.80 | 2772.60 | 13.01 | 201.23 |
| Avg. | 36.83 | 2785.15 | 12.01 | 186.37 |
| S.D. | 0.57 | 20.58 | 1.11 | 19.49 |

Table A.11 Tensile properties of PLA/NR films at BUR 1.8 in TD

| No. | Tensile strength (MPa) | Young's Modulus (MPa) | Elongation at break (%) | Tensile toughness (mJ) |
|---|---|---|---|---|
| 1.00 | 33.74 | 2704.67 | 9.40 | 130.47 |
| 2.00 | 34.10 | 2688.23 | 12.61 | 180.87 |
| 3.00 | 34.68 | 2724.40 | 8.50 | 121.80 |
| 4.00 | 35.86 | 2731.00 | 11.17 | 154.90 |
| 5.00 | 35.30 | 2760.30 | 8.91 | 130.67 |
| Avg. | 34.74 | 2721.72 | 10.12 | 143.74 |
| S.D. | 0.86 | 27.36 | 1.73 | 24.15 |

Table A.12 Tensile properties of PLA/NR films at BUR 2.0 in TD

| No. | Tensile strength (MPa) | Young's Modulus (MPa) | Elongation at break (%) | Tensile toughness (mJ) |
|---|---|---|---|---|
| 1.00 | 52.47 | 2914.25 | 6.08 | 121.95 |
| 2.00 | 48.52 | 2868.61 | 7.51 | 129.56 |
| 3.00 | 57.69 | 2993.97 | 6.79 | 134.74 |
| 4.00 | 51.34 | 2845.22 | 8.16 | 153.98 |
| 5.00 | 48.95 | 2873.58 | 9.40 | 131.53 |
| Avg. | 51.80 | 2899.13 | 7.59 | 134.35 |
| S.D. | 3.68 | 58.55 | 1.28 | 11.94 |

Table A.13 Tensile properties of PLA/NR films at drawing ratio = 0% in MD (TUR = 15)

| No. | Tensile strength (MPa) | Young's Modulus (MPa) | Elongation at break (%) | Tensile toughness (mJ) |
|-----|------------------------|-----------------------|-------------------------|------------------------|
| 1 | 40.36 | 1967.62 | 23.52 | 229.69 |
| 2 | 36.08 | 1816.11 | 35.74 | 307.01 |
| 3 | 35.76 | 1881.07 | 19.39 | 165.27 |
| 4 | 41.66 | 1859.77 | 18.90 | 191.24 |
| 5 | 41.02 | 1891.08 | 19.78 | 195.83 |
| Avg. | 38.98 | 1883.13 | 23.47 | 217.81 |
| S.D. | 2.83 | 55.32 | 7.10 | 54.88 |

Table A.14 Tensile properties of PLA/NR films at drawing ratio = 50% in MD (TUR = 15)

| No. | Tensile strength (MPa) | Young's Modulus (MPa) | Elongation at break (%) | Tensile toughness (mJ) |
|-----|------------------------|-----------------------|-------------------------|------------------------|
| 1 | 43.25 | 1912.90 | 59.46 | 481.41 |
| 2 | 42.52 | 1882.90 | 56.92 | 386.75 |
| 3 | 41.83 | 1965.90 | 45.81 | 362.10 |
| 4 | 40.88 | 1818.59 | 39.23 | 330.30 |
| 5 | 47.40 | 1977.53 | 54.93 | 496.64 |
| Avg. | 43.18 | 1911.56 | 51.27 | 411.44 |
| S.D. | 2.52 | 64.75 | 8.47 | 73.79 |

Table A.15 Tensile properties of PLA/NR films at drawing ratio = 100%
          in MD (TUR = 15)

| No. | Tensile strength (MPa) | Young's Modulus (MPa) | Elongation at break (%) | Tensile toughness (mJ) |
|---|---|---|---|---|
| 1 | 73.64 | 2471.76 | 42.10 | 511.10 |
| 2 | 66.08 | 2262.78 | 45.03 | 500.05 |
| 3 | 59.61 | 2239.74 | 52.95 | 509.29 |
| 4 | 67.00 | 2424.78 | 33.71 | 389.57 |
| 5 | 61.54 | 2298.77 | 39.21 | 415.29 |
| Avg. | 65.57 | 2339.57 | 42.60 | 465.06 |
| S.D. | 5.46 | 102.79 | 7.14 | 58.04 |

Table A.16 Tensile properties of PLA/NR films at drawing ratio = 0%
          in TD (BUR = 1.6)

| No. | Tensile strength (MPa) | Young's Modulus (MPa) | Elongation at break (%) | Tensile toughness (mJ) |
|---|---|---|---|---|
| 1 | 26.33 | 1882.10 | 22.78 | 129.70 |
| 2 | 26.67 | 1848.90 | 19.55 | 114.95 |
| 3 | 27.27 | 1834.80 | 21.83 | 129.21 |
| 4 | 26.73 | 1820.00 | 23.83 | 138.12 |
| 5 | 29.91 | 1971.60 | 23.24 | 148.50 |
| Avg. | 27.38 | 1871.48 | 22.25 | 132.10 |
| S.D. | 1.46 | 60.50 | 1.67 | 12.39 |

Table A.17 Tensile properties of PLA/NR films at drawing ratio = 50%
in TD (BUR = 1.6)

| No. | Tensile strength (MPa) | Young's Modulus (MPa) | Elongation at break (%) | Tensile toughness (mJ) |
|---|---|---|---|---|
| 1 | 36.56 | 2150.80 | 44.78 | 300.08 |
| 2 | 41.50 | 2146.69 | 41.64 | 358.51 |
| 3 | 41.02 | 2016.49 | 49.93 | 378.51 |
| 4 | 41.05 | 2089.25 | 44.68 | 339.17 |
| 5 | 39.84 | 2080.23 | 43.83 | 394.55 |
| Avg. | 39.99 | 2096.69 | 44.97 | 354.16 |
| S.D. | 2.02 | 55.20 | 3.05 | 36.72 |

Table A.18 Tensile properties of PLA/NR films at drawing ratio = 100%
in TD (BUR = 1.6)

| No. | Tensile strength (MPa) | Young's Modulus (MPa) | Elongation at break (%) | Tensile toughnes (mJ) |
|---|---|---|---|---|
| 1 | 71.49 | 2510.63 | 50.54 | 505.48 |
| 2 | 70.78 | 2146.48 | 56.01 | 479.45 |
| 3 | 76.69 | 2441.41 | 61.08 | 581.15 |
| 4 | 81.38 | 2526.55 | 51.67 | 524.67 |
| 5 | 79.07 | 2575.93 | 53.16 | 514.04 |
| Avg | 75.88 | 2440.20 | 54.49 | 520.96 |
| S.D. | 4.65 | 171.11 | 4.22 | 37.58 |

Table A.19 Tear strength of PLA/NR films for different BUR

| Sample | Tear strength (Nm) | |
|---|---|---|
| | MD | TD |
| BUR 1.6 | 7.38±1.81 | 9.62±1.28 |
| BUR 1.8 | 5.40±1.91 | 9.00±0.00 |
| BUR 2.0 | 4.91±3.36 | 9.43±1.31 |

Table A.20 Tear strength of PLA/NR films for different TUR

| Sample | Tear strength (Nm) | |
|---|---|---|
| | MD | TD |
| TUR 15 | 9.30±2.60 | 11.43±3.34 |
| TUR 20 | 5.40±1.91 | 9.00±0.00 |
| TUR 25 | 3.25±2.01 | 5.45±1.81 |

Table A.21 Impact strength of PLA/NR films for different BUR

| Sample | Impact strength (J/cm) |
|---|---|
| BUR 1.6 | 7.95±1.02 |
| BUR 1.8 | 6.47±0.98 |
| BUR 2.0 | 5.56±0.95 |

Table A.22 Impact strength of PLA/NR films for different TUR

| Sample | Impact strength (J/cm) |
|---|---|
| TUR 15 | 9.73±1.25 |
| TUR 20 | 6.47±0.98 |
| TUR 25 | 4.24±0.94 |

## Appendix B

### Gas Permeability

Table B.1 Oxygen and Water vapor permeation of PLA/NR films at TUR 15

| No. | Oxygen permeation $(cc.mil/m^2.day.atm)$ | Water vapor permeation $(gm.mil/m^2.day.atm)$ |
|-----|------------------|-----------------|
| 1 | 707.24 | 278.46 |
| 2 | 711.49 | 280.72 |
| 3 | 787.32 | 305.10 |
| 4 | 709.74 | 287.83 |
| Avg. | 728.95 | 288.03 |
| SD | 38.95 | 12.06 |

Table B.2 Oxygen and Water vapor permeation of PLA/NR films at TUR 20

| No. | Oxygen permeation $(cc.mil/m^2.day.atm)$ | Water vapor permeation $(gm.mil/m^2.day.atm)$ |
|-----|------------------|-----------------|
| 1 | 807.12 | 292.88 |
| 2 | 841.61 | 293.23 |
| 3 | 682.05 | 291.12 |
| 4 | 797.19 | 310.13 |
| Avg. | 781.99 | 296.84 |
| SD | 69.29 | 8.91 |

Table B.3 Oxygen and Water vapor permeation of PLA/NR films at TUR 25

| No. | Oxygen permeation (cc.mil/m$^2$.day.atm) | Water vapor permeation (gm.mil/m$^2$.day.atm) |
|---|---|---|
| 1 | 893.98 | 308.68 |
| 2 | 835.16 | 312.60 |
| 3 | 777.60 | 315.64 |
| 4 | 789.66 | 326.63 |
| Avg. | 824.10 | 315.89 |
| SD | 52.77 | 7.71 |

Table B.4 Oxygen and Water vapor permeation of PLA/NR films at BUR 1.6

| No. | Oxygen permeation (cc.mil/m$^2$.day.atm) | Water vapor permeation (gm.mil/m$^2$.day.atm) |
|---|---|---|
| 1 | 635.29 | 305.27 |
| 2 | 770.14 | 288.46 |
| 3 | 778.23 | 283.90 |
| 4 | 787.78 | 288.86 |
| Avg. | 742.86 | 291.62 |
| SD | 72.07 | 9.38 |

Table B.5 Oxygen and Water vapor permeation of PLA/NR films at BUR 1.8

| No. | Oxygen permeation (cc.mil/m$^2$.day.atm) | Water vapor permeation (gm.mil/m$^2$.day.atm) |
|---|---|---|
| 1 | 807.12 | 305.27 |
| 2 | 841.61 | 288.46 |
| 3 | 682.05 | 283.90 |
| 4 | 797.19 | 288.86 |
| Avg. | 781.99 | 291.62 |
| SD | 69.29 | 9.38 |

Table B.6 Oxygen and Water vapor permeation of PLA/NR films at BUR 2.0

| No. | Oxygen permeation (cc.mil/m$^2$.day.atm) | Water vapor permeation (gm.mil/m$^2$.day.atm) |
|---|---|---|
| 1 | 795.98 | 302.03 |
| 2 | 822.07 | 310.92 |
| 3 | 792.36 | 316.12 |
| 4 | 812.02 | 303.09 |
| Avg. | 805.61 | 308.04 |
| SD | 13.91 | 6.69 |

Table B.7 Oxygen permeation of PLA/NR films for different drawing ratios in MD (TUR = 15)

| No. | Oxygen permeation (cc.mil/m$^2$.day.atm) | | |
|---|---|---|---|
| | TUR 15 | | |
| | 0% | 50% | 100% |
| 1 | 834.74 | 1225.509 | 846.658 |
| 2 | 711.49 | 1202.751 | 946.5213 |
| 3 | 787.32 | 1364.07 | 873.7557 |
| 4 | 943.38 | 1486.872 | 938.2019 |
| Avg. | 819.23 | 1319.801 | 901.2842 |
| SD | 97.09 | 132.2424 | 48.82331 |

Table B.8 Oxygen permeation of PLA/NR films for different drawing ratios in TD (BUR = 1.6)

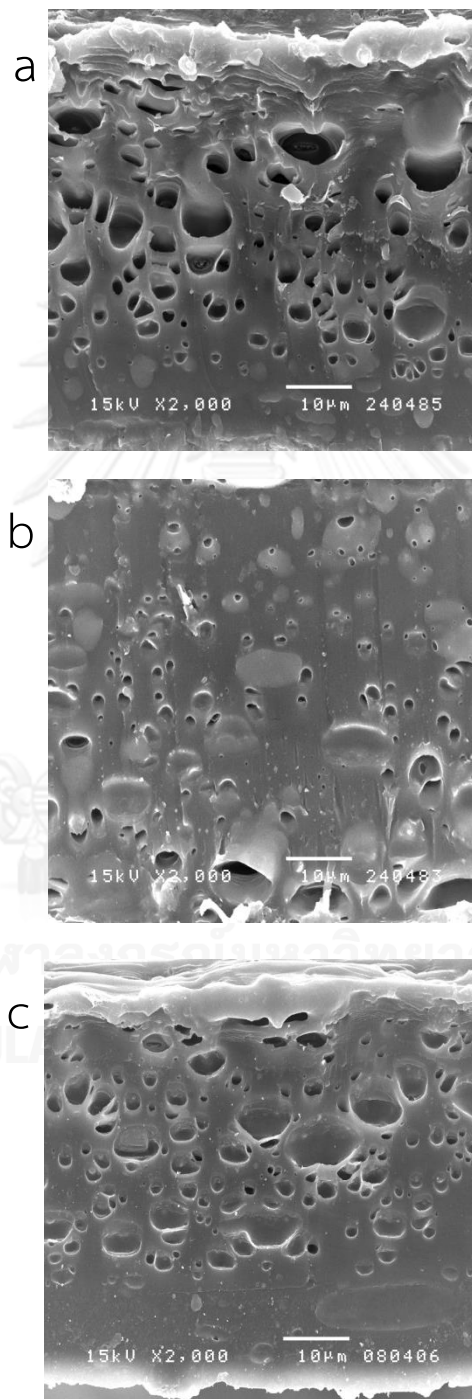| No. | Oxygen permeation (cc.mil/m$^2$.day.atm) | | |
|---|---|---|---|
| | BUR 1.6 | | |
| | 0% | 50% | 100% |
| 1 | 794.11 | 976.33 | 986.79 |
| 2 | 899.91 | 948.10 | 986.79 |
| 3 | 867.68 | 979.07 | 949.63 |
| 4 | 787.78 | 969.74 | 955.79 |
| Avg. | 837.37 | 968.31 | 969.75 |
| SD | 55.26 | 14.03 | 19.84 |

## Appendix C

## Morphology of PLA/NR films



Figure C.1 Morphology of cross-sectional fractured surfaces and in the
PLA/NR films in MD films for different TUR at fixed BUR = 1.8
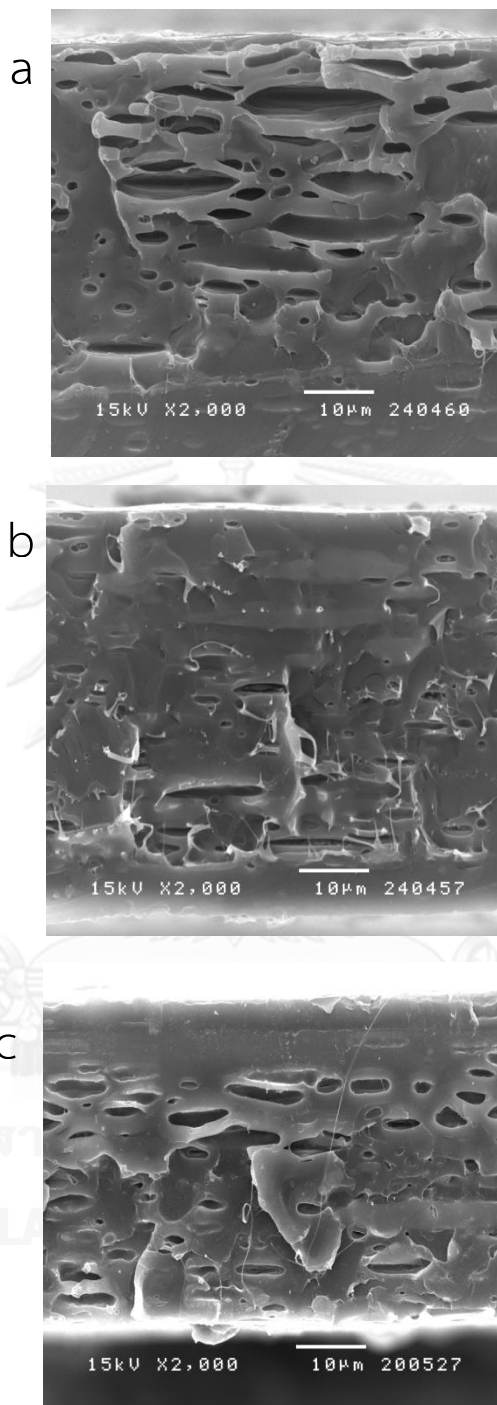(a) TUR = 15, (b) TUR = 20  and (c) TUR = 25.

Figure C.2 Morphology of cross-sectional fractured surfaces and in the
PLA/NR films in TD for different BUR at fixed TUR = 20 (a) BUR
= 1.6, (b) BUR = 1.8 and (c) BUR = 2.0

## Appendix D

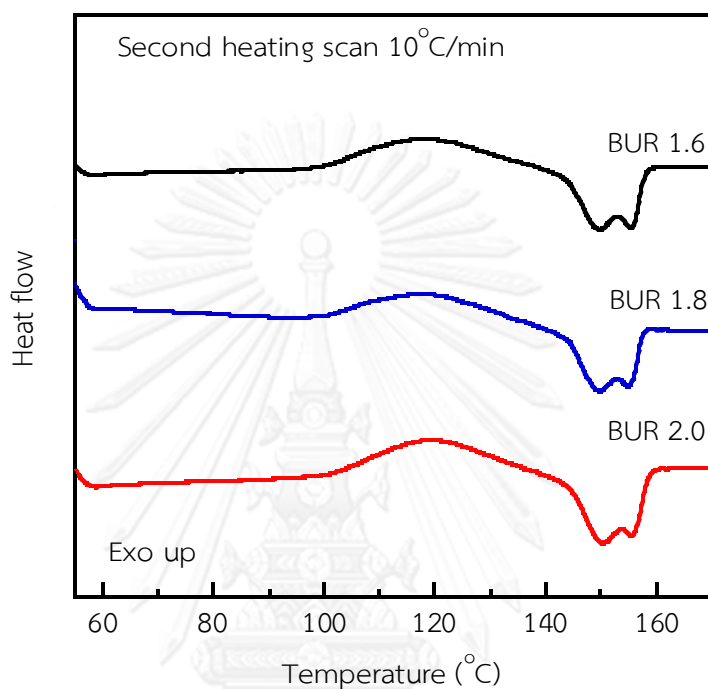## Thermal properties of PLA/NR films



Figure D.1 DSC thermograms of the PLA/NR films for different
BUR at fixed TUR = 20

Table D.1 Thermal properties of PLA/NR films for different BUR determined from the
second DSC heating scan at fixed TUR = 20

| Samples | Tg ($^{o}$C) | $T_{cc}$ ($^{o}$C) | $T_{m1}$ ($^{o}$C) | $T_{m2}$ ($^{o}$C) | $\Delta H_{cc}$ (J/g) | $\Delta H_{m}$ (J/g) | %$X_{c}$ |
|---------|------|------|------|------|------|------|------|
| BUR = 1.6 | 59.5 | 118.3 | 149.7 | 155.7 | 19.75 | 19.75 | 0.00 |
| BUR = 1.8 | 60.0 | 120.0 | 149.8 | 155.3 | 17.77 | 17.77 | 0.00 |
| BUR = 2.0 | 59.7 | 118.3 | 150.3 | 155.9 | 18.44 | 18.44 | 0.00 |

.

## VITA

Mr. Thawatchai Wongchaichana was born on October 20, 1989 in Bangkok, Thailand. He finished high school at Nawamintharachinuthid Horwang Nonthaburi School, Nonthaburi. In 2012, He received the Bachelor's Degree from Department of Chemical Engineering, Faculty of Engineering, Chulalongkorn University. He continued his study for Master's Degree in Chemical Engineering at the Department of Chemical Engineering, Faculty of Engineering, Chulalongkorn University in June, 2012.

He was invited for poster presentation in the title of "Effect of Blown Films Processing on Properties of Poly(lactic acid)/Natural Rubber Film", During January 8-10, 2014 at Pure and Applied Chemistry International Conference 2014 in Khon Kaen, Thailand.